This is to certify that the

dissertation entitled

A Continuous Magnetofluidized Bed Bioreactor for Production of Plant-Cell Secondary Metabolites

presented by

Tyler T. Ames

has been accepted towards fulfillment
of the requirements for

Ph.D. degree in Chemical Engineering

R. Mark Worden

Major professor

Date May 1, 1997

A CONTINUOUS MAGNETOFLUIDIZED BED BIOREACTOR FOR PRODUCTION OF PLANT-CELL SECONDARY METABOLITES

By

Tyler T. Ames

A DISSERTATION

Submitted to
Michigan State University
in partial fulfillment of the requirements
for the degree of

DOCTOR OF PHILOSOPHY

Department of Chemical Engineering

1997

ABSTRACT

A CONTINUOUS MAGNETOFLUIDIZED BED BIOREACTOR FOR PRODUCTION OF PLANT-CELL SECONDARY METABOLITES

By

Tyler T. Ames

Plant cells have the potential to produce a wide variety of economically important products. The magnetofluidized bed bioreactor (MFB) which offers continuous, plug-flow biocatalyst throughput, is well suited for production of intracellularly stored plant metabolites. A MFB system, featuring a magnetic valve for solids (MVS), has been assembled, operated, and refined. The MFB has been operated with soybean cell culture, producing daidzein and genistein for up to 2 months. Soybean cells were co-immobilized with ferritic stainless steel in calcium alginate beads. Biocatalyst microscopy and Thiele modulus calculations indicated that oxygen diffusion in the biocatalyst was not rate limiting in this system. Continuous operation of the MFB, featuring dissolved O_2 and CO_2 control, has been demonstrated past start-up to the point of steady growth rates. An unsteady-state model of the system provided insight on experimental data as well as protocol for steady-state operation. MFB feasibility was confirmed by the scale-up calculations. Power per volume requirements decrease with size and microbubble aeration was demonstrated as an efficient method for providing oxygen at large scale. MFB development was paralleled by development of the Diffusion Gradient Chamber (DGC) for rapidly optimizing plant cell culture growth and product formation. The DGC provides exposure of immobilized plant cells to a continuum of essentially steady-state

concentrations in a single experiment. Image acquisition and analysis provided a non-invasive method for tracking growth. Growth and isoflavonoid accumulation responded to several chemical effector gradients including carbon source, nitrogen source, basal salts, hormones, antibiotics, and an isoflavonoid precursor. Optimal conditions were generally within normal ranges and did not provide a new medium formulation for the MFB.

ACKNOWLEDGMENTS

I would like to thank Dr. Mark Worden for his guidance, dedication, and support throughout my doctoral program. I also thank Dr. Ken Sink for his collaboratory efforts and of course for our soybean cultures. I greatly appreciate the advice and job search assistance given by Dr. Bruce Dale. I would like to thank Dr. Daina Briedis not only for participation on my guidance committee, but also for her role in my choice of MSU for graduate school.

I would like to thank Mark Widman, Marshall Bredwell, and Mark Mikola for countless instances of assistance and humor over the past three years in the lab. We have had the privilege of several undergraduate researchers, all appreciated, but especially Casey Preston for his dedicated work and good spirit. I would also like to thank Joseph Leykam for graciously providing mass spectrometry method development and analysis. Funding for this work was provided by the MSU Crop and Food Bioprocessing Center, Center for Plant Lipids and Starches, and the MSU Biotechnology Training Program.

I am especially grateful to Julie Caywood, Candy McMaster, and Faith Peterson for helping with innumerable hurdles. As always, I am forever grateful to my mother and father for giving me this opportunity and believing in me.

TABLE OF CONTENTS

LIST OF TABLES

LIST OF FIGURES

1. INTRODUCTION

Plant cells have the potential to produce a wide variety of economically important products. However, commercial development of this potential is limited by slow growth rates, relatively low rates of product formation, and consequently, low bioreactor productivities (Sahai and Knuth, 1985). The research presented here addresses this problem on two levels. First, a continuous bioreactor for plant-cell culture which offers several advantages over traditional systems such as CSTRs was developed and demonstrated. Second, a novel tool was developed for determining concentrations of medium components that optimize growth and product expression. Soybean cell culture, which produces the isoflavonoids genistein and daidzein, was used a model system. The medical and agricultural potential of these compounds gives added value to the work, which is relevant to a broad range of plant cell systems and products.

The research is presented in 6 sections. Section 2, Objectives and Significance, presents the goals and hypotheses of the research as well as the significance of the work. Background information and a review of relevant literature comprises Section 3, Background. Preliminary development of the magnetofluidized bed bioreactor (MFB) is described in Section 4, MFB Development and Continuous Operation. Section 5, Protocol and Modeling for Long-Term Operation, expands upon key aspects of operation, examines steady-state operation, and provides a mathematical description of the system. Scale-up feasibility issues including use of a third (gas) phase and magnetic field generation are addressed in Section 6, MFB Bioreactor Scale Up. Development of

the Diffusion Gradient Chamber (DGC) as a tool for plant bioprocess is detailed in Section 7, Plant Studies in the DGC.

2. OBJECTIVES AND SIGNIFICANCE

2.1 Continuous MFB Operation

The primary objective of the research was to demonstrate continuous operation of a MFB for production of isoflavonoids from soybean cell culture. Furthermore, achievement of steady-state growth and product formation was a goal. Demonstration of continuous, steady-state operation at the lab scale is considered an important prerequisite for further development (scale-up) of the system. It was hypothesized that by maintaining key process variables at steady values, growth and product concentrations can be maintained at a steady-state. Key process variables were considered to be sucrose and antibiotic concentrations, pH, temperature, dissolved oxygen, and carbon dioxide content of the gas phase.

The MFB bioreactor is ideally suited for production of intracellular plant-cell secondary metabolites because it provides continuous processing of immobilized cells while maintaining a uniform residence time. By eliminating solids mixing the MFB has the potential for a significant increase in productivity over conventional fluidized beds. Two specific isoflavonoids produced by soybeans, genistein and daidzein, were the target compounds for this research project. In contrast to the current extraction method for isoflavonoids, the proposed bioprocess would allow soybean cell cultures to be maintained under optimal conditions for isoflavonoid production, and would allow continuous, rather than seasonal production by field crops. Genistein and daidzein concentrations in soybean cell culture (Zacharius and Kalan, 1990) have been reported as

one to two orders of magnitude higher than in soybeans (Wang and Murphy, 1994; Naim *et al.*, 1974). It is therefore anticipated that the proposed process could reduce the costs of genistein and daidzein by more than an order of magnitude.

Shuler *et al.* (1990) has noted that the primary determinant of economic viability for a bioprocess, the volumetric productivity of the reactor times the wholesale price of the product, is 0.12 $/L-day +/- 60% for a wide variety of fermentations. A volumetric productivity can be calculated for MFB productivity as shown in Table 1.

Table 1. Volumetric productivity calculation for MFB.

Variable	**Value**	**Source**
Value of Isoflavonoid	$1000 per gram	Sigma: $4,800 /g natural genistein $700 /g synthetic genistein ICN: $1,400 /g daidzein
Concentration in soybean	600 ppm	Genistein content in Worden lab Glycine max Reported as high as 15,600 ppm (Zacharius and Kalan, 1990)
Soybean density in biocatalyst	10 g/L	Achieved in MFB (Fall 1995)
Biocatalyst packing	0.7 L per L	estimate
Biocatalyst residence time	20 days	Used in MFB (Fall 1995), approx. end of growth in batch cultures
Volumetric productivity	0.21 $/L-day	

The calculated volumetric productivity falls within the range of commercial fermentations. This result is encouraging as the values in Table 1 should be obtainable in a successful

steady-state run. Furthermore, these numbers do not take into account improvements which may result from proposed research with the DGC.

2.2 Bioreactor Scale Up

For lab scale bioreactors using a continuous liquid recycle, pre-saturation of the liquid phase with gaseous substrates may be adequate. Bramble *et al.* (1990) conducted 2-phase MFB experiments with *C. arabica*, using a dialysis cartridge to aerate the liquid phase before it entered the reactor. However, for commercial-scale bioreactors where higher cell densities and longer liquid residence times would be needed, this approach is not feasible because the dissolved oxygen would be depleted from the liquid phase as it rises through the bioreactor. Addition of gas is needed to replenish what is consumed by the cells.

A secondary objective of the research was to demonstrate a useful pairing of microbubble aeration and the magnetofluidized bed bioreactor. It was hypothesized that power required to stabilize the bed will be reduced by using microbubbles instead of conventional gas sparging. A positive result would translate to increased gas mass transfer and reduced operating costs. Microbubble aeration is attractive method of supplying oxygen for two reasons. First, microbubbles provide very high mass-transfer coefficients. Second, microbubble aeration causes less disruption of a magnetofluidized bed than traditional gas sparging.

The feasibility of a commercial scale MFB also depends on the economics scaling up to large scale. Both power requirements for magnetic field operation and capital costs

of construction are important issues. It was hypothesized that the MFB would scale favorably by the criteria of decreasing power-per-volume ratio with increasing reactor volume. It was further hypothesized that capital costs would be a small fraction of typical fermentation system capital costs. Validation of this hypothesis is significant in determining the commercial potential of the process.

2.3 Diffusion Gradient Chamber for Plant Cell Culture

An additional objective of the research was to develop the Diffusion Gradient Chamber (DGC) as a tool for optimizing conditions in bioprocesses which utilize plant cell culture. The DGC was explored as a highly efficient tool for collecting data on plant cell response to environmental conditions. The stimulus which causes the response is defined as a chemoeffector. The DGC can be used to optimize concentrations of both a positive chemoeffector (e.g. substrate such as sucrose) and a negative chemoeffector (e.g. antibiotics inhibiting growth). Optimization is used here in a broad sense, not limited to maximization. Optimization could include determination of the lowest sugar concentration which yields growth at 95% of the maximum rate. Balancing antibiotic effectiveness against microbes and plant toxicity (both dependent on concentration) is another example. It was hypothesized that plant cell concentration (and thus growth) could be quantified noninvasively with video capture and image analysis. The logical step beyond growth optimization is optimization of product accumulation. It was hypothesized that accumulation of genistein and daidzein could be optimized as a function of chemoeffectors which may be important to secondary metabolism (e.g. phenylalanine) using the DGC.

simult
effect
could
Petri
time
and c
broad
prog
more
conc
by c
cell
tech
wha
inf
cell

The DGC allows plant cells to be grown under a spectrum of conditions simultaneously. Image analysis and/or chemical assays are then used to determine the effects of those conditions on cell growth and product formation. One DGC experiment could potentially supply information equivalent to dozens of individual experiments in Petri dishes or Erlenmeyer flasks. This approach is expected to significantly reduce the time and effort required to determine environmental conditions which maximize growth and/or product accumulation. Furthermore, success with product correlation has even broader applications. Even if the product correlation hypothesis cannot be validated, progress towards the objective may establish protocols for other plant cell systems where more sensitive or non-invasive assays are available or where products are found in higher concentrations. Examples could include: production of pigments which can be quantified by color image analysis, production of valuable oils comprising a significant fraction of cell mass, or production of secondary metabolites for which a non-invasive assay technique is available such as fluorescence. The DGC provides an additional advantage when applied to immobilized cell systems. As cells can be immobilized in the DGC gel, information specific to a solid phase can be gained. Such information could include data on cell mass and substrate gradients as well as effects of immobilization.

3. BACKGROUND

3.1 Fluidized Beds for Immobilized Plant Cells

Several reactor schemes are available for plant cell cultures, including stirred tanks, bubble columns, air-lift reactors, hollow-fiber membranes, liquid-dispersed trickle and incline reactors, and mist bioreactors for hairy root culture (McKelvey *et al.*, 1993; Whitney, 1992; Taya *et al.*, 1989). However, each of these reactors has limitations, such as cell death from shear, insufficient mixing at high cell densities, dead zones, settling of cells, and difficulty in scale-up (Panda *et al.*, 1989). Furthermore, many of these reactors are poorly suited for continuous operation in which the product is accumulated intracellularly.

Fluidized bed bioreactors offer several advantages for immobilized plant cells. Low shear forces and pressure drops prevent damage to fragile cells. Excellent contact between the gas, liquid, and solid phases eliminates the need for mechanical mixing. Shuler *et al.* (1990) noted that high cell densities and continuous operation lead to increased volumetric productivity over non-immobilized or batch processes. Cell densities may reach 110 g/L in alginate beads, while suspension culture is limited to about 30 g/L (Sahai and Knuth, 1985). The close proximity of immobilized cells allows intercellular communication and transport that can be important for differentiation and secondary-metabolite production (Shuler *et al.*, 1990). Attachment and plugging caused by free cells are eliminated by immobilization (Sahai and Knuth, 1985).

An important disadvantage of conventional immobilized systems, however, is that most plant secondary metabolites are typically stored intracellularly. Soybean isoflavonoids exist predominantly as glucoside-malonylated conjugates (Graham *et al.*, 1990; Kudou *et al.*, 1991) which are located in the vacuole (Barz and Welle, 1992). Permeabilization methods for release of products into the media result in low culture viability. Brodelius (1990) notes that it appears very difficult, if not impossible, to release vacuolar substances into the medium by permeabilization of the plasma membrane and the tonoplast without killing the cells.

Continuous solids throughput eliminates the need for metabolite release. Fresh cells can be continually added at the reactor, maintained in the reactor for the optimal length of time, and then removed for product recovery. The solids residence time can be chosen to optimize the intracellular product concentration, and controlled by the rate of solids throughput. Continuous operation also minimizes bioreactor down time, and thus offers increased productivity over batch operation.

3.2 Magnetofluidized Bed (MFB)

3.2.1 Principle of Operation

A magnetofluidized bed (MFB) consists of a fluidized bed of magnetically susceptible particles to which a direct-current (DC) magnetic field is applied. The magnetic field induces dipoles in the particles and causes them to align along the field lines (Figure 1), thus eliminating the solids mixing that occurs in fluidized beds. However, like conventional fluidized beds, the magnetized solids can still be passed though the bed. As a result, illustrated in Figure 2, continuous solids throughput without mixing (i.e. "plug

flow") is possible (Rosensweig, 1978; Rosensweig, 1979; Rosensweig *et al.*, 1981; Siegell, 1988; and Liu *et al.*, 1991). Several applications have been found for MFB, and reviewed by Liu *et al.* (1991). Magnetic fields have been successfully applied to fluidized bed bioreactors including continuous ethanol fermentation (Weng *et al.*, 1992), as well as phenol degradation (Hu and Wu, 1987). Bramble *et al.* (1990) operated a two-phase magnetically stabilized fluidized bed with plant cells (*C. arabica*). However, none of these bioreactors were operated in a solids-throughput mode.

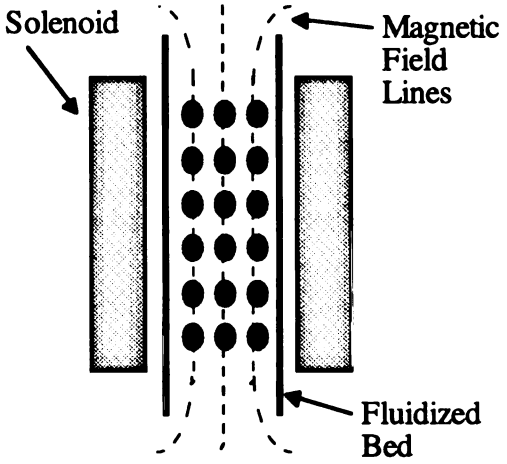

Figure 1. Magnetic field lines and elimination of mixing in a MFB.

Preliminary MFB development has been ongoing in the research lab of Dr. Mark Worden. Phase hold-up, liquid-mixing, and gas-mass-transfer properties of a prototype MFB have been characterized (Freund and Worden, 1990; Thompson and Worden, 1991, 1992; Thompson, 1993; Thompson and Worden, 1997). These studies have indicated that magnetization increases the gas volume fraction, decreases the axial liquid mixing, and increases the volumetric gas-to-liquid mass-transfer coefficient (k_la) in the fluidized bed.

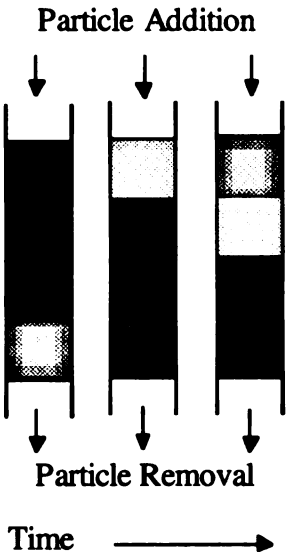

Figure 2. Plug-flow movement of solids through a MFB.

Magnetic valves for solids (MVS) have been developed to control movement of solids out of fluidized beds. An MVS consists of a magnetic-valve coil surrounding the column in the vicinity of a magnetically susceptible screen. The screen openings are large enough to allow free passage of solids when no current is applied to the valve coil. Supplying power to the valve coil results in an induced magnetic field at the screen which stops solids flow. Magnetic valves can be operated fully open, fully closed, or partially open, to control solids flow (Jaraiz-M. *et al.*, 1984b). The MVS have no moving parts and consume little power (Yang *et al.*, 1982). Complete theory and design considerations regarding screen sizes, capture and release currents, solids mass flux, and magnetic coils are given by Jaraiz-M. *et al.*, (1984).

3.2.2 Features as a Bioreactor

The primary advantage of the MFB bioreactor is that it allows continuous processing of the biocatalyst particles with tight control of their residence time in the

reactor. This capability, which has not been demonstrated for any other type of bioreactor, allows the bioreactor productivity to be optimized, as illustrated in the following example calculations.

The productivity of a bioreactor producing intracellular products is a function of both the cellular kinetics and the residence-time distribution (RTD) of the biocatalyst. The RTD, in turn, is determined by the degree of solids mixing as the solids pass through the reactor. The mixing can be quantified either in terms of a Peclet number or a number of stirred-tanks in series (Fogler, 1986). For a conventional fluidized bed, assuming a four-week growth and product-formation cycle for the plant cells, a typical dispersion coefficient of 4 cm^2/s (Dorgelo *et al.*, 1985), and a bioreactor length of 60 cm, the number of stirred tanks in series needed to approximate the solids mixing was calculated to be 1.000. Thus, the biocatalyst would become perfectly mixed, and the RTD would be described by a stirred-tank model. In contrast, solids mixing is virtually eliminated in the MFB, and the RTD would be approximated by a plug-flow model. These two limiting cases were used to demonstrate the increase in productivity possible with the MFB. Figure 3 includes a lag phase, exponential growth, a stationary phase during which the product is formed, and an exponential death phase during which the product decays according to first-order kinetics. Decrease in product concentration with time has been observed for a variety of plant systems, including genistein and daidzein production by *Glycine max* (Zacharius and Kalan, 1990). For these kinetics and a 4.8 week mean residence time, a plug flow bioreactor gives an average product concentration (and hence bioreactor productivity) almost three times higher than a stirred-tank bioreactor. While

the actual increase in productivity realized by using the MFB will depend on the soybean kinetics and the small degree of mixing at the ends of the column, this calculation indicates the magnitude of improvement which may be expected.

A potential disadvantage of the MFB, which arises from its ability to continuously process biocatalyst in plug flow, is that it is impossible to change (program) the medium composition in accordance with the age of the cells. Medium programming is not needed for soybean isoflavonoid synthesis (Zacharius and Kalan, 1990) which is the subject of this research.

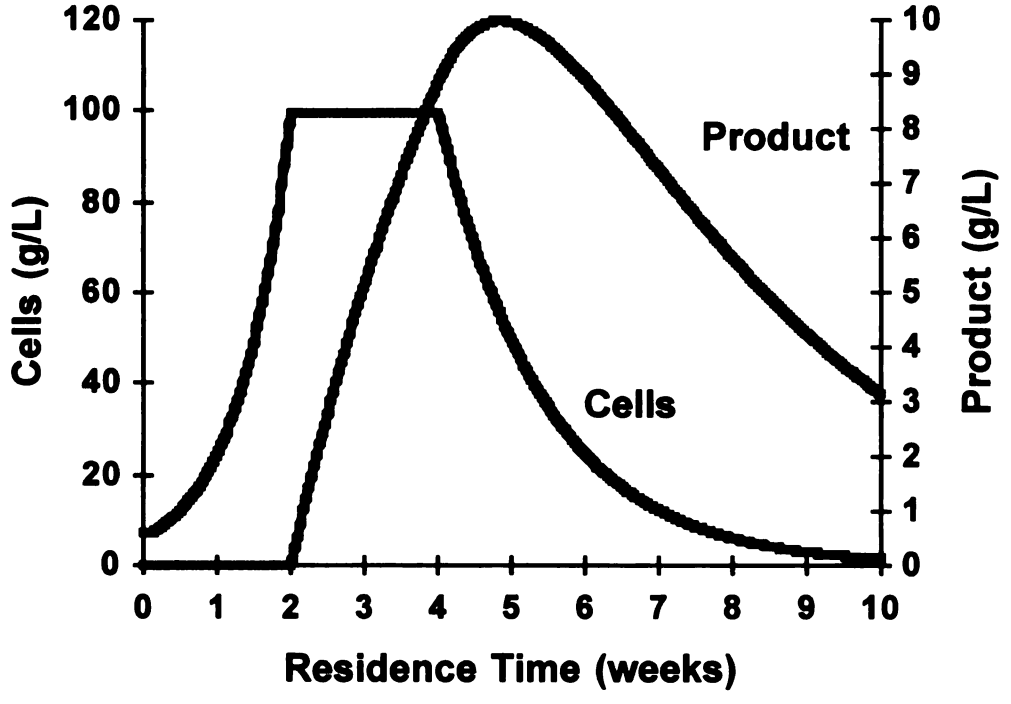

Figure 3. Hypothetical plant-cell growth and secondary-product-formation kinetics.

3.3 Microbubble Gas-Liquid Mass Transfer

Oxygen is commonly the rate-limiting nutrient in aerobic bioprocesses due to its low aqueous solubility (about 8 mg/L for water in equilibrium air at 30°C and 1 atm

pressure). The main resistance to oxygen mass-transfer may lie in the gas-liquid interface, the liquid-solid interface, or within the solid phase. For commercial-scale bioreactors, the gas-liquid resistance is usually large, resulting in relatively low dissolved-oxygen concentrations (van't Riet, 1983). In such cases, increasing the volumetric mass-transfer coefficient ($k_l a$) increases the oxygen mass-transfer rate, and hence the reactor productivity. An increase in $k_l a$ is typically achieved by either increasing the gas flow rate or the power-to-volume ratio (van't Riet, 1983). Both of these approaches work by increasing the interfacial area between the gas and liquid. Unfortunately, they both add significantly to the operating costs of the process.

Microbubbles are surfactant-stabilized bubbles about 50 μm in diameter. The surfactant layer surrounding microbubbles generates a diffuse electric double layer that acts to repel other bubbles and prevent coalescence (Sebba, 1987). A microbubble dispersion exhibits colloidal properties and is stable enough to be pumped (Longe, 1989). The microbubble dispersion can thus be made remotely and then pumped, as needed, into the bioreactor The effects of surfactant type and concentration, as well as salts, on microbubble formation, drainage and stability have been characterized in the lab of Mark Worden (Bredwell *et al.*, 1995).

Conventional gas bubbles are about 100 times larger in diameter than microbubbles (Kaster *et al.*, 1990). Because surface area is inversely proportional to the bubble diameter squared, microbubbles could potentially increase $k_l a$ values by orders of magnitude. Significant mass-transfer enhancement by microbubbles has been demonstrated in yeast fermentations (Kaster *et al.*, 1990). Microbubble dispersions are easily produced, are

biocompatible, and can produce extremely high $k_l a$ values, even in the absence of mechanical agitation (Bredwell *et al.*, 1995a; Bredwell *et al.*, 1995b, Kaster *et al.*, 1990). Values for $k_l a$ of up to 1800 h^{-1} in an unagitated bubble column using a gas volume fraction less than 5% have been measured (Bredwell *et al.*, 1995b). Furthermore, because of their extremely small size, microbubbles equilibrate with the surrounding liquid phase within about 15 s (Bredwell *et al.*, 1994).

Power requirements for microbubble aeration are expected to be quite low during scale-up. The Power number for our microbubble generator was measured as 0.036 (Bredwell *et al.*, 1995b). Using this value, a specific oxygen-uptake rate of 10 mg O_2/g cells h, and previously reported details of microbubble formation (Bredwell *et al.*, 1995a), the power required to make enough microbubbles to sustain a 1 m^3 reactor containing 30 g/L soybean culture was calculated to be 0.013 kW (i.e., 0.013 kW/m^3) (Bredwell *et al.*, 1995b). By comparison, power-consumption rates for mechanically agitated microbial fermentations are on the order of 1 kW/m^3 (van't Riet, 1983).

3.4 Isoflavonoids

Isoflavonoids constitute an important class of 15-carbon phenolic compounds sharing a similar carbon skeleton. Found in all plant tissues, isoflavonoids have been shown to exhibit a wide range of biochemical activities, including providing defense against invading organisms (Rao, 1990). This research focused on the production of two key isoflavonoids, genistein and daidzein, from soybean cell culture. The chemical

structures of these compounds are shown in Figure 4. These compounds, which are found in high concentrations in soybeans, have important medical and agricultural applications.

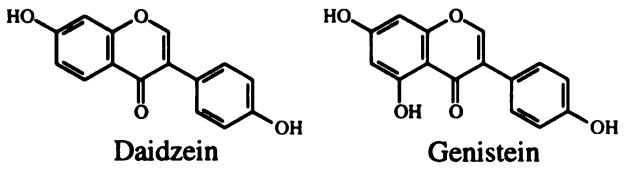

Daidzein Genistein

Figure 4. Structure of the isoflavonoids daidzein and genistein.

3.4.1 Medical Applications

Recent studies have shown that the isoflavonoid genistein is a potent chemotherapeutic agent that blocks several key steps in cancer induction and proliferation. Protein tyrosine kinases (PTKs) play a key role in cancer induction, proliferation, and metastasis (Akiyama *et al.*, 1987; Mueller *et al.*, 1992; Mustelin and Burn, 1993). Genistein, a potent inhibitor of PTKs, has been shown to have antiprolific effects on human hepatocarcinoma (Mousavi and Adlercreutz, 1993) and stomach cancer cells (Yanagihara *et al.*, 1993). It can induce Erythroleukemia cells to differentiate into non-cancerous Erythroid cells (Watanabe *et al.*, 1991). Daidzein was also found to have potent differentiation-inducing activity for human leukemia cells, both *in vitro* and *in vivo* (Jing *et al.*, 1993). Genistein has also been shown to block the invasion of normal cells by tumor cells (Mueller *et al.*, 1992) and block bacterial uptake by epithelial cells (Rosenshine *et al.*, 1992).

Topoisomerase is involved in breaking DNA for replication, transcription, recombination, integration, all necessary steps in cell proliferation. Genistein limits the

ability of ras oncogenes to transform cells by inhibiting topoisomerase, and this inhibition was found to occur only in transformed cells (Okura *et al.*, 1988). Angiogenesis (formation of new capillaries) is necessary for proliferation and metastasis of tumors beyond the 1-2 mm size. Genistein was found to inhibit angiogenesis of endothelial cells in vitro as well as proliferation of several types of cancer (neuroblastoma, rhabdyosarcoma, and Ewings Sarcoma) (Fotsis *et al.*, 1993).

Evidence suggests that reactive oxygen species, such as hydrogen peroxide, play an important role in mutagenesis and carcinogenesis, particularly in tumor promotion. Reactive oxygen species may damage macromolecules such as proteins, RNA, and DNA, which is related to carcinogenic initiation, promotion, and progression. Genistein has been shown to inhibit both hydrogen peroxide production by leukemic cells and mouse skin damage by hydrogen peroxide (Wei *et al.*, 1993).

Isoflavonoids in soybean (primarily genistein and daidzein) may suppress endogenous oestrogenic activity and inhibit hormone-dependent carcinogenesis of the breast. A soybean rich diet has been associated with a reduced risk of breast cancer (Lee *et al.*, 1991). Rats showed a significant decrease in chemically induced mammary cancers when fed a soy diet (Messina and Barnes, 1991).

3.4.2 Agricultural Applications

Isoflavonoids such as genistein and daidzein are potential environmentally compatible alternatives to synthetic pesticides for defense against pathogenic organisms. Several studies suggest that isoflavonoids are part of the natural defense mechanisms of plants. Soybean plants respond to infection or wounding by the production of the

enzymes phenylalanine lyase and chalcone-flavanone isomerase, which are part of the isoflavonoid synthesis pathway (Partridge and Keen, 1977). Genistein was found to strongly inhibit the growth of *Sclerotium rolfsii*, which is responsible for southern-blight disease (Gazaway and Hagan, 1989). Genistein has been shown to be toxic to *Phytophthora megasperma* f. sp. *glycina* (Graham and Graham, 1991) which causes root and stem rot in soybeans. In tissue infected by *P. megasperma*, production of phytoalexins increased and there was rapid hydrolysis of isoflavone conjugates to produce inhibitory levels of genistein at the site of infection (Graham and Graham, 1991). Soybean isoflavones at 50 ppm of the growth medium inhibited growth of six species of fungi by 60 to 85% (Naim *et al.*, 1974). Genistein and daidzein concentrations of 50-75 ppm completely inhibited spore formation of *Aspergillus niger*, the causal factor in deterioration of seeds in the field following weather-delayed harvests (Jacobsen and Meronuck, 1989; and Adesanya *et al.*, 1986).

The symbiotic relationship between soybean and *Bradyrhizobium japonicum* is responsible for the formation of nitrogen-fixing root nodules. Genistein and daidzein have been shown to induce the nod genes of *B. japonicum* (Kosslak *et al.*, 1987). Roots and seeds exude these isoflavonoid compounds, suggesting that the plant attracts the nodule-producing bacteria (Rao, 1990).

3.5 Soybean Culture

3.5.1 Development

Soybean tissue is rich in daidzein and genistein, the isoflavonoids targeted in this proposal (Barz and Welle, 1992). Both compounds have been identified in hydrolyzed

soybean root and leaf extracts (Porter *et al.* 1986), soybean seedling tissue and root exudates (Graham, 1991b), and soybean roots (Cho and Harper, 1991). Genistein and daidzein have also been found in soybean cell cultures in concentrations as high as 15,600 and 4410 μg per gram of dry cells, respectively (Zacharius and Kalan, 1990). Genistein and daidzein in soybean are found together with their 7-O-glucoside 6"-O-malonate conjugates (Barz and Welle, 1992). The conjugates can be hydrolyzed to free genistein and daidzein by strong acid or almond β-glucosidase (Graham *et al.,* 1990) for product recovery.

Suspension cultures of *Glycine max* cv. Mandarin were provided by Dr. Ken Sink, Department of Horticulture. Callus cells were initiated according to Fett and Zacharius (1982). Briefly, soybean seeds are surface sterilized and epicotyl, cotyledon or hypocotyl explants are placed aseptically on B5 agar medium (Gamborg *et al.*, 1968) with 1.0 or 2.0 mg/L 2,4-D. Calluses are subsequently transferred to B5 agar medium with 2.0 mg/L 2,4-D and after about 1 month into liquid B5 to initiate cell suspensions.

3.5.2 Enhancement of Isoflavonoid Synthesis

A possible means to enhance production of isoflavonoids in unorganized cell cultures is through elicitor promotion by phytoalexins (Dougall, 1986), which are produced in a defensive response to infection by pathogens. Isoflavonoids are intermediates in the biosynthetic pathways of phytoalexins. Elicitation occurs via activation of genes involved in the biosynthetic pathway (Chappell and Hahlbrock, 1984). This pathway begins with the conversion of phenylalanine to cinnamic acid by phenylalanine ammonia-lyase. This enzyme is considered to be a key switchpoint

between primary and secondary metabolism of phenolics, and increased enzymic activity has led to increased product synthesis (Holden and Yeoman, 1987). Additionally, the supply of phenylalanine has limited capsaicin accumulation (secondary phenolic) in *Capsicum frutescens*. The conversion of phenylalanine is apparently important in regulation of phenolics production, and may thus be an important rate-limiting step in the pathway.

Several types of phytoalexin elicitors have been studied including fungal cell wall, plant cell wall, and microbial enzymes (Darvill and Albersheim, 1984). Hahlbrock *et al.* (1981) first showed that UV light, a non-biological elicitor, stimulated biosynthesis of flavonoids. A variety of other abiotic inducers have also been investigated including heavy metals, autoclaved ribonuclease, chloroform, and detergents, although they are typically associated with tissue damage (Darvill and Albersheim, 1984). As isoflavonoids such as genistein and daidzein are intermediates in the production of phytoalexins, production of these isoflavonoids may also be stimulated by phytoalexin elicitors. Kochs and Grisebach (1987) found that microsomal preparations from normal soybean cells or from elicitor-challenged cells (*P. megasperma* or *Alternaria carthami*) catalyzed the conversion of (2S)-naringenin to genistein. Miller *et al.* (1994) showed that the beta-1, 6-1, 3-glucans isolated from *B. japonicum* elicited the production of both daidzein and glyceollin in a soybean cotyledon assay. In a contrasting study, Zacharius and Kalan (1990) studied biotic stresses on soybean cell cultures with particular reference to quantifying daidzein and genistein levels (precursors of the phytoalexin glyceollin). Glyceollin levels were generally promoted while the precursor (daidzein and genistein) concentrations always decreased

after 40-68-96 h treatment with the intact bacterial (*Pseudomonas syringae* pv. *glycinea*, strains A-29-2 and 2159) or isolated fungal elicitor (*Phytophthora infestans*). While phytoalexin elicitors promoted an enzyme upstream of genistein (Kochs and Grisebach, 1987), the downstream portion of the pathway is apparently also promoted. As a result, except for daidzein in the Miller *et al.* (1994) report, there is typically a net decrease in the concentrations of genistein and daidzein following elicitation. In contrast, cool white fluorescent light was found to promote genistein accumulation in line Sb-1a (Zacharius and Kalan, 1990). Exposure of Sb-1a cells in culture to a synthetic photon flux of 17.5 versus 5.3 $\mu mol/m^2s$, on a 24 h photoperiod, yielded up to ten times more daidzein and genistein.

Gas-phase reactants are also expected to influence soybean-cell growth and product synthesis in the MFB. The importance of carbon dioxide and ethylene in the gas phase of bioreactors has been documented, but is poorly understood. Addition of 2% carbon dioxide improved growth and viability of *C. roseus* in a 20 L airlift bioreactor, while 5% carbon dioxide was detrimental (Archambault, 1991). Both carbon dioxide and ethylene were important for product formation by *Thalictrum rugosum* in a 2.3 L airlift bioreactor (Kim *et al.*, 1991). The specific berberine content was doubled by supplying these gases at levels comparable to closed shake-flask cultures. Cho *et al.* (1988) used ethephon, an ethylene precursor, to stimulate alkaloid production in *Coffea arabica* and *T. rugosum* which have widely different biochemical pathways. Gas recycle was found to increase product synthesis for *Catharanthus roseus* cultures in a stirred tank reactor (Schlatmann *et al.*, 1993). In contrast, carbon dioxide enrichment of sparging air did not

enhance growth of *Hyoscyamus muticus* root cultures (McKelvey *et al.*, 1993). More recently, Schlatmann *et al.* (1997) have suggested a focus on dissolved gaseous metabolites (DGM), represented by their largest constituent CO_2, for plant-cell bioreactor design.

3.6 Diffusion Gradient Chamber

3.6.1 Description

The level of secondary metabolites produced by plant cells is strongly influenced by key effector variables such as carbon source, nitrogen source, hormones, precursor compounds and pH. However, these effects are poorly understood and efforts to increase production levels typically rely on trial-and-error studies. Because of the large number of potential effectors (and much larger number of permutations), and slow plant-cell growth rates, screening studies in shake flasks or petri dishes can be very labor intensive and time consuming.

A research tool used to-date for microbiological work has great potential to greatly accelerate these trial-and-error studies with plant cells. The Diffusion Gradient Chamber (DGC) generates multiple, simultaneous, chemical gradients within a semi-solid growth medium (Emerson *et al.*, 1994). It consists of a transparent, sterilizable, plastic box that houses a 5 cm x 5 cm x 1 cm slab-shaped arena containing agar gel illustrated in Figure 5. The arena is separated from the four liquid reservoirs that bound it by membranes that allow diffusion of small molecules but are impermeable to gel or cells. A continuous flow of fresh medium through the reservoirs replenishes solute molecules that diffuse across the membrane, thus maintaining a constant concentration in the reservoirs. When different

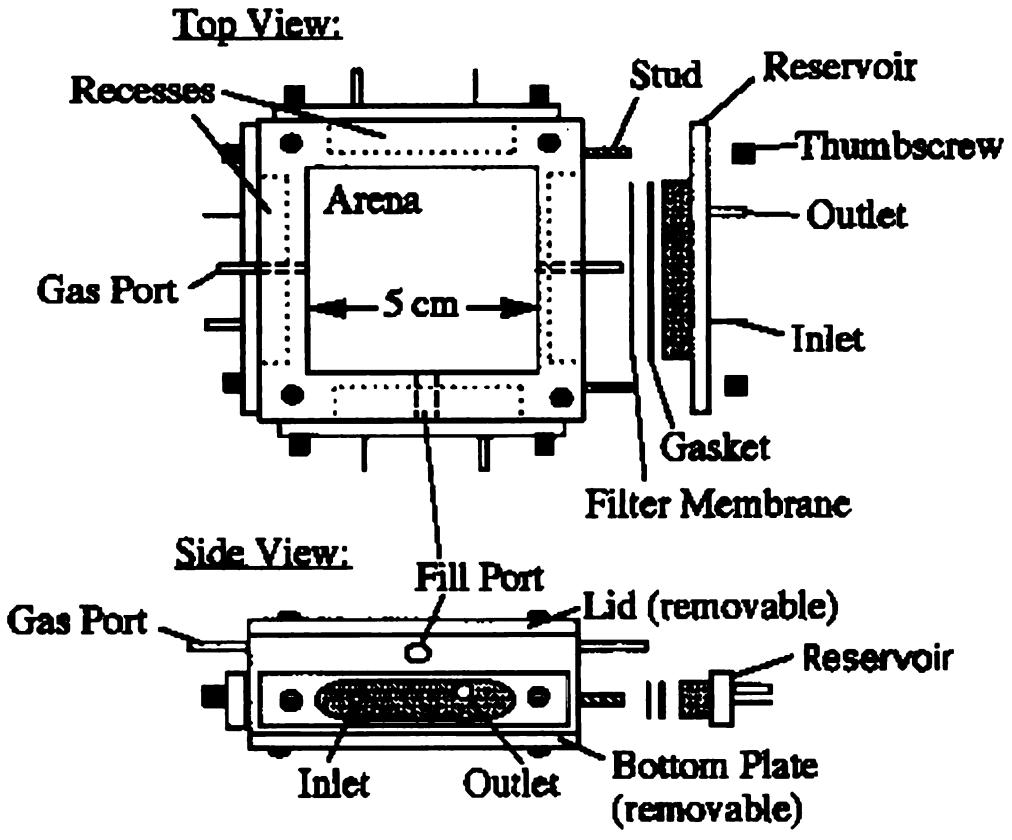

Figure 5. Diffusion Gradient Chamber.

solute concentrations are used in the reservoirs, diffusion generates a continuous concentration gradient across the arena. Gradients of multiple solutes may be established simultaneously, either parallel or perpendicular to one another. In this way, the influence of multiple stimuli on cells may be tested simultaneously. Bacterial growth and migration are measured using a CCD camera and image processing. Applied lighting is diffracted by cells while a light-absorbing background is placed behind the DGC. Therefore, cells appear as white on a black background. Bacterial concentrations are directly proportional to greyscale value over a range of concentrations (M. Widman, unpublished data).

3.6.2 Microbial Research

DGC research has centered around the behavior of bacteria in environments containing chemical gradients. The growth and migratory behavior of *E coli.* in response to chemoattractants (aspartate, α-methyl aspartate, and serine) and a chemorepellent (valine) have been examined by Emerson *et al.* (1994). Chemoeffector gradients were also used to separate *E. coli* from *Pseudomonas fluorescens* based on differential chemotactic responses. Bacterial behavior in the DGC has agreed well with predictions of mathematical models. Fickian diffusion in the gel arena and a first-order mass-transfer resistance at the membrane have accurately predicted gradient concentrations (Emerson *et al.*, 1994; M. Widman, personal communication). Extensive modeling of bacterial growth and chemotaxis in response to both consumable and non-consumable substrate gradients has been completed (Widman *et al.*, 1995). Oxygen and glucose gradients have been measured utilizing microelectrodes and microbiosensors which allow non-disruptive assaying (Emerson *et al.*, 1993, Brune *et al.*, 1995).

4. MFB DEVELOPMENT AND CONTINUOUS OPERATION

4.1 Introduction

A wide variety of plant secondary metabolites have value as pharmaceuticals, food colors, flavors and fragrances. Plant cell culture offers a high-quality, uniform product while reducing labor costs (Shuler et al., 1990) and eliminating the effects of weather and disease. Furthermore, continuous production may provide increased productivity over traditional batch systems.

Bramble et al. (1990) previously demonstrated the use of plant cells in a magnetically stabilized fluidized bed. *Coffea arabica* cells were co-immobilized with magnetite in calcium-alginate beads. These beads comprised the solid phase of a two-phase bed, where solids mixing was prevented by a DC magnetic field. Continuous solids throughput was discussed but not achieved in their system. Solids throughput with minimal solids mixing is desirable for plant cells as it allows tight control of residence time. Intracellular products which are difficult or impossible to release into the medium by permeabilization (Brodelius, 1990) can be extracted from the plant tissue after it has spent an optimal residence time in the bioreactor.

The goal of this work was to achieve continuous production of daidzein and genistein from soybean in a magnetofluidized bed (MFB) with continuous biocatalyst throughput. The isoflavonoids are high-value compounds having both medical and agricultural applications. A magnetic valve for solids (MVS) was used to control the rate

of solids throughput. Supporting work included batch shake flask experiments to study the effects of immobilization and antimicrobial agents on soybean culture growth.

4.2 Materials and Methods

4.2.1 Chemicals

All chemicals for soybean culture medium were purchased from Sigma Chemical (St. Louis, MO) except sucrose from J. T. Baker (Phillipsburg, NJ). LB medium was purchased from Gibco (Paisley, Scotland). Sodium alginate and genistein were purchased from Sigma Chemical. Stainless steel powder (grade 410-L) was purchased from Alfa Aesar (Ward Hill, MA). Daidzein was purchased from ICN Biomedicals (Aurora, OH). Ampicillin and gentamicin were purchased from Sigma Chemical, and Timentin was purchased from SmithKline Beecham (Philadelphia, PA). Benlate was supplied by DuPont (Wilmington, DE). Helium was purchased from AGA Gas (Cleveland, OH). Acetonitrile, ethyl acetate, and acetic acid were purchased from EM Science (Gibbstown, NJ). All other chemicals were purchased from J. T. Baker.

4.2.2 Equipment

4.2.2.1 MFB System

The MFB system used in this work is illustrated in Figure 6. The main components of the MFB bioreactor system are the fluidized bed, solenoids, biocatalyst reservoirs, and mixing vessel. The fluidized bed was comprised of a 60 cm long, 5 cm diameter Pyrex glass column with grooved ends for O-rings. Custom machined stainless steel endplates were sealed with Viton O-rings. The head plate, as illustrated in Figure 7, had a port for solids inlet and a port for liquid outlet. The base plate, shown in Figure 8

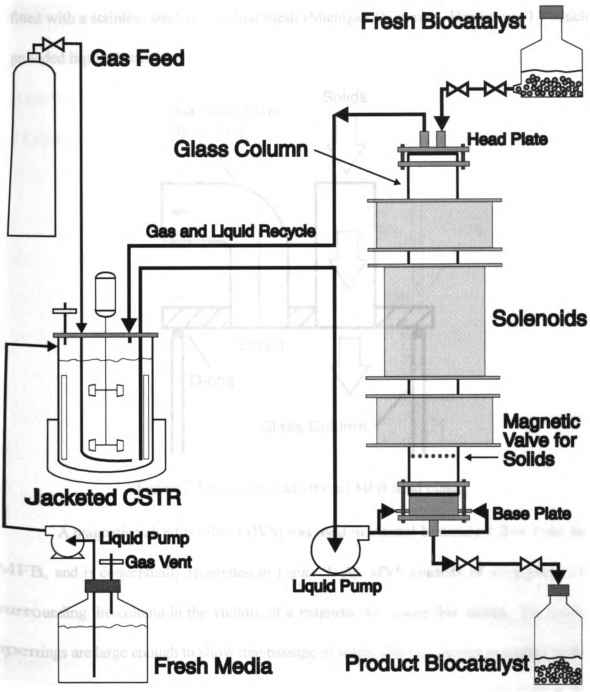

Figure 6. Diagram of the magnetofluidized bed bioreactor.

had a center outlet for solids and an annular region for liquid inlet. The annular region was fitted with a stainless steel fluidization mesh (Michigan Dynamics, Heathrow FL) which provided liquid distribution.

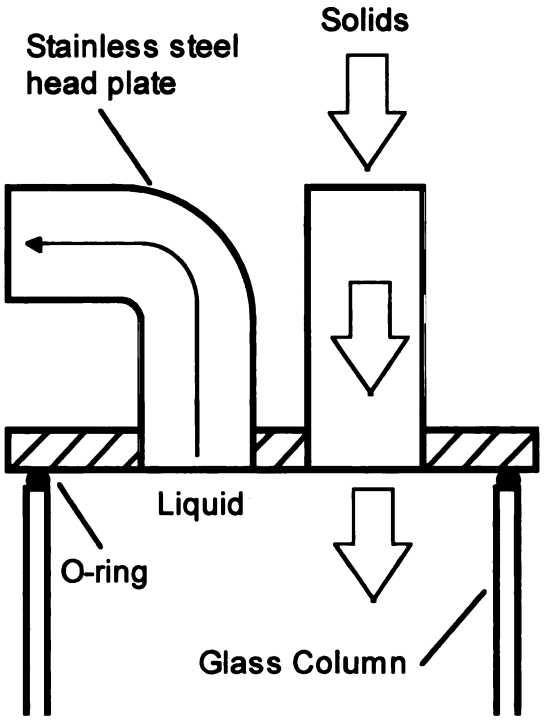

Figure 7. Cross-sectional view of MFB head plate.

A magnetic valve for solids (MVS) was used to control biocatalyst flow from the MFB, and is conceptually illustrated in Figure 9. An MVS consists of a magnetic coil surrounding the column in the vicinity of a magnetically susceptible screen. The screen openings are large enough to allow free passage of solids when no current is applied to the valve coil. Supplying power to the valve coil results in an induced magnetic field at the screen that stops solids flow. Details of MVS construction and operation are given by Jaraiz-M. *et al.* (1984) and Yang *et al.* (1982). The magnetic valve screen, which consisted of a 430 stainless steel wire mesh 4 x 4 (Belleville Wire Cloth, Cedar Grove NJ), was fixed

to the glass with silicone sealant near the bottom of the column. An axial, DC magnetic field was supplied by three solenoids designed to provide an approximately even field strength over the total length of the solenoids. The bottom solenoid also provided the magnetic field for the magnetic valve for solids. Power for the solenoids was supplied by a Kepco (Flushing NY) DC power supply (ATE 100-5M) rated at 100 volts and 5 A.

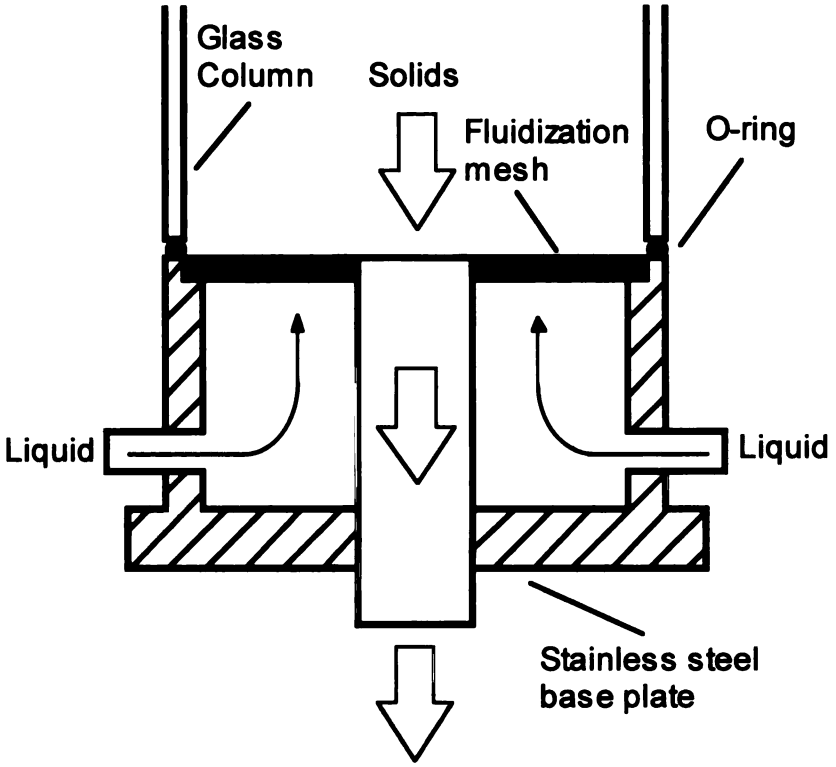

Figure 8. Cross-sectional view of MFB base plate.

The feed biocatalyst reservoir was a 2 L aspiration vessel sealed with a foam stopper and aluminum foil. A Wheaton solvent flask with a modified screw cap served as the product biocatalyst reservoir. Biocatalyst outlet tubing passed through the cap via a hole that was sealed with silicone sealant. Both reservoirs were connected to their respective headplates with silicone tubing. Clear tubing (1.5 cm ID) allowed visualization of biocatalyst movement as it was controlled with pinch clamps. The mixing vessel was a

Bioflo II (New Brunswick, Edison NJ) fermentation system with a 1.5 L vessel. The Bioflo II system provided agitation, temperature control, and dissolved oxygen monitoring. Connections to the vessel included a suction line to the baseplate of the column, a return line from the headplate of the column, a fresh medium inlet, a sparging gas inlet, and a head space vent. All tubing was norprene or silicone. Liquid was pumped to the column with a high capacity Masterflex peristaltic pump (Cole Parmer, Chicago). Liquid returned from the column by gravity. A 20 L carboy provided fresh medium via a peristaltic pump (Cole Parmer) as needed. An oxygen cylinder regulated at 5 psi was connected to the vessel sparge line. The gas flow rate was controlled by a peristaltic pump (Cole Parmer).

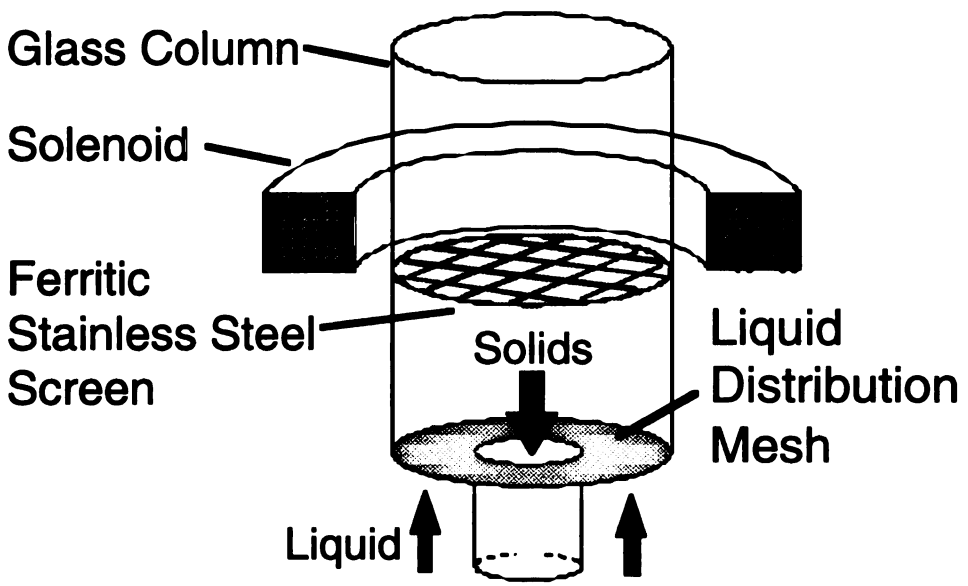

Figure 9. 3-D diagram of the magnetic valve for solids.

4.2.2.2 HPLC

Isoflavonoid analysis was conducted using high performance liquid chromatography (HPLC). A Waters (Milford, MA) 600 multisolvent pump, Waters 490 multiwavelength UV absorbance detector, Waters system interface module, and a PC for data acquisition and processing comprised the system. A 25 cm by 4.6 mm Rainin (Woburn MA) Microsorb-MV column containing 5 μm C-18 packing was used. A refillable 3 cm guard column with pellicular C-18 packing (Alltech, Deerfield IL) was used to protect the analytical column.

4.2.2.3 Gas Chromatography

Gas chromatography of the MFB gas phase was performed on a Perkin Elmer (Norwalk CT) Autosystem Gas Chromatograph with a thermal conductivity detector. Fixed gases were separated on a 9.1 m by 2.2 mm Hayesep DB 100/120 SS column (Alltech) with helium as the mobile phase. A Perkin Elmer 600 Series Link and PC were used for data acquisition and instrument control.

4.2.3 Plant Cell Culture and Analysis

Suspension cultures were maintained on a Lab-Line (Melrose Park IL) 3590 Orbital Shaker. All culture transfer and immobilization was conducted in a sterile laminar flow hood (Baker Company, Sanford ME). A Stir Pak lab stirrer (Cole Parmer) and a Teflon microcentrifuge sample pestle (Fisher, Pittsburgh) were used for extraction of isoflavonoids. Samples were centrifuged in an Eppendorf 5415C centrifuge (Brinkmann Instruments, Westbury NY). A Cenco drying oven (Central Scientific, Chicago) was used for dry weight analysis. All sterilization was performed in a Amsco (Farmington, MI)

steam autoclave at 121°C. A Reichert Microstar IV microscope (Cambridge Instruments, Buffalo NY) was used for light microscopy of biocatalyst. A Pulnix TM-7CN CCD camera (Sunnyvale, CA) was used for image capture. Image data were acquired using Quanta (Mountain View CA) WinVisionPro software on a PC.

4.2.4 Respiration

Dissolved oxygen was measured with an Ingold O_2 sensor (12 mm diameter) and an Ingold Model 170 oxygen amplifier (Mettler-Toledo, Wilmington MA). Data were acquired with a PC, DT2801 analog and digital I/O board (Data Translation, Marlboro MA), and Labtech Notebook software (Laboratory Technologies, Wilmington MA). For suspension culture, the oxygen sensor was inserted into a 100 mL graduated cylinder via a rubber stopper. For immobilized soybean, a miniature packed bed system was assembled using a 15 cm by 2.5 cm ID Pyrex column. Column ends were plugged by rubber stoppers which were connected via Tygon tubing (Cole Parmer). The bottom stopper was fitted with a metal screen to prevent passage of biocatalyst. The oxygen sensor entered the column through the top stopper. Liquid was circulated with a Masterflex peristaltic pump (Cole Parmer).

4.2.5 Soybean Culture

Suspension cultures of *Glycine max* cv. Mandarin were maintained at 25-27 °C on a rotary shaker at 125 rpm in 250 mL Erlenmeyer flasks. They were subcultured by passing two-week-old culture through a 400 μm sieve. Twenty mL of this inoculum was added to 50 mL of fresh 1-B5 medium as listed in Table 2 (Gamborg *et al.*, 1968). All transfers were conducted in a laminar flow hood. Subculturing had been ongoing for over

one year and had produced stable suspension cultures. While undocumented, a decrease in average aggregate size (finer suspensions) and increase in average growth rate have been observed. Both results are advantageous for productivity and immobilization.

Table 2. Composition of soybean medium.

Item	Concentration
Gamborg B5 Salts	3.1 g/L
Nicotinic acid	1 mg/L
Pyridoxine HCl	1 mg/L
Thiamine HCl	10 mg/L
Myo-inositol	100 mg/L
Sucrose	20 g/L
2,4-D	1 mg/L
Kinetin	0.15 mg/L

4.2.6 Immobilization

Immobilization solution (150 mL aliquots) consisting of 2% medium viscosity sodium alginate and 25% (w/w) stainless steel was prepared and autoclaved in 500 mL Erlenmeyer flasks. A soybean inoculum was prepared by passing an approximately 2 week-old (since last sub-culture) culture through a 1 mm sieve. The filtrate was added to the immobilization solution and peristaltically pumped through a sterile bead-making apparatus into hardening solution. Figure 10 illustrates the section of the beadmaker where formation of beads occurred. The bead-making apparatus consisted of feed tubing leading to four 16 gauge syringe needles with flattened tips. Each needle was fitted with concentric tubing to provide a shearing stream of sterile filtered air that decreased bead

size. Beads were approximately 2 mm in diameter. Hardening solution (400 mL) consisted of 0.1 M calcium chloride and 20 g/L sucrose. After 20 minutes, the hardening solution was decanted and replaced with 200 mL of 1-B5 medium. For MFB use, antibiotics/antimycotics were added (50 mg/L ampicillin, 100 mg/L Timentin, and 25 mg/L Benlate). Before addition to the MFB, each batch of fresh biocatalyst was sampled (approximately 10 mL) with a sterile 25 mL wide-mouth pipette for dry weight analysis. The entire process was conducted in a laminar flow hood.

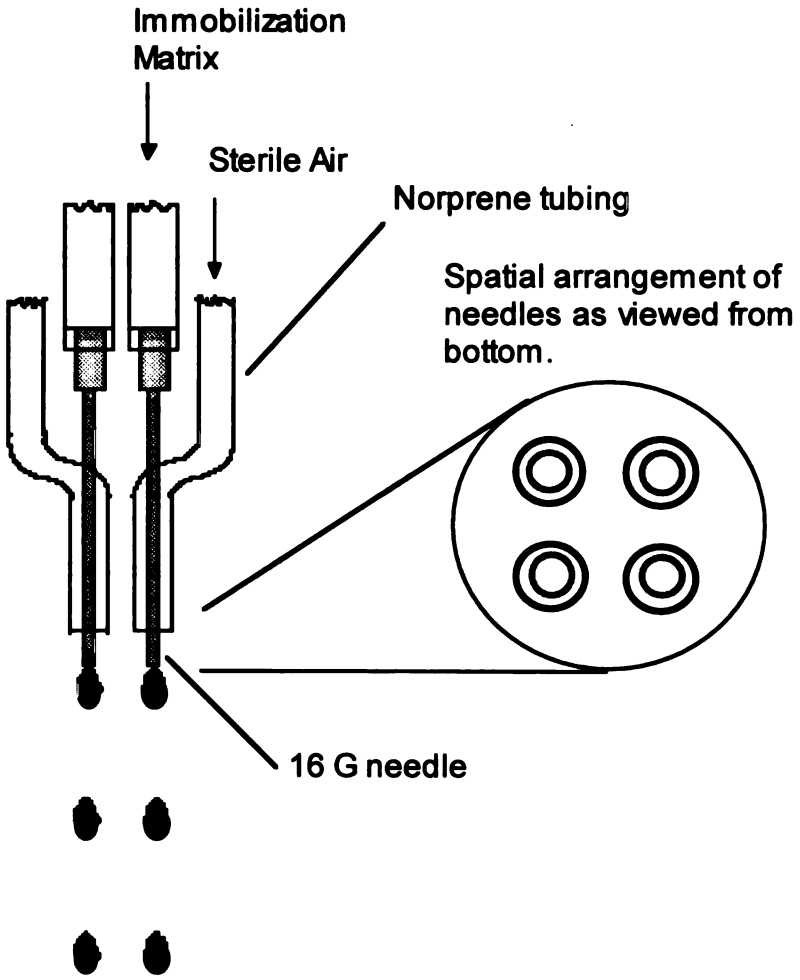

Figure 10. Beadmaker for co-immobilization of soybean and stainless steel.

4.2.7 Cell Recovery

Biocatalyst volume was measured by volume displacement in a 50 mL graduated cylinder. Sample volumes were approximately 10 and 20 mL for feed and product samples respectively. Samples were placed in 125 mL Erlenmeyer flasks with approximately 50 mL of 0.2 M sodium citrate to dissolve the alginate matrix. Flasks were placed on a rotary shaker for 30 minutes at 300 rpm. Suspended cell mass was decanted while stainless steel was retained by placing a magnet on the bottom of the flask. Complete recovery of cell mass was achieved by removing the magnet, adding deionized water to wash the stainless steel, and decanting suspended cell mass with the magnet on the bottom of the flask.

4.2.8 Analytical Procedures

4.2.8.1 Dry Weight

Decanted cell mass was collected by filtering through dried and tared Whatman 41 ashless filter paper using a glass microanalysis filter holder (Fisher, Pittsburgh PA). Samples were dried overnight at 70°C and weighed. Samples immobilized with stainless steel were then ashed in tared, ceramic crucibles over a Bunsen burner, cooled in a desiccator, and weighed. The ash in the crucible was taken as the mass of residual stainless steel which was not separated from the soybean tissue.

4.2.8.2 Biocatalyst Microscopy

Product biocatalyst was sliced to obtain a cross-section from the center of the particle. The cross-sections were examined at 40 times magnification for distribution of

cell mass. Both transmission and dark-field illumination were utilized. Images were acquired by mounting a CCD camera on the microscope.

4.2.8.3 Extraction of Isoflavonoids

Soybean tissue recovered from product biocatalyst was extracted by the following method adapted from Graham (1991). Product biocatalyst was stored frozen until used. Approximately 0.200 g of soybean tissue was extracted twice with 0.4 mL of 80% ethanol (20% water) in a 1.5 mL microfuge tube by grinding with a Teflon microfuge pestle for 5 minutes. Previous testing verified a greater than 95% average recovery of the isoflavonoids using this extraction protocol. The combined extracts were injected directly into the HPLC after centrifugation. Following HPLC analysis of the extracts, a portion of each sample was subjected to a hydrolysis treatment to liberate daidzein and genistein from sugar moiety compounds. In a screw-top test tube, 0.4 mL of sample was combined with 4 mL of 1 N HCl and put in a 100 °C water bath for 1 hour. The hydrolysis mixture was then extracted with 1 mL of ethyl acetate. The ethyl acetate extract was dried at 40°C in a microfuge tube and dissolved in 0.4 mL methanol (ethyl acetate adversely affected chromatograms). The hydrolyzed extracts were analyzed by HPLC in the same manner as raw extracts.

4.2.8.4 Isoflavonoid Analysis

HPLC analysis was performed with gradient programming. Mobile phase A was acetonitrile with 0.5% acetic acid and mobile phase B was water with 0.5% acetic acid. Adjustment of pH with acetic acid significantly reduced band tailing. The gradient linearly increased from 30% A to 45% A over 20 minutes, followed by a 2 minute linear increase

to 90%A, a 10 minute hold, and a 5 minute linear return to 30% A. Retention times were 8.0 and 14.9 minutes for daidzein and genistein respectively. UV absorbance was monitored at 254 nm.

Identities of daidzein and genistein where verified by sample spiking and mass spectrometry. Retention times of daidzein and genistein in the sample matrix were checked by adding standards to soybean extracts. Fractions of the HPLC effluent were collected and analyzed by electrospray mass spectrometry in negative ion mode (M-1). Daidzein and genistein were verified by peaks at 253 and 269 amu, respectively.

4.2.8.5 Respiration

For suspension culture, the entire contents of a 250 mL shake-flask culture were put into the graduated cylinder along with fresh medium to approximately 100 mL total volume. The liquid was then sparged with air for 5 minutes. The oxygen sensor was inserted with care to remove any head space, and the stirring speed was set to give complete mixing in the cylinder. Dissolved oxygen concentration data were collected until a steady value was reached.

For immobilized culture, the apparatus described above was filled with product biocatalyst. The oxygen sensor was inserted, and the remaining volume was filled with deionized water. The pump speed was set to keep the liquid well mixed.

4.2.9 Batch Shake Flask Cultures

Shake flask cultures were conducted to study the effects of immobilization on soybean growth. The study compared suspension culture, cells immobilized in alginate, and cells immobilized in alginate with 25% (w/w) stainless steel. Replicate cultures in 1 L

Erlenmeyer flasks contained 400 mL of 1-B5 medium. Suspension cultures had 30 mL of inoculum while immobilized cultures had 20 mL of inoculum in approximately 200 mL of beads. A common inoculum was used for all flasks to reduce error due to soybean variation. Immobilization followed the procedure described above. Cultures were maintained on an orbital shaker at 125 rpm.

Shake flask cultures were also conducted to study the effects of antimicrobial agents on soybean growth. Effects of ampicillin (100 mg/L), gentamicin (50 mg/L), Timentin (200 mg/L), and Benlate (50 mg/L) were studied in 1 L Erlenmeyer flasks containing 400 mL of 1-B5 medium. A common inoculum (30 mL) was used for all flasks, including two controls.

4.2.10 MFB Operation

4.2.10.1 Start-up

As the entire MFB system was designed to fit in the autoclave, system connections made after autoclaving were minimized. Only the two connections to the column headplate were made post-autoclaving as necessitated by the solenoids. The fresh medium reservoir was also filled prior to autoclaving and did not contain antibiotics/antimycotics. After mounting and final connections were made, the system was filled from the medium reservoir and liquid circulation started. The liquid flow rate was set to approximately 1.6 L/min. Ampicillin, Timentin, and Benlate were added to the circulating medium yielding 50, 100, and 25 mg/L concentrations respectively. The solenoid power supply was set at 2 A, yielding a magnetic field strength of 150-180 gauss depending on position in the column. The column was loaded with immobilized soybean

(feed biocatalyst) in four aliquots over the first three days of operation. Agitation in the Bioflo vessel was set at 250 rpm. Sparging was not started until the dissolved oxygen concentration dropped below 80% of the initial value.

4.2.10.2 Continuous Biocatalyst Processing

At intervals varying from one to several days, product biocatalyst was removed from the bottom of the column, and feed biocatalyst was added to the top. Intervals during the first 12 days were chosen with the goal of demonstrating growth during that period. From day 12 through 34, scheduling obligations resulted in irregular biocatalyst addition/removal. Past day 34, biocatalyst was exchanged roughly every four days. To minimize bed mixing, the liquid flow rate was reduced to 1 L/min before biocatalyst removal operations. The power supply to the solenoids was increased to 3 A. The upper of two pinch clamps on the outlet tubing was opened slightly to allow the length of tubing between the upper and lower pinch clamps to fill with medium from the column. At the same time, air was displaced into the column. Once the tubing was filled with liquid, the upper clamp was completely removed. The magnetic valve was operated by decreasing the solenoid power to 0.6 A which reduced the magnetic interaction between the biocatalyst and screen. The magnetic field strength was approximately 40 Gauss at the magnetic valve. Squeezing the outlet tubing induced the biocatalyst to fall through the stainless steel screen into the region of the column above the fluidization mesh. Once entering this region of free movement, the biocatalyst fell through the center opening in the baseplate. No mixing in the bed was observed due to the stabilization afforded by the 50-60 gauss magnetic field in the column.

After the desired quantity of beads had passed through the screen, the solenoid power was returned to 3 A. While the greater portion of the released biocatalyst fell through the outlet hole in the baseplate, the remainder which came to rest on the fluidization mesh was removed by briefly increasing the liquid flow rate to 3 L/min. Once all the biocatalyst was in the outlet tubing, the liquid flow rate was returned to 1.6 L/min. The bottom clamp was then removed, releasing the biocatalyst into the product reservoir. The bottom clamp was replaced, and the process repeated once more, resulting in 150-200 mL of biocatalyst in the reservoir. Following biocatalyst removal, additional medium was drained into the product reservoir making room for addition of fresh medium. The solenoid power was returned to 2.0 A. The final step in removal was a aseptic exchange of the full biocatalyst reservoir with an empty one.

After product biocatalyst was removed, feed biocatalyst was added using a similar pinch-clamp technique. Freshly prepared biocatalyst and medium were added to the feed biocatalyst reservoir. The upper of two pinch clamps was removed allowing fresh medium and biocatalyst to fill the inlet tubing. Repeated squeezing of the tubing facilitated movement of solids from the reservoir to the tubing, displacing the liquid. Once the tubing was full of biocatalyst, the top pinch clamp was replaced and the bottom pinch clamp removed allowing the biocatalyst to enter the column through the headplate. The bottom clamp was replaced and the process repeated until all biocatalyst was removed from the reservoir (4-5 times). Fresh medium was then added (approximately 200 mL) by releasing the pinch clamps. The pinch clamps were then replaced, completing the removal/addition process.

Aseptic conditions during continuous operation were verified by periodically inoculating a rich medium (LB broth) with MFB medium from the product reservoir. Both LB agar in petri dishes and LB medium in 125 mL Erlenmeyer shake flask cultures were employed. Shake flasks were incubated at room temperature while petri dishes were incubated at both room temperature and 30°C for a minimum of two weeks.

4.2.11 Theoretical

4.2.11.1 Specific Growth Rates

Growth rates during continuous operation were estimated from residence times and cell densities in the feed and product biocatalyst. For exponential growth, the average specific growth rate (μ) is described by

$$\mu = \frac{\ln\left(\frac{X}{X_0}\right)}{\tau} \qquad (1)$$

where τ is the biocatalyst residence time, and X and X_0 are the soybean concentrations in the product and feed biocatalyst, respectively. Residence times were calculated from the known volumes and times of biocatalyst addition and removal, assuming plug flow of the solid phase. Uncertainty in residence times stems from error in measurement of biocatalyst volume added and removed as well as any mixing which may have occurred in the column. As error in residence time calculations may lead to erroneous pairing of X and X_0 values, feed biocatalyst cell densities (X_0) were taken as the averaged value over the entire run.

4.2.11.2 Thiele Modulus Calculations

The possibility of oxygen diffusion within the biocatalyst limiting the overall reaction rate was assessed with Thiele modulus calculations. An observable modulus (Φ) has been described by Bailey and Ollis (1986) for Michaelis-Menten kinetics which does not require knowledge of intrinsic-rate parameters:

$$\Phi = \frac{\upsilon_0}{D_s s_0}\left(\frac{V_p}{A_p}\right)^2 \qquad (2)$$

where υ_0 is the observed volumetric reaction rate, D_s is the diffusion coefficient of substrate in the biocatalyst, s_0 is the bulk substrate concentration, V_p is the biocatalyst volume, and A_p is the biocatalyst surface area. For observable modulus calculations, immobilized-soybean respiration rates were measured as described above. Volume and area parameters assumed a 2 mm diameter sphere. An oxygen diffusion coefficient of 1.91 x 10^{-5} cm^2/sec was calculated by multiplying the diffusion coefficient in water at 25°C (Perry and Green, 1984) by correction factors of 0.85 for 2% calcium alginate gel (Westrin and Axelsson, 1991) and 0.9 for 25% w/w magnetite (Thompson, 1993). The second correction factor assumes the effects of magnetite and stainless steel at 25% w/w on the effective diffusion coefficient to be equal. The bulk oxygen concentration at 25°C was taken to be 8.43 mg/L (Bailey and Ollis, 1986).

The possibility of oxygen diffusion limitations within individual soybean aggregates was assessed with the generalized modulus:

$$\phi = \frac{V_p}{A_p}\sqrt{\frac{n+1}{2}\frac{k_v C_s^{n-1}}{D_e}} \qquad (3)$$

where k_v is the intrinsic rate constant, C_s is the bulk substrate concentration, D_e is the effective diffusivity, and n is the reaction order (Froment and Bischoff, 1979). The intrinsic respiration rate was assumed to be that of suspension cultures, and measured as described above. The effective diffusivity was taken as 2% of the value for oxygen in water (Ananta *et al.*, 1995). Respiration rates measured on a mass basis were translated to a volumetric basis assuming a cell density of 1.02 g/mL (Ananta *et al.*, 1995) and a dry weight to fresh weight ratio of 0.07 g/g (unpublished data).

4.3 Results and Discussion

4.3.1 Batch Shake Flask Cultures

4.3.1.1 Immobilization

Specific growth rates for suspension (control), alginate immobilized, and alginate/stainless steel immobilized cultures were 0.35±0.01, 0.21±0.08, and 0.26±0.06 day^{-1} respectively. All cultures exhibited exponential growth with r^2 values ranging from 0.977 to 0.999 for fitted exponential curves. Figure 11 shows the results for replicate, alginate immobilized cultures. Batch shake flask cultures indicated immobilization slows soybean growth. Immobilization with stainless steel reduced the growth rate by about 25% compared to suspension culture. However, the addition of stainless steel in the immobilization matrix did not further hinder growth compared to alginate only. While the average specific growth rate for stainless steel cultures was higher than for alginate only, the difference was not statistically significant at the 95% confidence level.

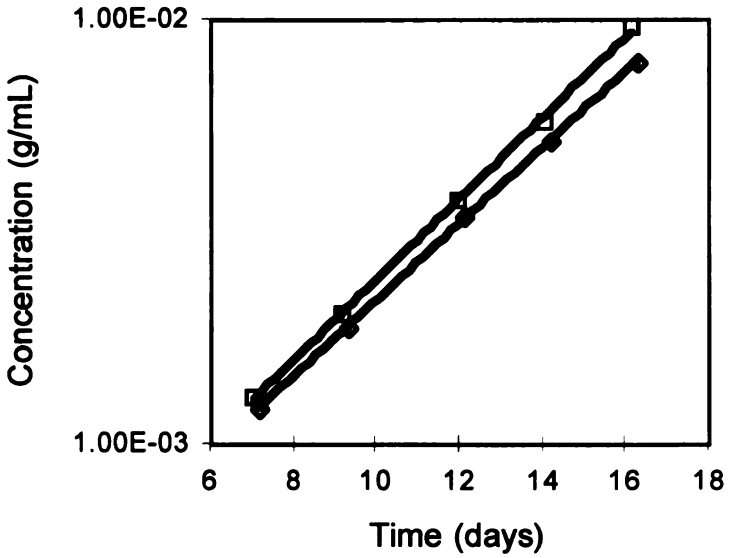

Figure 11. Immobilized soybean cell densities for replicate shake flasks.

Three aspects of the immobilization protocol merit discussion. First, this work used ferritic stainless steel, a novel material for creating a magnetically susceptible biocatalyst, in place of magnetite. The stainless steel powder chosen for this work offers several advantages over magnetite including a higher magnetic permeability, inherent biological inertness, and easier separation from dissolved immobilization matrix due to increased particle size and density. Stainless steel concentrations employed in this study were much higher than magnetite concentrations reported previously (Bramble *et al.*, 1990), and considered realistic for stable bed operation with continuous solids throughput.

Second, the use of concentric air streams to shear immobilization matrix droplets from needles was valuable in maintaining a small biocatalyst diameter. The use of concentric, shearing air reduced bead diameters by roughly 50%. Smaller diameters reduce diffusional mass transfer limitations. The minimum size is limited, however, by the

relatively large size of suspension culture aggregates. In order to utilize the majority of a 2 week-old culture for inoculum, a 1 mm screen was used. This mesh size sets the minimum practical needle size at about 16 gauge.

Third, experimental evidence suggests that stainless steel became entrapped within soybean aggregates as they grew. While separating soybean cells released from the alginate matrix from stainless steel, some soybean aggregates appeared to be drawn to the magnet. Tissue resting on the side of a flask could be moved with a magnet. It was unclear however, if the movement was due to entrapped metal or the presence of metal around the aggregates. Examination at 100 times magnification showed steel particles on or in the aggregates (results not shown). Again, a clear distinction could not be made. Finally, complete separation of soybean cells and stainless steel was not achieved following dissolution of the alginate, as determined by ashing of dry weight samples. Due to the density of stainless steel, it was necessary to account for the mass of steel when determining cell dry weights.

4.3.1.2 Antimicrobial Agents

Table 3 lists the antibiotic-antimycotic compounds tested, concentrations used and resulting specific growth rates. Of the four agents tested, three were found to have limited toxicity at concentrations useful in inhibiting microbial growth. Only gentamicin was found to be completely toxic to plant cells at the tested concentration. The remaining compounds offer a broad spectrum cocktail to prevent contamination during extended, continuous bioreactor operation. Ampicillin is a broad range antibiotic effective mainly against Gram positive bacteria (Pollock *et al.*, 1983). Timentin contains ticarcillin,

effective against Gram positive and negative bacteria, as well as clavulanic acid, an anti-betalactamase. Timentin therefore bolsters the stability of ampicillin. Benlate is a broad spectrum antifungal agent (Brown *et al.*, 1982).

Table 3. Antibiotics successfully tested with soybean cell culture.

Agent	mg/L	Specific Growth Rate (day^{-1})
Control	-	0.40±0.13
Ampicillin	100	0.37
Benlate	50	0.32
Timentin	200	0.31
Gentamicin	50	no growth

4.3.2 Asepsis Testing

Trial runs of the MFB were conducted to verify aseptic operation. Initially, the column and endplates assembly was partially filled with LB medium, sealed, and autoclaved. No microbial growth was apparent after 8 days at room temperature. The complete MFB system was then tested including liquid circulation and air sparging using LB medium. Asepsis was verified by plating of medium on LB agar after 4 and 6 days of operation. A final trial run was made to verify that biocatalyst could be added and removed from the system aseptically. Alginate beads containing 25% stainless steel were added/removed four times over 24 days without contamination as verified by LB plating of the medium. No antimicrobial agents were used in asepsis testing.

4.3.3 Continuous Operation

4.3.3.1 Soybean Growth

Continuous operation of the MFB utilizing immobilized soybean culture was accomplished during a 62 day run. No evidence of contamination was seen on LB petri dishes or shake flasks. The product biocatalyst loadings are shown as a function of time in Figure 12. Over the first two weeks, the goal of operation was demonstration of soybean growth in the MFB system. Residence times were therefore kept short, and process monitoring was limited to product biocatalyst cell densities and dissolved oxygen concentrations. Figure 12 shows that cell densities increased over the first 12 days, in part due to increasing residence times during start-up. The limited oxygen demand was met by sparging the liquid each day until the dissolved oxygen level returned to the air saturation level.

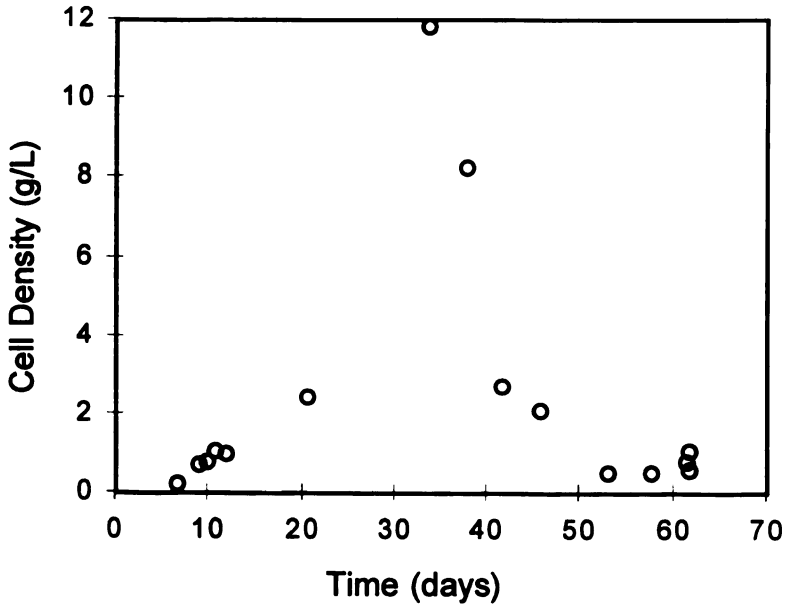

Figure 12. Product biocatalyst loading as dry weight per biocatalyst volume.

Following start-up was a period of irregular biocatalyst addition/removal. During this time, residence times were increased, and additional monitoring methods were developed. Daily (periodic) sparging was replaced with continuous, peristaltic-pump addition of oxygen to the Bioflo vessel to match the increased oxygen uptake. As seen in Figure 12, only two product biocatalyst aliquots were removed between days 12 and 34. Soybean concentration in the product biocatalyst peaked at day 34. The significant decrease in growth after day 34 is likely explained by two experimental problems that are described below.

On day 30, agitation in the Bioflo vessel ceased due to bearing failure. Gas-liquid mass transfer was therefore hindered for the remainder of the experiment. Within three days after agitation ceased, dissolved oxygen levels dropped considerably below air saturation levels. An effort to counter decreasing oxygen levels was made by gradually increasing oxygen feed to the Bioflo vessel. However, dissolved oxygen levels continued to drop through day 45 while head space analysis indicated oxygen levels well above ambient conditions (results not shown). During the same time, product biocatalyst loadings in the MFB decreased significantly. These results support the hypothesis that loss of agitation resulted in poor gas-liquid mass transfer, depletion of oxygen in the medium, and poor soybean growth.

A second cause of poor growth after day 34 may be dilution of endogenous growth factors (Bramble *et al.*, 1990). During biocatalyst removal on day 34, the soybean culture was found to be growing out of the biocatalyst at the bottom of the MFB. Some biocatalyst particles were connected by plant tissue, making the removal procedure

difficult. Growth outside of the immobilization matrix also resulted in high medium turbidity. Between days 34 and 38, 2.4 L out of the approximately 3 L working liquid volume was exchanged with fresh medium to counter this problem. While soybean growth in the liquid phase was avoided, dilution of important plant hormones may have reduced growth rates.

Figure 13 shows specific growth rates as a function of time. Growth rates mirror product biocatalyst densities as expected. With caution regarding uncertainties in residence time calculations, the MFB growth rates can be compared to batch shake flask cultures of immobilized soybean. The peak MFB value of 0.17 day^{-1} compares well to the shake flask value of 0.26 day^{-1}. The average MFB growth rate is roughly one-third of that in shake flask culture. Furthermore, at least part of the lower growth rates can be explained by stress due to the antibiotic cocktail used in the MFB, as illustrated by batch shake flask studies. Growth rates fell to their lowest values after day 50, but showed a rebound in the biocatalyst removed on the last day of operation.

4.3.3.2 Respiration and Oxygen Diffusion

Thiele modulus calculations suggested that soybean respiration was not rate limited by oxygen diffusion in the biocatalyst. In all respiration measurements, the oxygen-uptake rates were found to be independent of dissolved oxygen concentration. The respiration rate of soybean in MFB product biocatalyst was measured at 8.9 mg O_2/g cells-hr. The observed volumetric rate was 2.9×10^{-9} g O_2/mL biocatalyst-sec yielding an observable modulus of 0.02. A graphical solution of η as a function of Φ is available for Michaelis-Menten kinetics in the zero-order regime (Bailey and Ollis, 1986). The

resulting effectiveness factor of 1.0 indicates that oxygen diffusion within the biocatalyst is not rate limiting. The immobilized cell respiration rate was roughly one-third of that for suspension culture in exponential growth phase, 28 mg O_2/g cells-hr. The difference is consistent with the growth rate of the immobilized culture being approximately 0.1 day^{-1} (roughly one-third of suspension culture). Furthermore, the immobilized soybean residence time was approximately 16 days. The respiration rate of a post-exponential phase suspension culture (19 days old) was 8.7 mg O_2/g cells-hr, which is very close to that of the immobilized soybean culture.

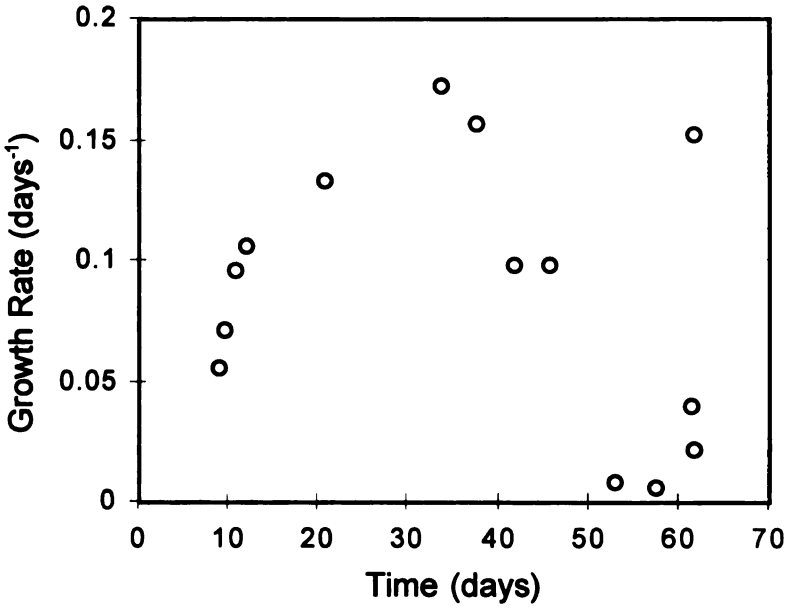

Figure 13. Soybean specific growth rates in the MFB.

Microscopy of product biocatalyst cross-sections supported the idea that oxygen diffusion was not rate limiting. Typical pictures of biocatalyst cross-sections are shown in Figure 14. Figure 14a shows the dark-field image of a bead with soybean aggregates appearing as lighter regions. Figure 14b shows the same bead under transmission

illumination with soybean appearing as darker regions in the center, and stainless steel preventing passage of light around edges. Figure 14c shows a different bead with three dark regions of soybean, illustrating larger aggregate sizes. No radial dependence of cell concentration was observed in the biocatalyst. Soybean aggregates appeared to be randomly distributed throughout the biocatalyst, as opposed to preferentially located near the biocatalyst surface. The latter trend was observed by Bramble *et al.* (1990) with *C. arabica* in 3-4 mm alginate beads. Images from days 38, 42, and 62 showed soybean aggregates to be large relative to suspension culture. Aggregates up to 1 mm across were seen, with aggregates from 0.1 to 0.5 mm being most common. The general observation of large and dispersed aggregates may be explained by immobilization technique and hormone dependent growth. Large aggregates are expected to develop from inoculum aggregates which are above some minimum size. Growth of such aggregates may be explained by the feeder and dividing aggregate model proposed by Shuler (1981). Thus, aggregates which started large may continue increasing in size while smaller ones grow poorly or not at all. Poorly growing aggregates may however, be bolstered if they are surrounded or engulfed by rapidly growing large aggregates. Furthermore, the somewhat dispersed nature of the soybean in the biocatalyst suggests that higher inoculation densities would provide higher final densities for a given residence time. Higher inoculation densities could reduce the void volume observed in the cross-section images.

While intrabiocatalyst oxygen diffusion does not appear to be rate limiting, oxygen diffusion within soybean aggregates may be important. Modulus values for typically observed aggregates (0.1 to 0.5 mm diameter) range from 0.5 to 2.3. Based on a modulus

of 1.0, rate limitation due to oxygen diffusion would be expected for aggregates larger than 0.2 mm. For zero order kinetics where ϕ is greater than unity, η is equal to ϕ^{-1} (Froment and Bischoff, 1979). The effectiveness factor for 0.5 mm aggregates is therefore 0.4. For the largest aggregates observed (roughly 1 mm), the calculated effectiveness factor is 0.2. These results indicate that soybean aggregates may become diffusion limited as they move through the MFB. However, Ananta *et al.* (1995) found that experimental results do not agree with Thiele modulus calculations. Aggregates ranging from 3.0 to 12.5 mm in diameter were capable of active growth and respiration with retention of cell viability in at least 90% of the particle; observed specific oxygen uptake rates were within the range normally associated with plant cell suspensions. It is therefore unclear whether oxygen diffusion limits growth rates inside soybean aggregates.

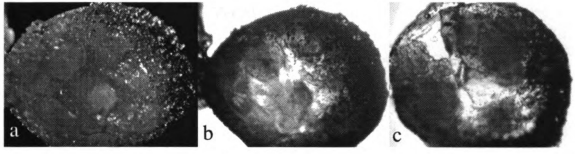

Figure 14. Product biocatalyst cross-sections at 40 times magnification.

4.3.3.3 Isoflavonoid Production

Daidzein and genistein were produced during the entire run with concentrations ranging from approximately 10 to 200 μg per gram of dry soybean tissue. The daidzein and genistein concentrations are shown as a function of time in Figure 15. The data are for hydrolyzed extracts, representing the total genistein or daidzein found in the soybean as

both free isoflavonoid and isoflavonoid with moieties. Acid hydrolyzed extracts averaged nearly 2.9 and 1.5 times the amount of daidzein and genistein respectively in raw extracts. Thus nearly two-thirds of the daidzein and one-third of the genistein exists with sugar moieties. The extraction protocol was also tested using two week-old soybean suspension cultures, providing isoflavonoid concentrations for comparison. Concentrations were 340 ± 50 ppm and 560 ± 160 ppm at a 95% confidence level for daidzein and genistein respectively. Daidzein concentrations in the MFB reached over one-half the average suspension culture level. Genistein concentrations reached nearly one-fifth the average suspension culture level. While peak isoflavonoid levels in the MFB were significantly below suspension culture values, the results are for the first continuous run attempted. Improved operating procedures and process control can reasonably be expected to raise the product concentrations considerably.

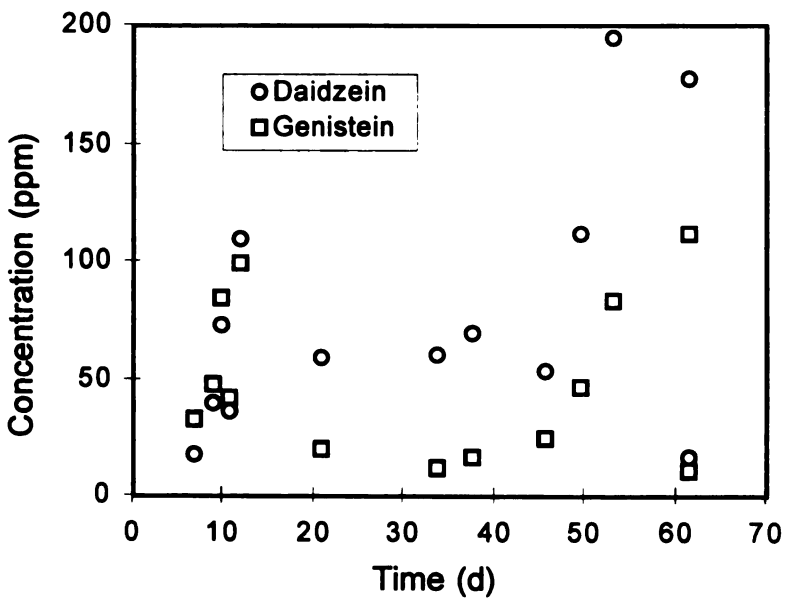

Figure 15. Isoflavonoid content of product soybean as mass per dry tissue.

4.3.4 System Improvements

The two month, continuous run demonstrated the feasibility of continuous production of plant secondary metabolites in an MFB. It also identified potential improvements in the experimental protocols that could yield steady-state operation. The ability to maintain steady-state growth and product accumulation is a likely prerequisite for further development toward a commercial process.

Automatic control of the dissolved oxygen concentration would help provide steady conditions for the plant cells. A gas recycle loop would be able to maintain good mass transfer between the gas and liquid while minimizing stripping of volatiles that may regulate the cellular metabolism. A controller could be used to adjust the total gas flow rate (fresh air) to match the oxygen demand. A high recycle gas flow rate and impeller speed should be able to maintain a high gas-liquid mass transfer coefficient independent of the total gas flow rate. This scheme would avoid volatiles stripping by excessive total gas flow rates typically used to maintain reasonable gas-liquid mass transfer.

In previous operation, liquid medium was added/removed along with biocatalyst addition/removal. For tighter control of net medium flow, fresh medium could be continually added to the mixing vessel, and removed via gravity through an overflow port. Improved solids metering during addition and removal could be achieved by use of graduated tubing for biocatalyst volume measurements. Evacuation of air from the biocatalyst outlet tubing should avoid large air bubbles rising through and disrupting the bed. Improved metering and decreased bed mixing would in turn lead to tighter residence time control.

4.4 Conclusions

Continuous isoflavonoid production from soybean with biocatalyst throughput has been demonstrated in a MFB bioreactor for over 2 months. Immobilization of soybean cell culture in alginate with stainless steel reduced the specific growth rate about 25% relative to suspension culture. Soybean growth rates and product concentrations were lower in the MFB than batch suspension cultures. Genistein and daidzein production ranged from 10 to 200 μg per gram of dry soybean tissue. Hydrolysis of bound daidzein and genistein was found to be important for product recovery. Both Thiele modulus calculations and biocatalyst microscopy suggested that intra-biocatalyst oxygen diffusion was not rate limiting. Ampicillin, Timentin, and Benlate had limited phytotoxicity at concentrations useful in preventing contamination during long, continuous bioreactor operation.

5. PROTOCOL AND MODELING FOR LONG-TERM MFB OPERATION

5.1 Introduction

Several reactor schemes are available for plant cell cultures, including stirred tanks, bubble columns, air-lift reactors, hollow-fiber membranes, liquid-dispersed trickle and incline reactors (van Gulik *et al.*, 1994; Reinhard, 1989; Panda *et al.*, 1989; Andrews, 1988). Each of these reactors is subject to trade-offs in advantages such as simplicity or effective mass transfer, and limitations such as shearing of cells, insufficient mixing at high cell densities, settling of cells, and difficulty in scale-up (Panda *et al.*, 1989). Bioreactor design also requires consideration of characteristics unique to plant cell culture including the importance of medium conditioning (Bramble *et al.*, 1990), dissolved gaseous metabolites (Schlatmann *et al.*, 1997), and difficulty in intracellular product recovery (Brodelius, 1990).

The magnetofluidized bed (MFB) bioreactor addresses several of the important issues for a plant-cell bioprocess. This bioreactor scheme was first introduced in a batch mode by Bramble *et al.* (1990). The authors co-immobilized *Coffea arabica* cells with magnetite in calcium-alginate beads. These beads comprised the solid phase of a two-phase bed, where solids mixing was prevented by a DC magnetic field. Continuous solids throughput in a similar system was achieved by Ames and Worden (1997) in a 2 month run. The residence time of immobilized soybean cell culture was tightly controlled independent of medium residence time. The need for permeabilization was avoided by extracting soybean tissue for isoflavonoids after harvesting from the reactor.

While the MFB has been demonstrated for continuous production of intracellular metabolites from plant cell culture, a framework for establishing operational protocols has not yet been developed. This work couples plant cell metabolism and bioreactor characteristics of the MFB system. The MFB has been operated using soybean cell culture, with the goal of understanding steady-state operation. The system has been described with appropriate mass balances, an unstructured metabolic model, and metabolic parameters drawn primarily from the literature.

5.2 Materials and Methods

5.2.1 Chemicals

Chemicals used for culture medium, immobilization, and analytical work have been reported in Section 4.

5.2.2 MFB System

The MFB system used in this work is illustrated in Figure 16. Details of the material and construction for the fluidized bed, reservoirs, and mixing vessel (Bioflo II, New Brunswick, Edison, NJ) have been reported in Section 4. Modifications to the original system included a gas phase recycle loop, dissolved oxygen control, a vacuum port on the biocatalyst outlet tubing, and drain lines from the feed biocatalyst reservoir and mixing vessel (see Figure 16). The gas phase recycle loop provided medium sparging independent of the feed gas flow rate. Gas was recirculated from the head space through the liquid return line to a fritted glass sparger via a peristaltic pump (Cole Parmer, Chicago). Head space samples were taken from this recirculation loop. The dissolved oxygen control loop consisted of an Ingold O_2 sensor (12 mm dia.) with Model 170

oxygen amplifier (Mettler-Toledo, Wilmington, MA), an IBM XT with a DT2801 analog and digital I/O board (Data Translation, Marlboro, MA) running Labtech Notebook (Laboratory Technologies Corporation, Wilmington, MA), and a peristaltic pump (Cole Parmer). The pump was fitted with two heads for 7.9 and 1.6 mm inside diameter tubing for air and oxygen, respectively. The outlet pressures for the air and oxygen cylinders were regulated at 35 kPa. The port added for vacuum provided removal of air in the biocatalyst outlet tubing which would otherwise rise through the magnetofluidized bed, potentially disrupting the particles. The drain from the feed biocatalyst reservoir was used to remove medium which was not used in transfer of biocatalyst into the column. The drain line from the mixing vessel maintained constant medium volume by overflow. The system required only two connections at the column headplate to be made post-autoclaving.

5.2.3 Soybean Culture and Medium

Soybean suspension cultures were *Glycine max* cv. Mandarin (Section 4). The liquid medium was Gamborg B5 supplemented with 1.0 mg/L 2,4-dichlorophenoxyacetic acid (2,4-D), 0.15 mg/L kinetin, 50 mg/L ampicillin, 100 mg/L Timentin, and 25 mg/L Benlate.

5.2.4 Batch Shake Flask Cultures

Shake flask cultures were conducted to study the effects of the antibiotic/antimycotic cocktail on isoflavonoid production. The study compared the medium described above to a control medium which contained no ampicillin, Timentin or Benlate. Replicate cultures in 1 L Erlenmeyer flasks contained 400 mL of medium and 30

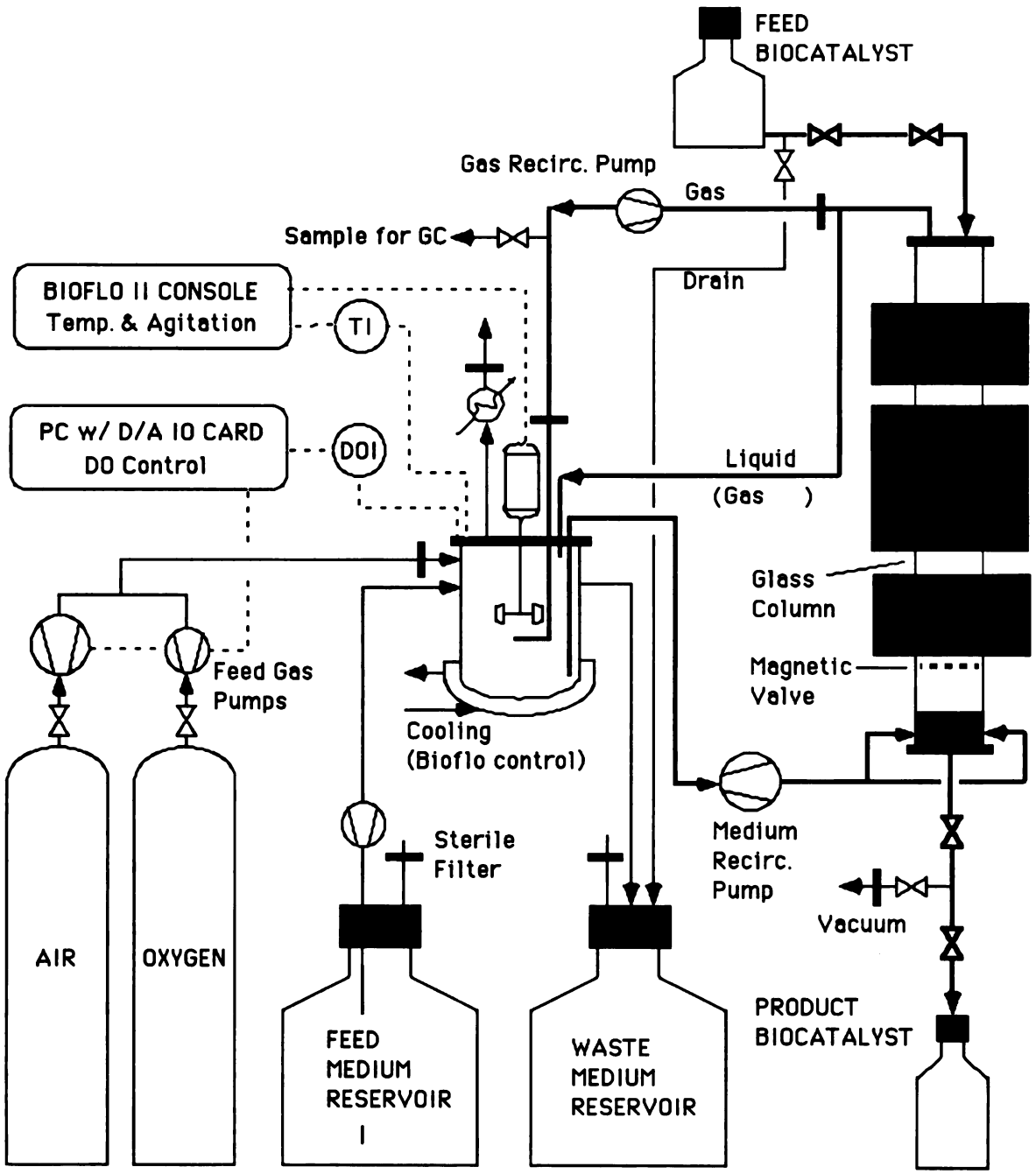

Figure 16. Diagram of the magnetofluidized bed bioreactor system.

mL of inoculum. A common inoculum was used for all flasks to reduce error due to soybean variation. Cultures were maintained on an orbital shaker at 125 rpm.

5.2.5 Analytical

Isoflavonoid assays based on the method of Graham (1991), and respiration measurements of suspension and immobilized culture have been reported elsewhere (Section 4). Sugar assays were conducted using high performance liquid chromatography (HPLC). A Waters (Milford, MA) 600 multisolvent pump, a 25 cm by 4.6 mm Supelco (Bellefonte, PA) LC-NH_2 column, and a Waters 410 differential refractometer comprised the system. Gas chromatography of the MFB head space was performed on a Perkin Elmer (Norwalk, CT) Autosystem Gas Chromatograph with a thermal conductivity detector. Fixed gases were separated on a 9.1 m by 2.2 mm Hayesep DB 100/120 SS column (Alltech) with helium as the mobile phase.

5.2.6 MFB Operation

The MFB biocatalyst (2 mm diameter) was 1-B5 medium with 2% medium-viscosity sodium alginate, 25% (w/w) stainless steel powder, and 30% (v/v) soybean inoculum. The details of soybean immobilization and recovery, and control of biocatalyst movement through the column using a magnetic valve for solids (MVS) have been reported previously (Section 4). Some aspects of the protocol including flow rates, biocatalyst exchange intervals, and use of dissolved oxygen control were modified. The volume of biocatalyst exchanged was metered by gradations on inlet and outlet tubing, allowing precise control of residence time. Average biocatalyst volumes exchanged (or "plugs") were around 150 mL. Change in bead volume was assumed to be negligible. The

21 and 27 day MFB runs reported in this work employed both variable and constant residence times, respectively. Biocatalyst was added to the latter every third day. Biocatalyst was removed starting on the ninth day yielding three plugs of biocatalyst in the column at all times once loaded.

The dissolved oxygen control loop was designed to maintain both dissolved oxygen (DO) and head space CO_2 near target levels. A respiration rate and gas to liquid mass transfer coefficient estimated from previous work were used in simplified versions of model equations described below. Target levels of 80% DO and 5% CO_2 were arbitrarily chosen based on a measured shake flask concentration of 5.5% after 2 weeks of growth, and literature values for shake flasks reaching 10% or more (Lee and Shuler, 1991). The mass balances yielded the percent oxygen required in the gas feed. Peristaltic pump tubing diameters for air and oxygen were chosen to most closely match the desired level of air enrichment. Rigorous control strategies have been published which maintain oxygen and carbon dioxide at their set points regardless of respiration rate (Smith *et al.*, 1990). However, the strategy used here utilized available equipment and afforded the simplicity of a single control loop.

5.3 Model

5.3.1 Scope and General Assumptions

The MFB system was conceptually modeled as three physical phases: solid biocatalyst, liquid medium, and gas head space. The gas phase was well mixed as its recycle rate was much greater than the feed. The solid phase was treated as three separate plugs, as each plug of biocatalyst in the column had a different age. Components of these

phases included in the model were cell mass, sucrose, glucose, oxygen, and carbon dioxide. General assumptions made in model development are listed as follows:

1. No mixing between plugs of biocatalyst.
2. Homogeneously distributed cell mass throughout the solid (biocatalyst) phase.
3. Well mixed liquid phase.
4. Rate limiting mass transfer step at the gas-liquid interface in transport of oxygen and carbon dioxide between the head space and plant cells.
5. Rate limiting cellular metabolism step in uptake of glucose and hydrolysis of sucrose.

Assumptions 1 and 2 were based on prior work which reported minimal solids mixing and a uniform distribution of soybean cell aggregates throughout the biocatalyst (Section 4). Therefore, the model does not include a radial dependence of cell concentration within the alginate spheres. An alternative assumption would have been the treatment of soybean and immobilization matrix as separate phases. However, the alternative treatment did not have value-added benefit as the measurements and information needed to effectively use a two-phase (soybean and alginate matrix) model were outside the scope of this work.

Assumption 3 requires that the dissolved oxygen is not significantly depleted across the length of the column. For steady-state and no liquid-solid mass transfer resistance, the dissolved oxygen concentration (O_l) is a function of vertical distance (z) as described by Equation (4)

$$v_z \frac{dO_l}{dz} = -\frac{1-\varepsilon}{\varepsilon} Q \qquad (4)$$

where v_z is the liquid velocity in the z direction, Q is the volumetric oxygen consumption rate in the solid phase, and ε is the void fraction in the column. For a velocity of 3.5 cm/s, a biocatalyst height of 40 cm, a respiration rate of 28 mg O_2/g cells-hr (Section 4), and an average cell density of 3.0 g/L, the dissolved oxygen would be depleted by only 4.7% across the length of the column for pre-saturation with air.

Assumptions 4 and 5 rely on the diffusion of dissolved substrates in the biocatalyst not being rate limiting. This assumption was justified by both the biocatalyst microscopy mentioned above, and Thiele modulus calculations presented in Section 4. Thiele modulus calculations also indicate that diffusion of sugars is not rate limiting. While sugar diffusion coefficients are somewhat lower than oxygen, bulk sugar concentrations are orders of magnitude higher than oxygen.

5.3.2 Mathematical Development

The cell balance given in Equation (5) for each solid-phase plug assumes exponential growth, and no loss of viability during the short residence time in the MFB.

$$\frac{dX_i}{dt} = \mu X_i \qquad (5)$$

The specific growth rate is described by Monod kinetics as a function of glucose. Other authors have used Monod kinetics dependent on glucose (van Gulik *et al.*, 1992), sucrose (Guardiola *et al.*, 1995), and internal glucose (Westgate *et al.*, 1991). Applying assumption 5 above, solid and liquid phase sugar concentrations are equal and Equation (5) can be written in terms of the liquid phase glucose concentration.

$$\mu = \mu_{max}\left(\frac{G_l}{K_G + G_l}\right)\phi \qquad (6)$$

In addition to carbon and energy source, the growth rate was also assumed to be a function of dissolved oxygen and dissolved carbon dioxide concentrations as defined by Equation (7).

$$\phi = \left(\frac{O_l}{K_O + O_l}\right)\left(\frac{C_l}{K_C + C_l}\right) \qquad (7)$$

Carbon dioxide was incorporated into the growth expression in order to account for DGM, as it was readily measured and represents the major component of DGM (Schlatmann *et al.*, 1997). While both the dependence (Archambault, 1991; Maurel and Pareilleux, 1985) and independence (Kim *et al.*, 1991; van Gulik *et al.*, 1994) of growth rates on CO_2 concentration have been reported, other DGM components which may affect growth rates would be accounted for by the model.

The balance for sucrose in each of the 3 solid phases is described by Equation (8)

$$\frac{dS_{b,j}}{dt} = Q_S - k_{hyd} \cdot X_i \cdot V_{b,j}\left(\frac{S_{b,j}}{K_{hyd} + S_{b,j}}\right) \qquad (8)$$

where sucrose is consumed by extracellular hydrolysis and replenished by the liquid medium. Sucrose is hydrolyzed by cell wall invertases (Fowler, 1982) and has been previously described with Michaelis-Menten kinetics (Hooker and Lee, 1992). Equation (9) is the liquid phase balance for sucrose which includes the net liquid flow through the system and loses to the biocatalyst.

$$\frac{dS_l}{dt} = F_l\left(S_{l,0} - S_l\right) - Q_S \qquad (9)$$

Combining Equations (8) and (9) yields Equation (10).

$$\frac{dS_l}{dt}V_l = F_l\left(S_{l,0} - S_l\right) - \sum_i \left(\frac{dS_{b,i}}{dt}V_{b,i} - k_{hyd}X_iV_{b,i}\left(\frac{S_{b,i}}{K_{hyd} + S_{b,i}}\right)\right) \qquad (10)$$

However, the assumption of negligible rate limitations for liquid-solid mass transfer (assumption 5 above) makes all liquid and solid phase concentrations equal. This allows rearrangement of Equation (10) to Equation (11) and elimination of the solid phase sucrose concentration variable.

$$\frac{dS_l}{dt}\left(V_l + \sum_i V_{b,i}\right) = F_l\left(S_{l,0} - S_l\right) - k_{hyd}\left(\frac{S_l}{K_{hyd} + S_l}\right)\sum_i X_iV_{b,i} \qquad (11)$$

The glucose balance in each solid phase is given by Equation (12)

$$\frac{dG_{b,i}}{dt}V_{b,i} = Q_G + k_{hyd}Y_{GS}X_iV_{b,i}\left(\frac{S_l}{K_{hyd} + S_l}\right) - q_G \qquad (12)$$

which includes transfer from the liquid, generation from hydrolysis, and uptake by the plant cells. Glucose is consumed for growth and maintenance as defined by Equation (13)

$$q_G = \left(\frac{\mu}{Y_{XG}} + m_G\phi\right)X_iV_{b,i} \qquad (13)$$

which includes a dependence for maintenance consumption on dissolved oxygen and carbon dioxide concentrations. Equation (14) is the liquid phase balance for glucose

$$\frac{dG_l}{dt}V_l = F_l\left(G_{l,0} - G_l\right) - Q_G \qquad (14)$$

which includes the net flow of medium through the system and loss of glucose to the biocatalyst. As with sucrose, Equations (13) and (14) can be combined into a single balance described by Equation (15).

$$\frac{dG_l}{dt}\left(V_l + \sum_i V_{b,i}\right) = F_l\left(G_{l,0} - G_l\right) + \left[k_{hyd} Y_{GS} \frac{S_l}{K_{hyd} + S_l} - \frac{\mu}{Y_{XG}} - m_G \phi\right] \sum_i \left(X_i V_{b,i}\right) \qquad (15)$$

A combined balance for oxygen, Equation (16), can be written by combining the liquid and solid phase balances as done with sucrose and glucose.

$$\frac{dO_l}{dt}\left(V_l + \sum_i V_{b,i}\right) = k_L a\left(\frac{O_g}{H_O} - O_l\right) V_l - \left[Y_{OX}\mu + m_O \phi\right] \sum_i \left(X_i V_{b,i}\right) \qquad (16)$$

Equation (16) includes transfer of oxygen from the gas phase and consumption by the plant cells for growth and maintenance. The gas phase balance for oxygen is given in Equation (17)

$$\frac{dO_g}{dt} V_g = F_g\left(O_{g,0} - O_g\right) - k_L a\left(\frac{O_g}{H_O} - O_l\right) V_l + k_{p,O} a\left(O_a - O_g\right) \qquad (17)$$

which includes the net flow of gas through the system, transfer of oxygen to the liquid phase, and transfer of oxygen due to permeability of the silicone tubing. Similar balances for carbon dioxide are given in Equations (18) and (19).

$$\frac{dC_l}{dt}\left(V_l + \sum_i V_{b,i}\right) = k_L a\left(\frac{C_g}{H_C} - C_l\right) V_l + \left[Y_{CX}\mu + m_C \phi\right] \sum_i \left(X_i V_{b,i}\right) \qquad (18)$$

$$\frac{dC_g}{dt} V_g = F_g\left(C_{g,0} - C_g\right) - k_L a\left(\frac{C_g}{H_C} - C_l\right) V_l + k_{p,C} a\left(0 - C_g\right) \qquad (19)$$

Equation (18) differs from Equation (16) in that carbon dioxide is generated rather than consumed. The amount of dissolved CO_2 reaction with the liquid medium is very low (Schlatmann *et al.*, 1997) and was not included in the model.

5.3.3 Solution Method

Equations (5), (11) and (15) - (19) form a set of 9 differential equations, as the balance in Equation (5) is written for each of the three solid phases. The continuous model was well suited for representation aspects including continuous feeds, exponential cell growth, and dynamic substrate concentrations. However, incremental plug-flow movement of the solid biocatalyst represented a discontinuity. The system was therefore solved in a piece-wise fashion. The differential equations were solved by the Fourth Order Runge-Kutta method with adaptive stepsize control for each interval between biocatalyst movement using Mathcad version Plus 6 for Macintosh. The results from each interval were passed as initial conditions to the next, including step changes in cell concentration and medium composition due to exchange of biocatalyst.

5.4 Results

5.4.1 Model Parameters

Model parameters were determined by experimental measurement, literature sources, and fitting. The list of non-adjusted model parameters and their source is given in Table 4. The value of the gas-liquid mass transfer coefficient (k_La) was determined directly from an MFB experiment using Equation (17) assuming steady-state conditions, as both liquid and gas phase oxygen concentrations were measured, and other parameters known. The same mass transfer coefficient was assumed for carbon dioxide balances. The

permeability mass transfer constants for silicone tubing were calculated from gas permeability constants (Cole Parmer, Chicago) given as volume per time as a function of pressure driving force and tube thickness and surface area. The oxygen saturation constant was determined by fitting a Michaelis-Menten kinetic model to suspension-culture batch respiration data.

The list of adjusted parameters is given in Table 5. Literature values for model parameters, where available, were used to bound the range of adjustment. Table 5 gives high and low literature values and the corresponding references. Optimization by goodness of fit of the model indicated that the saturation constant for hydrolysis (K_{hyd}) was much greater than the sucrose concentration, yielding first-order kinetics with respect to sucrose concentration. A first order rate constant (k'_{hyd}) was defined as the ratio of k_{hyd} and K_{hyd}. Values for these maximum rate and saturation parameters of 6.8 g/g cells-day and 0.5 g/L, respectively, were given by Hooker *et al.* (1992). These literature values could not predict the rapid hydrolysis seen during MFB startup. Glucose yield (Y_{XG}) and maintenance coefficients (m_G) were optimal by goodness of fit at the low and high ends of ranges, respectively, given in Table 5. This combination gives the highest glucose consumption rate possible for the given ranges. The glucose saturation coefficient (K_m) for growth was also found to be optimal at the high end of the range, introducing a significant dependence of growth on glucose concentration. Literature values for the CO_2 saturation coefficient for growth (K_C) were not available. The remaining metabolic parameters were found to be optimal at intermediate values. Feed gas flow rates (F_g) as a function of time were not available due to erroneous PC clock output, although a time-averaged value of

1.4 L/day was calculated. The flow rate was adjusted for each interval in order to mimic action of the dissolved oxygen control loop.

Table 4. Non-adjusted model parameters.

Parameter	Value	Source
V_l	2.7 L	measured by displacement
V_g	0.7 L	measured by displacement
F_l	0.115 L/day	measured
H_O	37.2 (g/L gas)/(g/L liquid)	calculated, Perry *et al.* (1984)
H_C	156 (g/L gas)/(g/L liquid)	calculated, Perry *et al.* (1984)
k_La	240 day^{-1}	measured
$k_{p,O}a$	16.4 L/m^2-day	calculated, Cole Parmer
$k_{p,C}a$	41.5 L/m^2-day	calculated, Cole Parmer
a	0.0547 m^2	calculated from tubing length, diameter
S_0	13.7 g/L	measured
G_0	3.06 g/L	measured
O_0	25%	measured
S_{int}	14.9	measured
G_{int}	0.564	measured
Y_{CX}	0.4 g CO_2/g cell mass	van Gulik *et al.* (1992)
Y_{OX}	0.4 g O_2/g cell mass	van Gulik *et al.* (1992)
Y_{GS}	0.53 g glucose/g sucrose	calculated, mass balance
K_O	0.38 mg/L	measured, respiration data

Table 5. Adjusted model parameters.

Parameter	Value	Range of Values
k'_{hyd}	1.67 L/g cells-day	-
μ_{max}	0.39 day^{-1}	0.105 - 0.468
		Guardiola *et al.* (1995), van Gulik *et al.* (1992)
Y_{XG}	0.28 g cells/g glucose	0.28 - 0.693
		Westgate *et al.* (1991), van Gulik *et al.* (1992)
K_m	6.0 g glucose/L	0.5 - 6.36
		Westgate *et al.* (1991), van Gulik *et al.* (1992)
K_C	0.3 mg CO_2/L	-
m_G	0.204 g glucose/g cells-day	0.142 - 0.204
		van Gulik *et al.* (1992), van Gulik *et al.* (1993)
m_O	0.161 g O_2/g cells-day	0.151 - 0.201
		van Gulik *et al.* (1992)
m_C	0.222 g CO_2/g cells-day	0.208 - 0.277
		van Gulik *et al.* (1992)
F_g	0 - 2.2 L/day	N/A

5.4.2 Biocatalyst Loading and Growth

Two MFB experiments were conducted which utilized gas phase recycle and dissolved oxygen control. Cell density and specific growth rate results are shown in Figure 17 for the second experiment. Biocatalyst loading (cell density) is reported as mass of dry tissue per volume of biocatalyst. Data are presented for 27 days of operation, as microbial contamination was detected on day 30. Feed biocatalyst data points which

correspond to product biocatalyst data are connected by a line for clarity. All feed plugs had a nine day residence time. Growth data are shown for each product biocatalyst point, and were calculated from initial and final cell densities of that plug, assuming exponential growth. Figure 17 shows that magnitudes in feed concentrations are reflected in product concentrations. Magnitudes are particularly well matched past 10 days, where growth rates are fairly constant. Specific growth appeared to become steady at approximately 0.15 day^{-1}.

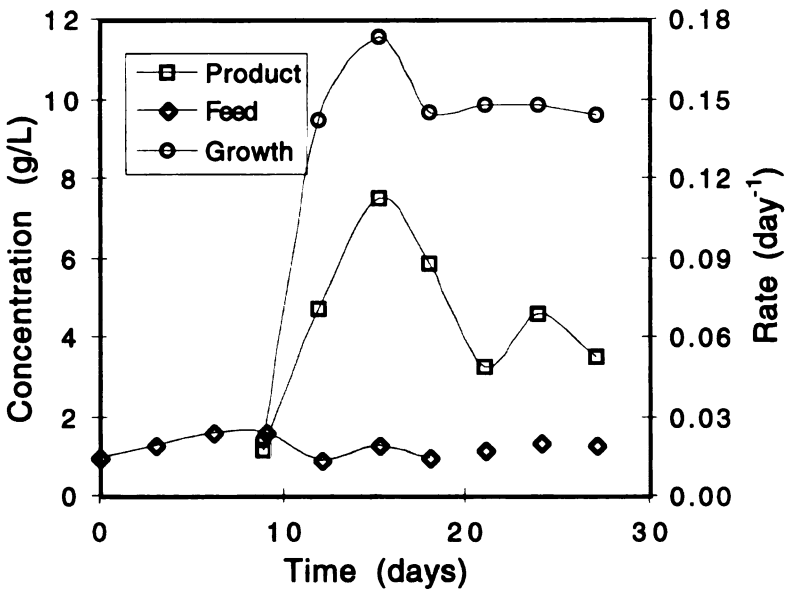

Figure 17. Biocatalyst plant-cell loadings and specific growth rates.

Similar results (not shown) were obtained for the first experiment, although operation lasted only 21 days. This experiment used longer and varied residence times of 11-18 days. Long residence times and growth rates up to nearly 0.12 day^{-1} resulted in soybean growth which joined biocatalyst particles, preventing MVS operation. Product biocatalyst densities reached over 11 g/L, where 10 g/L is considered the practical limit

before growth outside the immobilization matrix occurs. The data from this experiment were not used for modeling they involved non-uniform residence times.

Model predictions for soybean concentrations in the biocatalyst are shown in Figure 18 along with experimental data from Figure 17. Each line tracks the cell loading of a plug as it moves through the MFB over a nine day residence time. Feed concentrations were used as initial values. The model matched data well for biocatalyst harvested initially (day 9) and once growth rates became steady (days 21, 24, and 27). Specific growth rates, therefore, also matched well. The model could not accommodate the rapid increase in growth from days 10-15, underpredicting product biocatalyst loadings on days 12 and 15.

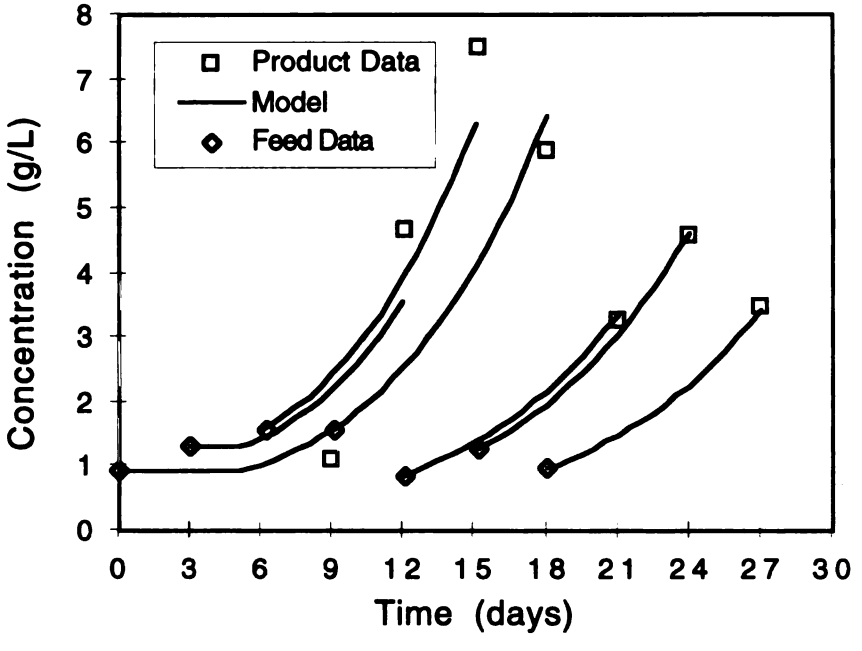

Figure 18. Data and model predictions for plant-cell loading of each biocatalyst plug.

5.4.3 Sugar Hydrolysis and Consumption

Data for sucrose, glucose, and fructose concentrations and model predictions for sucrose and glucose concentrations over the 27 day experiment are shown in Figure 19.

Rapid hydrolysis of sucrose to glucose and fructose was observed, resulting in sucrose concentrations of less than 2 g/L past day 9. Glucose and fructose concentrations increased accordingly, with glucose falling again due to consumption. Little or no consumption of fructose appeared to take place. These results were expected as diauxic growth of plant cells has been reported (Westgate *et al.*, 1991), and observed previously by the authors (unpublished data). Initial glucose and fructose concentrations were apparently the result of hydrolysis during the autoclave cycle. Model predictions match data reasonably well, although the model can not account for the apparent lag during the first 3 days of operation. Medium feed to the system included both the continuous feed started at day 9, and the medium exchanged with each biocatalyst exchange. The medium exchanges were step changes and give model predictions the saw tooth shape seen in Figure 19. Sugar assays were performed at the end of each interval and correspond to the saw tooth minima before each jump in concentration.

5.4.4 Head Space Composition and Dissolved Oxygen

Figure 20 illustrates the O_2 and CO_2 composition of the MFB head space and dissolved O_2 (DO) concentration in the medium. Model predictions are also shown for each variable. Head space O_2 and CO_2 content are given as percent volume. DO is shown as the percent of O_2 saturation, where medium in equilibrium with air would have a DO value of 20.9. Dissolved O_2 control and the feed gas pump were started on day 6 once oxygen uptake became appreciable. Head space assays were started when the GC became available on day 9. The model fit the data well excepting days 10 and 11 when a leak in the head space sampling line resulted in a significant flow of air into the head space. As

expected, the DO level remained steady at the setpoint of 16.3 (78% air saturation) excepting the disturbance caused by biocatalyst exchange at day 21 when vacuum was not available. The model shows a periodic behavior as a single feed gas flow rate is input at each interval, while in reality the controller matched the flow rate with increasing soybean concentration and oxygen uptake rate. Oxygen uptake rates were also calculated from the data shown in Figure 20 using Equation (17) assuming a constant gas flow rate of 1.4 L/day. Uptake held constant after day 12 at approximately 0.2 g O_2/day. The simulation predicted an average uptake rate of 0.22 g O_2/day for the last four intervals. The average uptake rate for the same period calculated from a previously measured immobilized soybean respiration rate of 8.9 mg O_2/hr was 0.39 g O_2/day.

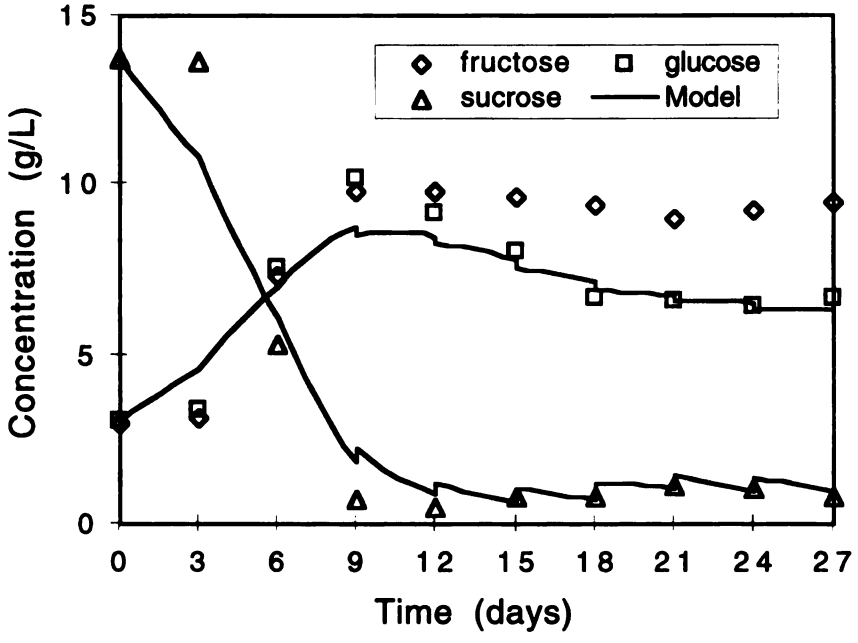

Figure 19. Sucrose, glucose, and fructose concentrations in MFB medium.

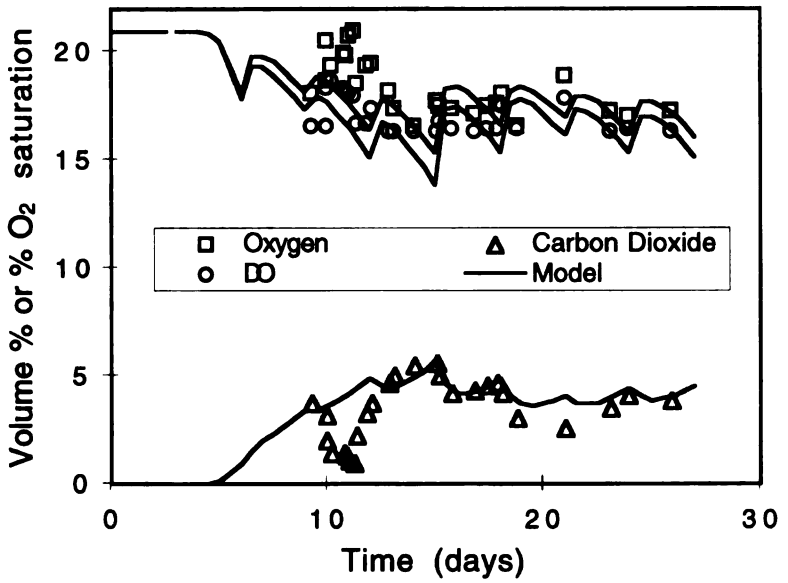

Figure 20. O_2 and CO_2 content of head space, and dissolved O_2 (DO).

5.4.5 Isoflavonoid Production

The concentrations of daidzein and genistein in soybean recovered from product biocatalyst are shown in Figure 21 on a dry soybean mass basis. Values are reported as mass per mass of dry tissue. The error bars represent the 95% confidence interval. Reported values are for total isoflavonoids, including both free isoflavonoids and isoflavonoids freed from moieties by acid hydrolysis. Isoflavonoids levels remained fairly constant and average values were 980 and 130 ppm for daidzein and genistein, respectively. The results in Figure 21 are an improvement over the prior 21 day MFB run discussed above in which concentrations averaged 180 and 30 ppm for daidzein and genistein, respectively. The results also compare well to prior MFB work in which average concentrations were 80 and 50 ppm (Ames and Worden, 1997). However, assays of stock cultures used as feed in the final MFB run averaged 24,000 and 5,700 ppm for

daidzein and genistein, respectively. An average of 2 stock cultures from the 21 day run had 4,900 and 2,900 ppm. Lower yet were the averaged concentrations from several stock cultures assayed prior to the original MFB work reported at 340 and 560 ppm for daidzein and genistein, respectively.

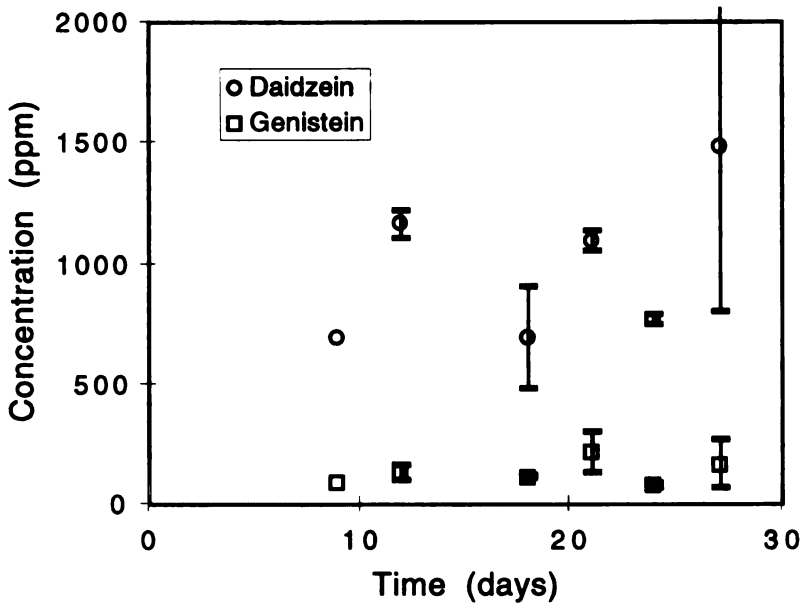

Figure 21. Isoflavonoid concentrations in product biocatalyst soybean.

The effect of the antibiotic/antimycotic cocktail on soybean growth and isoflavonoid production was evaluated in batch shake-flask cultures. Suspension culture concentrations are shown in Figure 22. Replicate results are shown. Average soybean specific growth rates were 0.35 ± 0.05 and 0.33 ± 0.01 d^{-1} for control and antibiotic cultures, respectively. The growth rates were calculated from the first three data points, considered to be log phase. As expected, the cocktail did not have a significant effect on growth rate. Daidzein and genistein concentrations on a mass of dry soybean basis are shown in Figure 23 and Figure 24, respectively. Changes in isoflavonoid concentrations

appeared to be independent of antibiotic effects for the first 6 days in batch culture, decreasing from initial values. Past 6 days, isoflavonoid concentrations increased for the control cultures, and continued decreasing for the antibiotic cultures. The change from decreasing to increasing concentrations appears to correspond with growth phase. The cultures no longer exhibited log growth past day 6. While temporally dependent, the effect of the antibiotic cocktail on isoflavonoid concentrations is significant. At day 9, average daidzein and genistein concentrations were less than 30% and 20% of the control values, respectively.

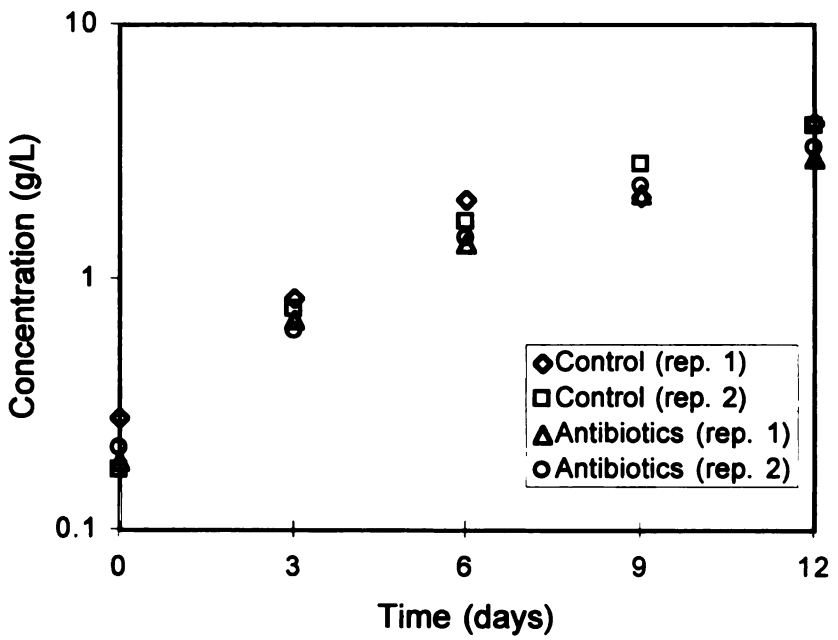

Figure 22. Effect of antibiotic cocktail on soybean cell growth.

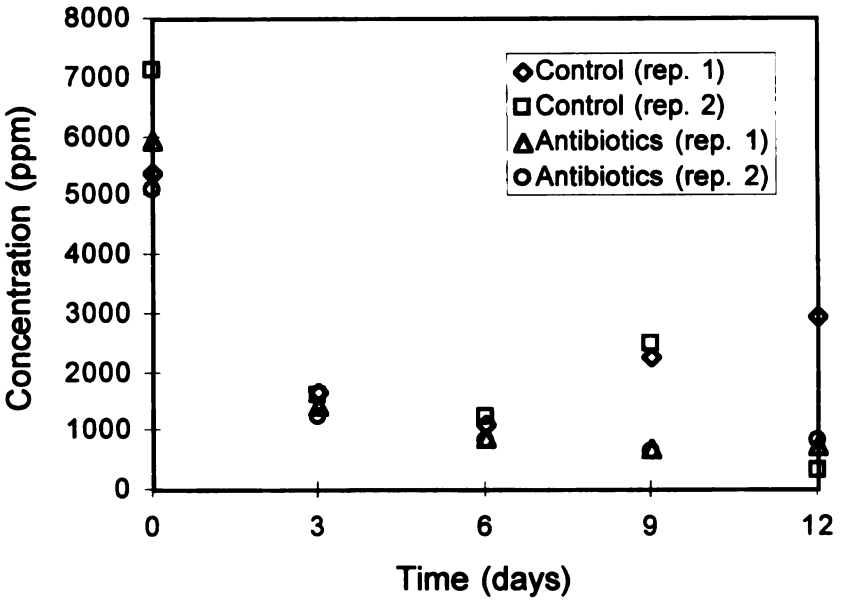

Figure 23. Effect of antibiotic cocktail on daidzein concentrations in soybean.

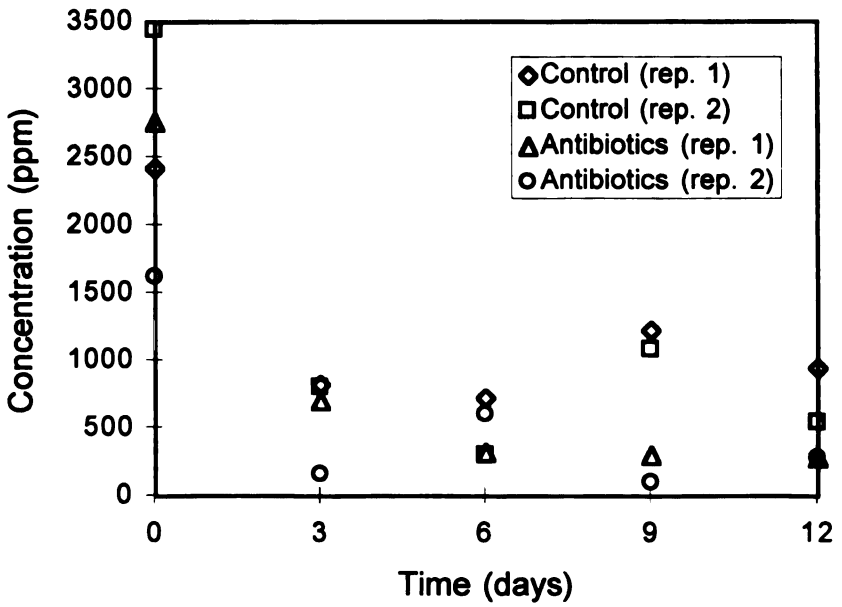

Figure 24. Effect of antibiotic cocktail on genistein concentrations in soybean.

Volumetric productivities were calculated for the final MFB run and are presented in Figure 25 along with total biocatalyst volumes contained in the MFB. Volumetric productivity is reported in $/L bioreactor-day assuming a value of $1000 per gram of isoflavonoid, and a 1 L working volume for bioreactor (column only). Shuler *et al.* (1990) has noted that the primary determinant of economic viability for a bioprocess, the volumetric productivity of the reactor times the wholesale price of the product, is 0.12 $/L-day +/- 60% for a wide variety of fermentations. Daidzein productivity falls into this range, but genistein productivity does not.

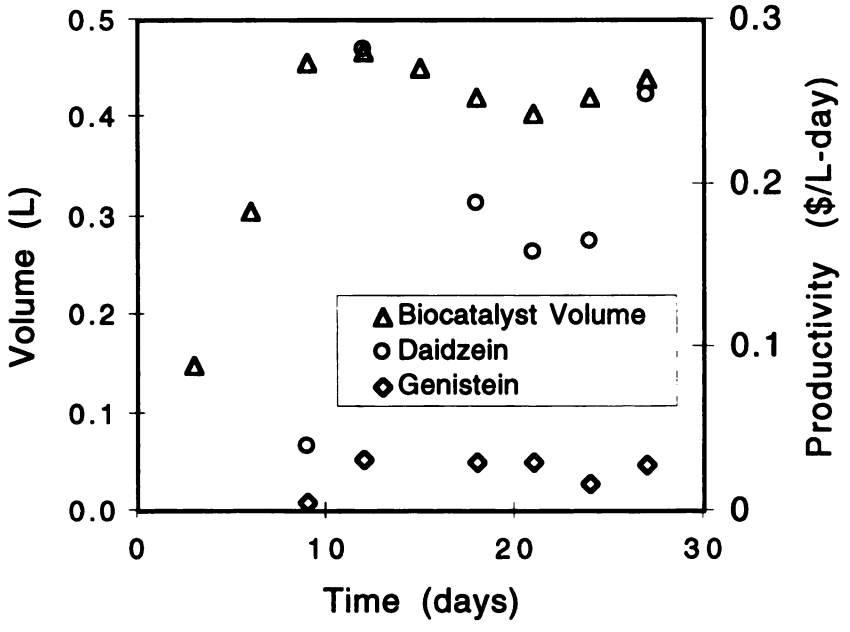

Figure 25. Total volume of biocatalyst and volumetric productivity.

5.4.6 Modeling of Steady State Operation

The experimental data shown in Figure 17 and Figure 19 indicates steady growth rates and sugar concentrations were achieved. Modeling presented in Figure 19 predicted that glucose concentrations, and thus growth rates, were still changing. An extended model

simulation is shown in Figure 26. All feed biocatalyst concentrations were 1.3 g/L starting at day 21. The cell density line shows the loading for the bottom plug. Cell concentrations leaving the MFB correspond to the top of the saw tooth waves. Concentrations were zero for the first 6 days as biocatalyst was present only in the top and middle plug positions. Figure 26 shows that the glucose level requires around 60 days to reach steady-state. This is in agreement with the heuristic for time to reach steady-state of 3 to 4 residence times (Fogler, 1992), as the liquid residence time was approximately 18 days. Sucrose levels out much quicker as the hydrolysis reaction is rapid. The glucose concentration appears to govern the time to steady-state. As the range for K_m values in Table 5 is large, the K_m value of 6 g/L may overestimate the effect of glucose concentration on growth. Figure 27 shows a simulation for a K_m of 0.5 g/L. The feed biocatalyst was 1.3 g/L for all intervals. Initial and feed medium concentrations were 20 g/L sucrose and 0 g/L glucose. While the time for glucose levels to reach steady-state is essentially the same as Figure 26, biocatalyst loadings and cell growth rates reach steady-state essentially within 21 days. This length of time reflects the biocatalyst movement rather than liquid residence time. Model simulations predict that the time to steady state could also be reduced by choice of sugar concentrations in the initial and feed medium. A simulation (not shown) with a K_m of 6 g/L can reach a glucose and growth rate steady-state in approximately 21 days by using an initial and feed reservoir concentration of 7 g/L glucose, and medium containing 25 g/L glucose for biocatalyst additions.

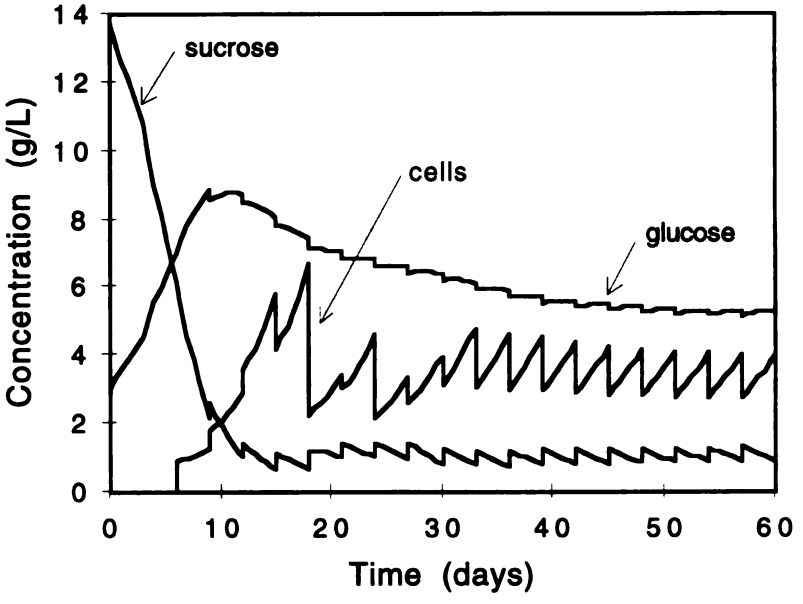

Figure 26. Extended simulation of MFB run.

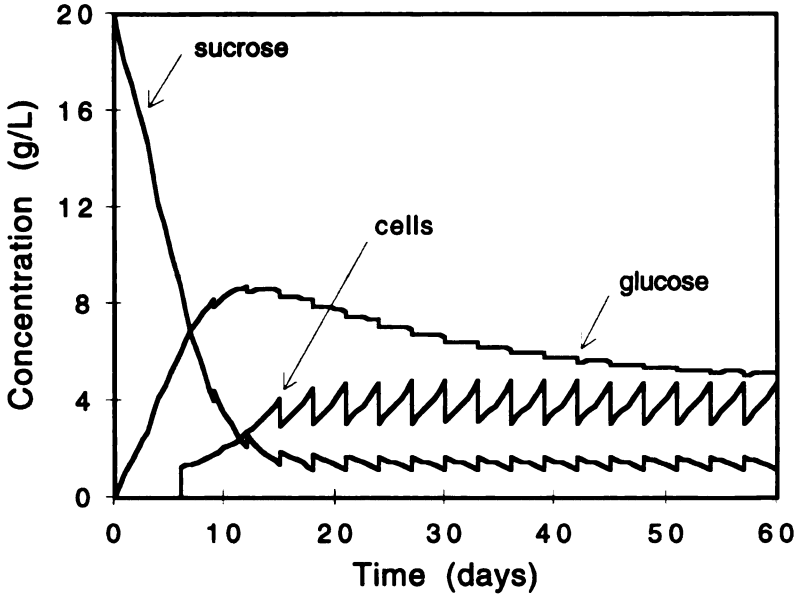

Figure 27. Simulation of MFB using a K_m of 0.5 g/L and 20 g/L sucrose feed.

Model simulations also provided insight into use of different biocatalyst residence times. Figure 28 shows simulations for 9 and 12 day residence times. Both simulations had a 1.3 g/L feed biocatalyst concentration, and feed and initial medium concentrations of 20 g/L sucrose. Sucrose levels are not shown in Figure 28 for visual clarity. Biocatalyst loadings were higher in the 12 day case as expected, and reached over 8 g/L. The magnitude of saw-tooth changes in glucose concentration showed no significant increase in the 12 day case compared to the 9 day case. The use of the longer residence time does not create excessive periodic fluctuations.

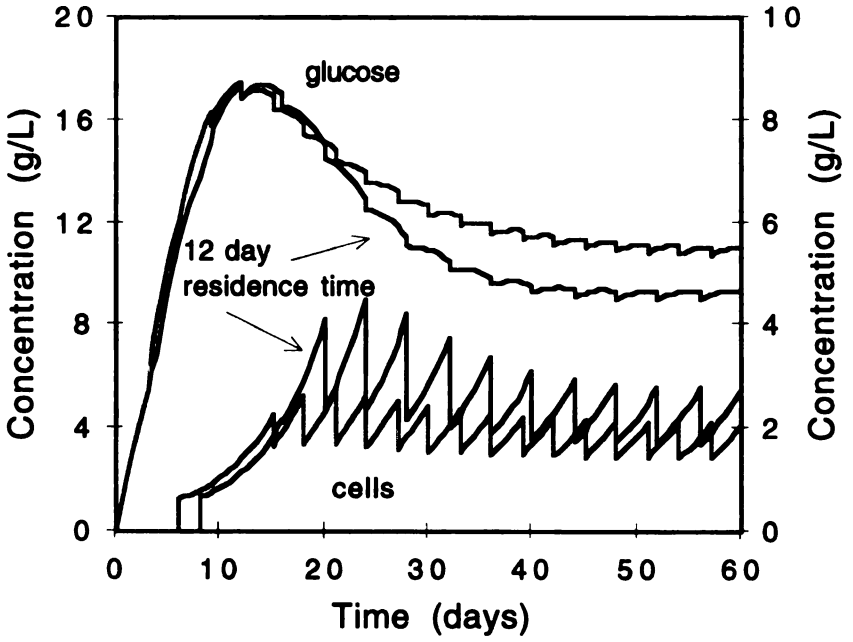

Figure 28. Simulations of MFB for 9 and 12 day biocatalyst residence times.

5.5 Discussion

The results depicted in Figure 17 represent a significant advance in continuous operation of the MFB with plant cell culture. While long-term operation was previously reported by the authors, the current work demonstrated stable operation where growth

rates reached a relatively steady value. Mixing of the biocatalyst during exchange appeared to be insignificant as feed and product biocatalyst loading levels closely paralleled each other over time. The dissolved oxygen control loop, which fed oxygen-enriched air to the system, successfully maintained a high dissolved O_2 level and head space CO_2 levels in the target range. Problems which remain with MFB operation include contamination and cell growth outside of the alginate spheres. While only the final MFB suffered contamination, difficulties in aseptic operation of a continuous, plant-cell bioreactor are expected to increase with scale. Plant cell growth outside the immobilization matrix posed a unique problem for the MFB configuration. While adhesion to reactor surfaces or significant clogging of the base plate fluidization mesh were not observed, interbiocatalyst attachment prevented solids removal at the end of the 21 day run. Feed biocatalyst loadings and residence times must be chosen to avoid this problem. In general, any system which has extended periods of immobilization particle contact may be susceptible. MFB operation may benefit from higher liquid velocities which yield more open packing structures such as chain-channel (Thompson and Worden, 1997), as opposed to the essentially frozen bed regime used here.

The isoflavonoid production levels presented in Figure 21 also represent an improvement over prior MFB operation. Product accumulation also showed less fluctuation over the course of the experiment. This is likely due to stable levels of dissolved oxygen and carbon dioxide. Despite this improvement, the kinetics of isoflavonoid production and degradation in the MFB are not fully understood. Lacking a fundamental basis, mass balances for daidzein and genistein were not included in the

modeling. MFB benefits including tight control of biocatalyst residence time, and independent control of solid, liquid, and gas residence times, need to be linked to isoflavonoid accumulation kinetics to be fully realized. MFB product levels were significantly below those of stock shake-flask cultures. Shake-flask tests determined that the use of the antibiotic/antimycotic cocktail was partially responsible for the lower values. Furthermore, long-term changes in soybean cell culture appear to be the most important factor in productivity results to date. Roughly a 2 order of magnitude increase in stock culture isoflavonoid concentrations has been observed over a 1.5 year period.

The MFB model yielded good prediction of process variables using metabolic parameters within ranges available in the literature. The exception was the use of a first order rate constant for hydrolysis. Otherwise, use of parameters outside of the literature bounds did not give significant improvement in model fits. A growth rate dependence on both glucose and dissolved CO_2 concentrations was important to the model's ability to fit the data. The CO_2 term is significant in matching the initially very slow growth rate followed by rapid increase before leveling off. In reality, one or more dissolved gaseous metabolites (DGM) may be important to growth (Schlatmann *et al.*, 1997). CO_2 monitoring provided a measure of DGM and incorporation of DGM into the model. Concepts such as medium conditioning with endogenous growth factors may explain gaps between data and modeling at some time points. However, the model in its presented form relies only on variables easily measured in a typical bioprocess.

An alternative CO_2 term is that which includes inhibition, as used by Schlatmann *et al.* (1997) to model ajmalicine production. The effect of including an inhibition constant

is illustrated in Figure 29. Growth data are plotted against average dissolved CO_2 concentrations to which each slug was exposed as predicted by the simulation. The relationship between CO_2 and growth is evident. While the inhibition model gives a better fit, the differences are small in the range of concentrations found in the MFB. The growth rates shown were also a function of a number of other variables besides CO_2. Neither the data nor the model fits in Figure 29 agree with the findings of Archambault (1991) regarding the gas phase where 2 and 5% CO_2 increased and decreased the growth rate with respect to no CO_2, respectively.

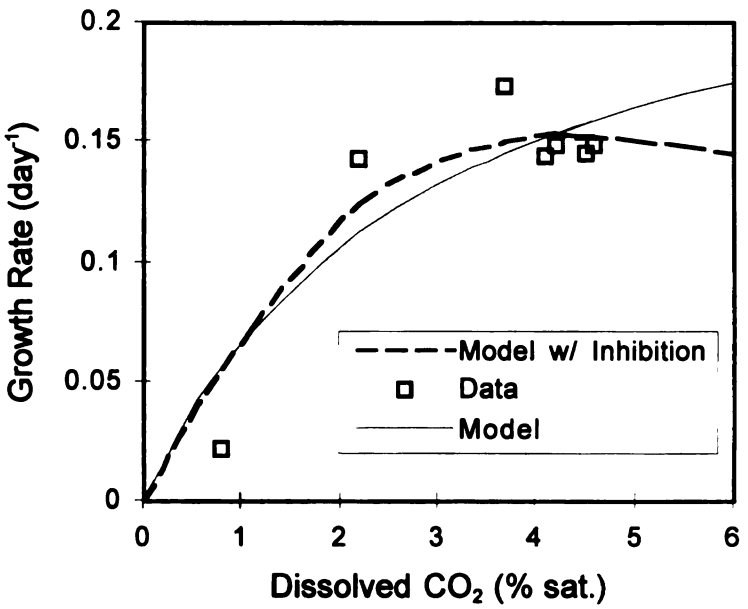

Figure 29. Comparison of saturation model with and without inhibition.

Modeling provided new insight into operational protocol for the MFB. As biocatalyst was exchanged at intervals, along with medium required for the exchange, periodic change in process variables was introduced. Simulations indicated that the amplitude of the periodic change is relatively small. Based on Figure 28, operation with a

12 day residence time should be a good choice. Biocatalyst loadings are higher without exceeding 10 g/L, and no significant increase in the amplitude of glucose periodic change is predicted. From results of 9 and 12 day residence times, it can be inferred that a 15 day residence time would risk bioreactor failure due growth outside of the biocatalyst. The increased soybean loading and therefore increased hydrolysis rate for the 12 day case also results in a quicker approach to the steady-state glucose concentration. This can be explained as the time to reach steady-state is inversely proportional to the rate for fast, first-order reactions in a CSTR (Fogler, 1992). Finally, the model was used to predict medium sugar concentrations which would provide the quickest approach to steady-state. Such strategies would require verification, as the model's robustness depends on the assumption that growth rates are more sensitive to glucose concentration than other factors. The model is also limited to conditions where glucose is the rate limiting carbon source as it does not include diauxic growth.

5.6 Conclusions

Continuous operation of the MFB bioreactor utilizing soybean cell culture has been demonstrated past start-up to the point of steady growth rates. A simple DO and CO_2 control strategy was able to maintain these variables near target levels. An unstructured model relying primarily on literature values for metabolic parameters provided a reasonable description of the process. The dependence of growth on both glucose and CO_2 was important to a good model fit. Model results indicated that time to achievement of steady-state is controlled by the liquid phase residence time and initial

conditions. Model results also predicted an optimum integer interval between biocatalyst exchange of 4 days, and that periodic changes in the medium would not increase significantly over the 3 day scenario. Contamination of the long-term continuous bioprocess and plant cell growth on the exterior of the immobilization matrix remain concerns for process feasibility. While isoflavonoid productivity was improved from earlier runs, possibly due to stable environmental conditions, concentrations were well below current shake flask levels. The use of an antibiotic/antimycotic cocktail was partly responsible for the lower values. Research is needed to better understand the relationship between isoflavonoid production kinetics and bioreactor process variables.

5.7 Nomenclature

5.7.1 Variables

μ	specific growth rate (day^{-1})
a	area for mass transfer (m^2)
C	carbon dioxide concentration (g/L)
F	volumetric flow rate (L/day)
G	glucose concentration (g/L)
H	Henrys law coefficient
K	saturation coefficient (g/L)
k'_{hyd}	hydrolysis constant (L/g cells-day)
$k_L a$	gas-liquid mass transfer coefficient (day^{-1})
k_p	tubing permeability constant (L/m^2-day)

m	maintenance coefficient (g/g cells-day)
O	oxygen concentration (g/L)
q	uptake rate (g/day)
Q_S	rate of sucrose transfer (g/day)
Q_G	rate of glucose transfer (g/day)
S	sucrose concentration (g/L)
V	volume of solid, liquid, or gas phase (L)
X	dry cell mass concentration in biocatalyst (g/L)
Y_{ab}	yield coefficient of compound a per compound b

5.7.2 Subscripts

0	(null) feed
a	ambient
b	biocatalyst (solid) phase
g	gas phase
hyd	sucrose hydrolysis
i	index for solid phase
int	interval
l	liquid phase
max	maximum

6. MFB BIOREACTOR SCALE UP

6.1 Introduction

Previous sections have described the benefits of a MFB bioreactor for plant cell culture and demonstrated its successful operation at the laboratory scale. Additional considerations are required, however, in designing a pilot or manufacturing scale MFB. These considerations fall into two categories: requirement and benefit of using a three-phase system, and economics of magnetic field generation.

MFB bioreactors can be operated with two or three phases. The third phase is a gas which replenishes the dissolved oxygen consumed by the plant cells. While systems described in Section 4 (Bramble *et al.*, 1990; Ames and Worden, 1997) were two-phase, the use of a third phase would be required at a scale where dissolved oxygen depletion was significant. The third phase can be supplied simply by a ring sparger as in a traditional fermentor. The physical characteristics of such a three-phase system have been studied in the lab of Dr. Mark Worden (Thompson and Worden, 1997). Alternatively, the third phase can be supplied by microbubbles (described in Section 3.3). Microbubbles not only provide high gas-liquid mass transfer rates, but may also reduce operating costs of a three-phase MFB. Due to their size, microbubbles cause less disruption to the bed than traditional sparger bubbles. Solenoid power, and thus cost, is directly related to the amount of disruption which must be overcome in the bed to prevent solids mixing.

For a MFB to be feasible at large scale, generation of a suitable strength magnetic field must be practical. Impractical situations would include excessively large solenoid

equipment or dramatic increases in power consumption with size. The analysis provided here compares MFB scale up with that of a traditional CSTR fermenter and illustrates the feasibility of the MFB. Additional capital costs of the MFB over the CSTR are also considered. While any of several parameters could be kept constant for scale-up, geometric similarity was chosen. Two cases of geometric-similarity scale up were studied. The first stemmed from an inherent optimum in the design of magnetic coils. There exists an optimum geometry where the power consumption, regardless of other considerations, will be minimized. With choice of reactor aspect ratio, an optimum coil thickness will exist which minimizes power consumption. The drawback to using optimum geometry is that coil thickness can become quite thick, and thus expensive. The second case was therefore and economic analysis considering operating costs versus capital cost of the coils. An optimal coil thickness was determined by minimizing the present value cost of the project.

6.2 Materials and Methods

Soybean culture and respiration measurements were described in Section 4. Equipment for microbubble studies including a 80 cm by 5 cm inner diameter magnetized fluidized bed system and 4 mm diameter alginate beads with 50% magnetite by weight have been detailed by Thompson and Worden (1997). Reverse-osmosis water was metered into the column and distributed through a 24 cm calming region. Compressed air was metered in just above the calming region through a stainless steel ring sparger 3.5 cm in diameter with 0.2 mm holes spaced at 5 mm intervals around the ring. Microbubbles

were metered into the liquid inlet line immediately prior to calming region. The microbubble generator and its operation have been described by Bredwell *et al.* (1995a). The unit consisted of a 6 L fermentation vessel with the impeller replaced by a 5 cm diameter, stainless steel disk. A motor mounted above the head plate rotated the shaft at speeds up to 9000 rpm. Baffles were approximately 2 mm from the spinning disk.

The power required to prevent mixing in a MFB was compared for three cases: liquid only, liquid sparged with air from fritted glass at the bottom of the column, and liquid with supplemented with microbubbles. Liquid flow rates were 6.1, 7.6, and 9.1 L/min, and gas flow rates were 0.24 and 0.54 L/min. For microbubble aeration, the gas fraction of the foam (approximately two-thirds) was used to determine the flow rate equivalent to 0.24 or 0.54 L gas/min. For each combination of flow rates, the solenoid current (and power) was increased from zero in 0.2 A increments, observing the bed through upper and lower view ports for 20 to 30 seconds. Bed regimes similar those described by Thompson and Worden (1997) were observed at each increment, while looking for the point at which mixing was prevented. Power was calculated from current and voltage meters on the power supply.

6.3 Theoretical

6.3.1 Oxygen Depletion in the Liquid Phase

A simple model neglecting mass-transfer resistances where a pre-saturated liquid phase flows up through a solid phase containing soybean has been used. For steady-state, plug-flow liquid movement, and no mass transfer resistance between the phases, the

dissolved oxygen concentration (C) is a function of vertical distance (z) as described by Equation (20)

$$v_z \frac{dC}{dz} = -\frac{1-\varepsilon}{\varepsilon} Q \qquad (20)$$

where v_z is the liquid velocity in the z direction, Q is the volumetric oxygen consumption rate in the solid phase, and ε is the void fraction in the column. Integration yields

$$C = C_{saturated} - \frac{1-\varepsilon}{\varepsilon} \cdot \frac{Q}{v_z} \cdot h \qquad (21)$$

for a column of height (h) and air saturated liquid entering at the bottom. For operation at 1.6 L/min (Section 4) and an assumed void fraction of 0.4, v_z was 3.5 cm/s. The bulk oxygen concentration at 25°C was taken to be 8.43 mg/L (Bailey and Ollis, 1986). Respiration rates and ranges for soybean densities in the biocatalyst were taken from Section 4. The oxygen consumption rate (Q) was calculated from the measured suspension culture respiration rate of 28 mg O_2/g cells-hr, and an integral average cell density of 3.0 g/L. The average density was based on feed and product biocatalyst densities of 0.4 and 10 g/L respectively.

6.3.2 Solenoid Equations

For a uniform-current-density solenoid the power consumption is described by Equation (22) taken from Montgomery (1969)

$$H_0 = G(\alpha,\beta) \cdot \left(\frac{W\lambda}{\rho a_1} \right)^{1/2} \qquad (22)$$

where H_o is the magnetic field vector, $G(\alpha,\beta)$ is the Fabry factor, W is power, λ is the fraction of coil cross section occupied by wire, ρ is the resistivity of the wire, and a_1, is the inner radius of the coil. The Fabry factor is given by Equation (23), also from Montgomery (1969)

$$G(\alpha,\beta) = \frac{1}{5}\cdot\left(\frac{2\pi\beta}{\alpha^2-1}\right)^{1/2}\cdot\ln\frac{\alpha+\left(\alpha^2+\beta^2\right)^{1/2}}{1+\left(1+\beta^2\right)^{1/2}} \qquad (23)$$

where α is the ratio of the outer to inner coil radii and β is the ratio of the coil height to the inner coil diameter. It is notable that β is also assumed to be the aspect ratio of the MFB. The Fabry factor can be thought of as a type of efficiency, and has a maximum near $\alpha = 3$ and $\beta = 2$. As an aspect ratio of 2 is reasonable for a large fluidized bed, these values were chosen for the first scale-up method of minimum power consumption (MP). Another important result is obtained from Equation (23). For a geometric similarity scale-up (constant Fabry factor) and given magnetic field strength, the power consumption varies with bed radius. This indicates that

$$power \propto volume^{1/3} \qquad (24)$$

$$\frac{power}{volume} \propto volume^{-2/3} \qquad (25)$$

which demonstrates a decrease in power consumption per volume with increasing size.

The resistivity (ρ) of copper wire at the cooling water temperature of 10 degrees Celsius was calculated to be 1.63×10^{-8} ohm-m. The fraction of space occupied by wire

(λ) for a staggered packing was calculated to be 0.8976, Two magnetic field strengths were specified, 100 and 300 Gauss. A field of 100 Gauss represents an adequate value for operation of a MFB bioreactor using 50% magnetite, alginate beads with an approximate diameter of 4 mm, and microbubble aeration as determined in bed studies above. A field of 300 Gauss represents a value more adequate for operation of the same system with conventional sparging aeration.

The specification for magnetic field strength is given at the axial and radial mid-point of the MFB bioreactor. The field will vary however, along the solenoid axis unless the solenoid is infinitely long. Solenoids with low aspect ratios (determined by the bed aspect ratio) may have an unacceptable decrease in field strength away from the axial mid-point. Equation (26) from Montgomery (1969) describes the variation in field strength along the axis

$$H_z\left(\frac{z}{a_1}\right) = H_z(0)\left[\frac{F(\alpha,\beta+z/a_1)+F(\alpha,\beta-z/a_1)}{2F(\alpha,\beta)}\right] \qquad (26)$$

where H_z is the field strength as a function of dimensionless axial position, $H_z(0)$ is the field strength at the axial mid-point (maximum field strength), and z is the axial distance from the center of the solenoid. The shape factor (F) is given by Equation (27).

$$F(\alpha,\beta) = \frac{4\pi\beta}{10}\cdot \ln\frac{\alpha+\left(\alpha^2+\beta^2\right)^{1/2}}{1+\left(1+\beta^2\right)^{1/2}} \qquad (27)$$

Equation (27) is used to determine the change in field strength along the axis for the original chosen aspect ratio (β = 2), as well as for an aspect ratio which yields a more uniform field strength (β = 8).

6.3.3 Economic Analysis

A present value cost analysis was performed in order to determine an minimum cost (MC) value for α as opposed to a minimum power (MP) value given by α = 3. The MC case was examined as very thick coils (α = 3) will yield very low power consumption, but high capital costs for the coils. For a given volume, α was optimized to give a minimum present value cost. The parameters used in the analysis are given in Table 6. The rate of inflation on operating costs was assumed to be zero as the increase in electricity costs are expected to match the rate of inflation.

Table 6. Parameters for present value cost analysis.

Parameter	Value
Cost of electricity	0. 1 $/kW-hr
Cost of copper magnet wire	3.0 $/lb.
Project life	10 years
Scrap value of copper coils	20% of original cost
Rate of inflation on operating costs	0%
Rate of inflation on value of scrap	40%

6.3.4 Comparison with CSTR Fermentors

A variety of methods exist for scale-up of CSTR fermenters (Hubbard, 1987) which give very different relationships between the power per volume for agitation and volume of the vessel. A correlation based on industrial data was therefore chosen. Einsele (1976) correlated power input data for 0.5 to 300 m^3 fermenters with Equation (28).

$$\frac{power}{volume} \propto volume^{-0.37} \qquad (28)$$

In order to develop a curve for comparison with the MFB bioreactor, a proportionality constant is needed for Equation (28). Power consumption per volume for plant scale fermenters has been given as 1 - 3 kW/m^3 (Aiba *et al.*, 1973) and 1 - 2 kW/m^3 as a low value (van't Riet, 1983). A proportionality constant was determined in order to yield 1 kW/m^3 for a volume of 300 m^3. The correlation correctly yields 1 -3 kW/m^3 values over the range of industrial size fermenters.

Another consideration is the additional capital cost of the solenoid for a MFB bioreactor compared with the cost of a CSTR fermenter. Comparisons were made using fermenter cost correlations from Kalk *et al.* (1986) based on 1985 prices. The solenoid cost only accounts for the purchase of copper magnet wire, but use of 1985 fermenters costs likely balances the neglect of labor and power supply costs for the solenoid. These neglected costs are also likely to be offset as agitator and motor costs are eliminated in a MFB.

6.4 Results and Discussion

6.4.1 Oxygen Depletion in the Liquid Phase

For the lab scale MFB described in Section 4, the depletion of dissolved oxygen across the 0.4 m height of biocatalyst is predicted to be 4.7%. Thus presaturation appears to be satisfactory for the lab scale experimental conditions. Equation (21) yields roughly a 1 mg/L drop in dissolved oxygen concentration for every m of height. Thus, the liquid would be nearly 50% depleted at 4 m, and essentially devoid of oxygen at 8 m. Maintaining dissolved oxygen at 80% of air saturation (as in Section 5) or higher throughout the MFB would limit the height to 1.7 m. Addition of a gas phase in the MFB would prevent both low dissolved oxygen levels and large variations in dissolved oxygen across the column.

6.4.2 Reduction in Power Consumption by Microbubbles

Power required to prevent solids mixing was less for the microbubble case than the sparged case at all flow rate combinations. In order to quantify error in measurements, repeated studies of the 7.6 L/min and 0.24 L/min case were done. The results comparing no air, sparged, and microbubble cases for the top view-port are shown in Figure 30. Error bars show the 95% confidence interval. The reduction in power required for the magnetic field while supplying the same volume of air is quite substantial. This result indicates that disturbances from rising bubbles are large compared to disturbances caused by liquid turbulence. The disturbances may, in part, be liquid turbulence created by the bubbles. The results for the bottom view port are shown in Figure 31. Power requirements are much less at the bottom port, but the relationship between the three cases is similar. The

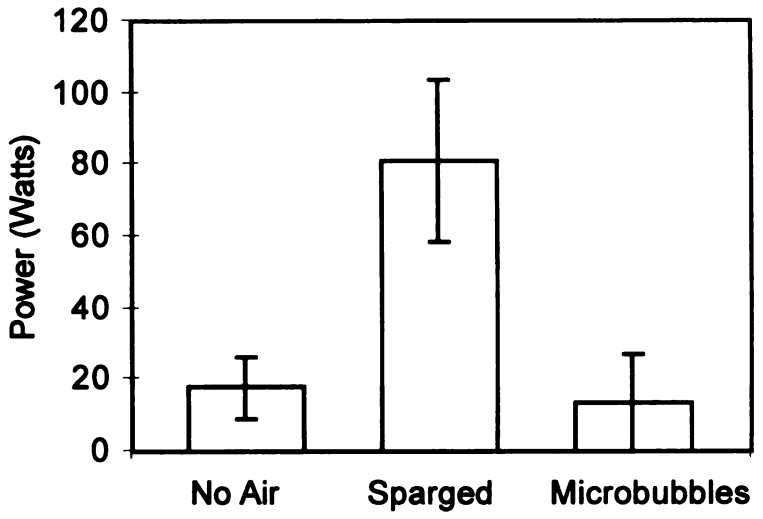

Figure 30. Power consumption required to prevent mixing at top view port.

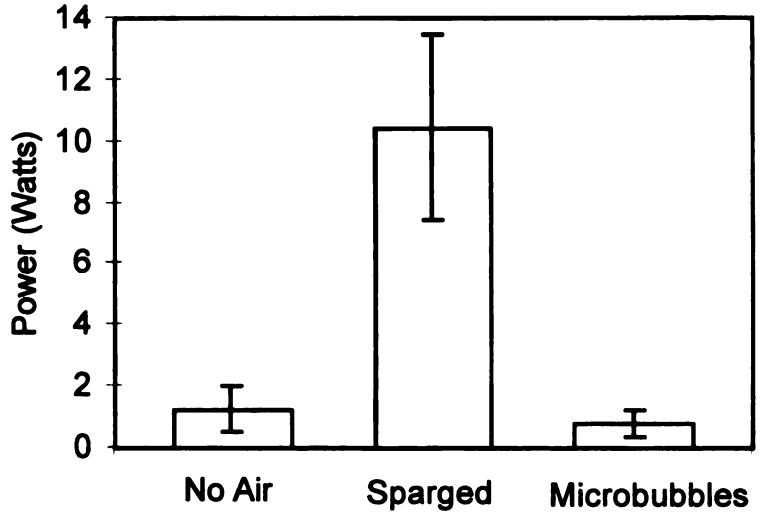

Figure 31. Power consumption required to prevent mixing at bottom view port.

results also indicate that the use of microbubbles may actually decrease the power required.

6.4.3 Uniformity of Magnetic Field

A limitation of short solenoids (and thus short MFBs) is the increasing axial nonuniformity of the field strength as the length decreases. The normalized magnetic field strength over one-half of the dimensionless length of the solenoid is shown in Figure 32 for $\beta = 2$, and in Figure 33 for $\beta = 8$. Two curves are plotted in each figure, one for the MP ($\alpha = 3$) case and one for $\alpha = 1.04$ which is typical for the MC case for a 12 - 13 m^3 MFB. Regardless of coil thickness, the results show that aspect ratios higher than 2 may be desirable in order to maintain field uniformity over the entire column. With this result, power per volume for scale-up was examined for $\beta = 8$.

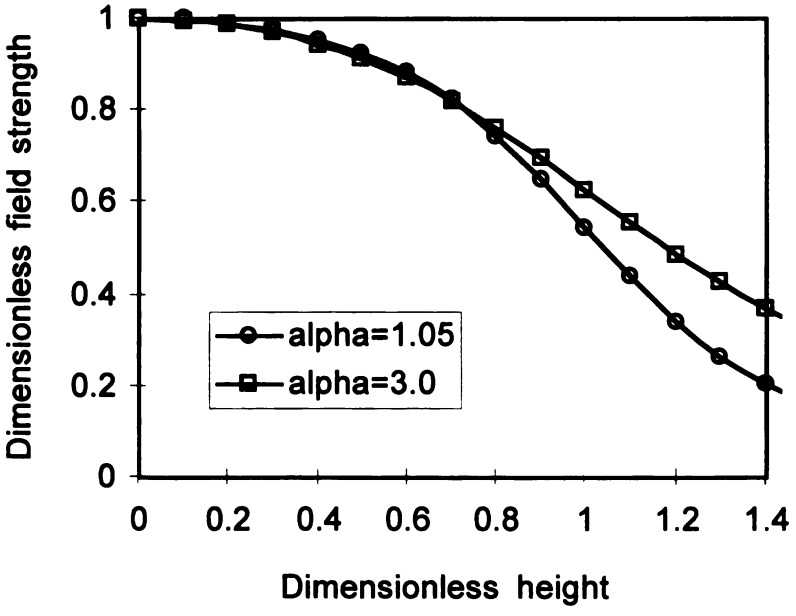

Figure 32. Field strength as a function of column height for an aspect ratio of 2.

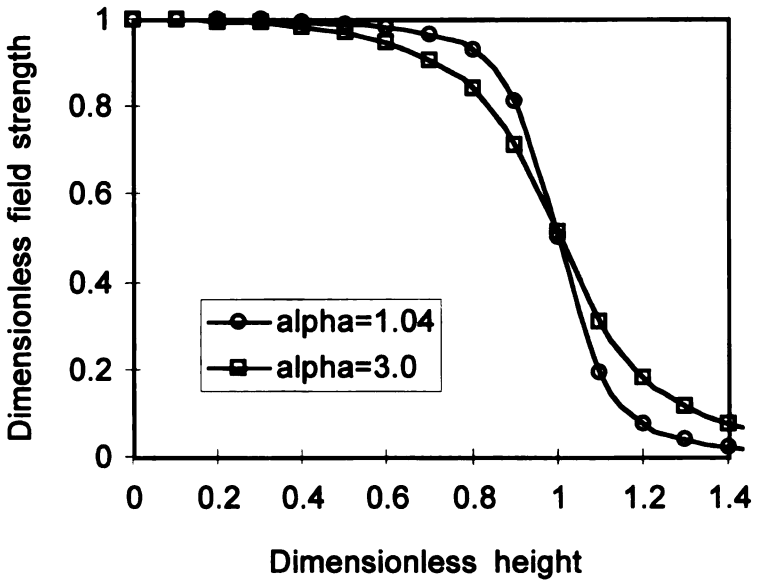

Figure 33. Field strength as a function of column height for an aspect ratio of 8.

6.4.4 Power Per Volume Ratios

The results of power per volume scale-up calculations are a comparison of three cases: (i) a CSTR fermenter, (ii) a MFB designed for minimum power consumption, and (iii) a MFB designed for the minimum cost. The results for the 100 and 300 Gauss specifications and an aspect ratio of 8 are shown in Figure 34 and Figure 35. The log-log plots show favorable scale up in all three cases. More importantly, both cases for the MFB show significantly less power consumption per volume than the CSTR. As expected, the MP case sets a lower bound while the MC case falls in between the other two. Depending on the volume and magnetic field specification, the MP case is roughly 1 to 3 orders of magnitude lower than the CSTR. The MC case is roughly 1.0 to 1.5 orders of magnitude lower than the CSTR.

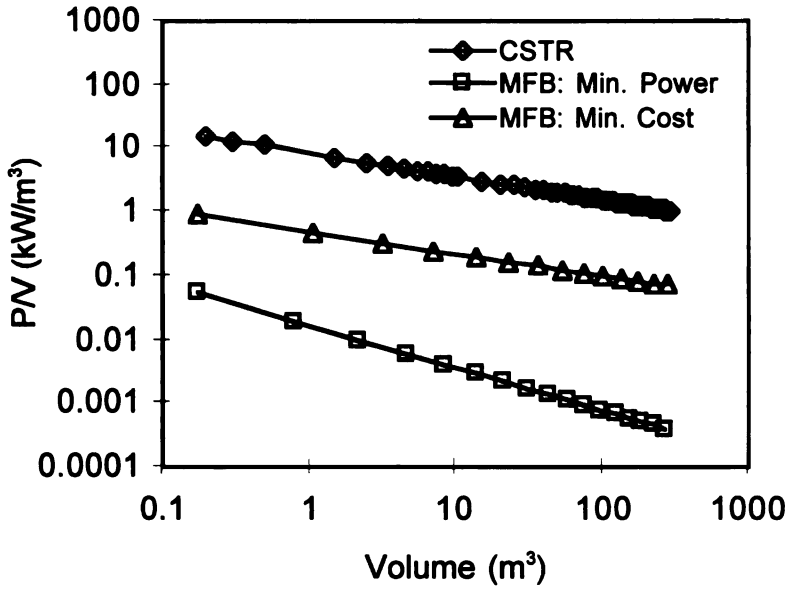

Figure 34. Power consumption of 100 Gauss MFB vs. CSTR.

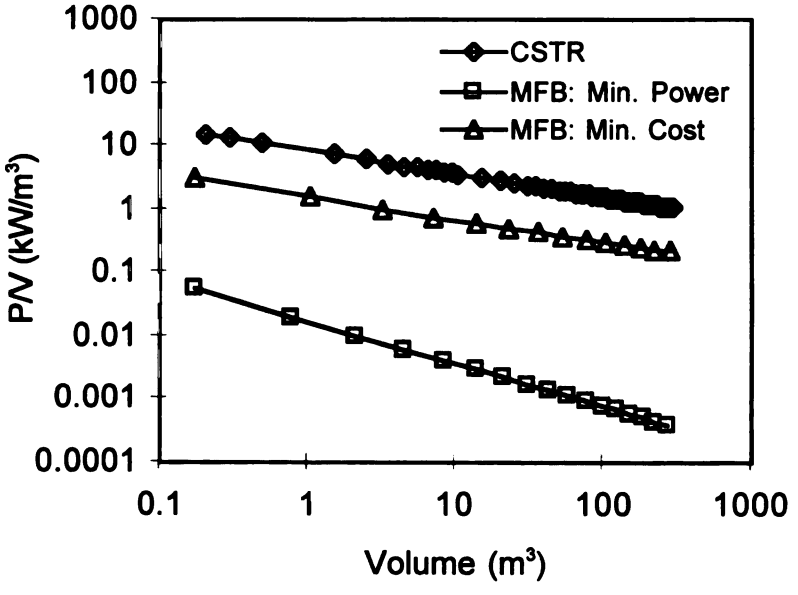

Figure 35. Power consumption of 300 Gauss MFB vs. CSTR.

The difference between the MFB cases in Figure 34 and Figure 35 is due solely to the difference in coil thickness described by α. Clearly, the difference is quite large. An example can be made with a column 1 m in diameter with a 100 Gauss field. The coil thickness for the MP case would be 1 m (α = 3). In contrast, the coil thickness for the MC case would be 1.3 cm. This indicates that the cost of the solenoid is significant in comparison with the cost of power. Similarly, the coil thickness for the 300 Gauss case is 3.8 cm. The increased thickness for higher field strength specification is as expected. Also of interest is the insensitivity of coil thickness to scale-up. For the range of volumes used in calculations, coil thickness was nearly constant, increasing only slightly with volume. As an example, the thickness for a 261 m^3, 300 Gauss system is 3.9 cm.

6.4.5 Capital Costs

A MFB will have a capital cost of the solenoid in addition to the cost of the fermenter. For the MFB to be feasible the added capital cost can not be excessive. Costs of the solenoid were calculated as the percent of the total capital investment (fermentation system and solenoid). Values range from roughly 2 to 10% for the 100 Gauss case, and roughly 5 to 25% for the 300 Gauss case. Results vary with size and also depend on whether the system is skid mounted or field erected (Kalk *et al.*, 1986).

6.4.6 Power Benefits of Microbubble Aeration

As previously described, 100 and 300 Gauss field strengths represent values appropriate for microbubble and traditional sparging operation of a MFB bioreactor respectively. Regardless of exact values, microbubble aeration has been demonstrated to reduce the magnetic field required (and thus power) to prevent mixing in a MFB as

compared to traditional sparging aeration. The comparison of power consumption per volume for the 100 and 300 Gauss cases demonstrates the power and cost savings potential of microbubble aeration. The 100 Gauss case has power per volume ratios roughly one-half order of magnitude lower than the 300 Gauss case.

While additional power is required to generate the microbubbles, the power required should be small compared to the amount saved over standard sparging. A microbubble MFB system may consist of a MFB and a smaller CSTR for microbubble generation. The microbubble CSTR is expected to be small in comparison with the volume of the MFB or a CSTR fermenter. The microbubble generation power is expected to be small in comparison with the power savings incurred by use of microbubbles instead of traditional sparging. Improved microbubble generator designs such as that of Michelsen *et al.* (1990) may further reduce power requirements. An additional benefit of microbubble aeration over traditional sparging is the reduction in capital costs. A decrease in required magnetic field strength yields a decrease in solenoid thickness and therefore cost.

6.5 Conclusions

The MFB bioreactor is a promising reaction system for plug-flow processing of immobilized plant cells. A three-phase system is not needed at the laboratory scale, but would become necessary at large scale. The MFB scales up favorably with regard to power per volume requirements. Calculations indicate that an order of magnitude reduction in power consumption can be achieved over a traditional CSTR fermenter. Added capital costs for the solenoid are expected to be very reasonable. MFB bioreactors

can be designed with aspect ratios approximating an axially uniform magnetic field. The benefits of microbubble aeration over sparging aeration include a significant reduction in power required to prevent solids mixing in the MFB.

7. PLANT STUDIES IN THE DGC

7.1 Introduction

A wide variety of plant secondary metabolites have value as pharmaceuticals, food colors, flavors and fragrances. Plant pharmaceuticals include taxol, genistein, codeine, morphine, quinine, shikonin, ajmalacine, and serpentine. Food product examples are anthocyanins, saffron, vanilla, mint, and a variety of fruit and vegetable flavors. Industrial application of plant cell culture has been limited by drawbacks including slow growth rates, low product yields, and poorly understood metabolic regulation. Plant growth rates and levels of secondary metabolites produced are strongly influenced by key effector variables such as carbon source, nitrogen source, hormones, precursor compounds and pH. However, efforts to increase production levels typically rely on trial-and-error studies. Because of the large number of potential effector combinations, and slow plant cell growth rates, screening studies in shake flasks or petri dishes can be very labor intensive and time consuming. The DGC has been proposed as a tool for greatly accelerating these trial-and-error studies.

The overall goal of this work was to establish the DGC as a tool for studying plant cell growth and product formation as a function of chemical concentration. Research was also conducted in order to demonstrate the use of image acquisition and processing as a non-invasive assay for plant cell growth. Immobilized soybean cells were exposed to pseudo-steady-state chemical gradients in a DGC. Images documenting cell growth in the DGC were acquired over two to three weeks, and the cell and chemical gradients were

measured at the end of the experiment. Soybean cells were also exposed to chemical gradients of compounds which were expected to effect secondary metabolism, and therefore the accumulation of daidzein and genistein. Experimental protocols developed in this study included a method of pouring DGC gels which provided a rapid approach to a steady-state gradient, and correlation of image grayscale with soybean cell concentration.

7.2 Materials and Methods

7.2.1 Chemicals

All chemicals for Gamborg B5 medium were purchased from Sigma Chemical (St. Louis, MO) except sucrose from J. T. Baker (Phillipsburg, NJ). Agar and 2,4-dichlorophenoxyacetic acid were purchased from Sigma Chemical. Ampicillin was purchased from Sigma Chemical, and Timentin was purchased from SmithKline Beecham (Philadelphia, PA). Helium was purchased from AGA Gas (Cleveland, OH). Acetonitrile and acetic acid were purchased from EM Science (Gibbstown, NJ). All other chemicals were purchased from J. T. Baker.

7.2.2 Diffusion Gradient Chamber System

A detailed description of the DGC has been given by Emerson *et al.* (1994). The system is comprised of a DGC (shown in Figure 36), lightbox, reservoir flasks, tubing, and peristaltic pump. The chamber, which is machined from a polycarbonate block by Koh Development (Ann Arbor, MI), consists of an arena and recessed reservoirs. The reservoirs are also made from polycarbonate, and each contains a stainless steel inlet port (1.0 mm i.d.) and outlet port (2.5 mm i.d.). The reservoirs are separated from the arena by a 0.05 μm pore size membrane, allowing permeation of small molecules. The arena is 5 cm

by 5 cm by 2.8 cm high. The reservoirs have a volume of 3 mL. Reservoir concentrations were maintained by pumping solutions from 1 L Erlenmeyer flasks to the reservoirs through 0.8 mm ID Norprene tubing (Cole Parmer, Chicago) using a peristaltic pump (Cole Parmer). The solution exiting the reservoir returned to the reservoir flask via 1.6 mm ID Norprene tubing. The entire DGC assembly was sterilized by autoclaving and subsequent manipulations were done in a laminar flow hood.

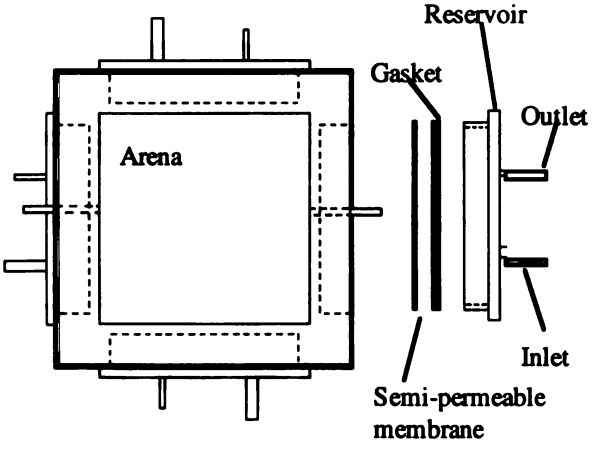

Figure 36. Diagram of the Diffusion Gradient Chamber top view.

The gel in the DGC was poured in three layers as shown in Figure 37. After tilting the chamber, Layer 1 was poured. This layer consisted of 20 mL of 0.3% agar and the chemoeffector of interest at the source flask concentration. The angle of the chamber was adjusted so that the gel extended along the bottom of the arena just reaching the side wall. Once the gel had cooled and solidified, the chamber was returned to level and Layer 2 was poured. This layer consisted of 20 mL of 0.3% agar containing the chemoeffector of interest at the sink flask concentration. Plant cell inoculum was prepared by passing a 2

week-old culture through a 400 micron mesh. Layer 3 was prepared by diluting a portion of the filtrate 1:2 with 0.6% agar containing the chemoeffector of interest at the source flask concentration. Once Layer 2 had solidified, 10 mL of the inoculum-agar (Layer 3) was poured and allowed to solidify.

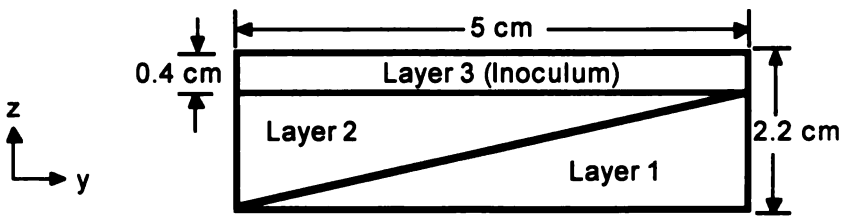

Figure 37. Schematic side-view of DGC showing three slabs.

A slightly different procedure was used for isoflavonoid accumulation studies. Soybean tissue which passed a 1 mm mesh was collected in a 100 micron mesh. The cells were added directly to 0.3% agar with the appropriate chemoeffector concentration. This method provided greater cell mass for isoflavonoid extraction and quantification. Experiments were run for approximately 1 week, compared to 2 to 3 weeks for growth studies.

Once the chamber lid was fastened, the DGC was placed on a lightbox that accommodated three chambers. The lightbox had (2) 30 cm fluorescent bulbs mounted on opposing sides of the box and black felt on the bottom. This arrangement provided diffuse, dark-field illumination of cells. The bottom of the lightbox was covered with black felt to provide contrast as viewed from above. Images of the chambers were captured with either a Macintosh system consisting of a Power Macintosh 7200/90 (Apple Computer, Cupertino, CA) and a Color QuickCam (Connectix, San Mateo, CA), or a PC system

consisting of a Gateway P5-60 (North Sioux City, SD), WinVisionPro video capture card (Quanta, Mountain View, CA), and a Pulnix TM-7CN CCD camera (Sunnyvale, CA). The lightbox and cameras were housed in a temperature controlled room at 28°C.

Swelling or drying of the gel in the arena was found to be sensitive to the height difference between the top of the agar in the DGC and the outlet of the reservoir flask return tubing. As the correct height difference could not be predicted *a priori,* flask heights were adjusted accordingly to prevent swelling or drying.

7.2.3 Chromatography

Sucrose and ampicillin analyses were conducted using high performance liquid chromatography (HPLC). A Waters (Milford, MA) 600 multisolvent pump, Waters 490 multiwavelength UV absorbance detector, and Waters 410 differential refractometer comprised the system. A 25 cm by 4.6 mm Supelco (Bellefonte, PA) LC-NH_2 column was used for sucrose. A 25 cm by 4.6 mm Rainin (Woburn, MA) Microsorb-MV column containing 5 μm C-18 packing was used for ampicillin. Gas chromatography of the DGC head space was performed on a Perkin Elmer (Norwalk, CT) Autosystem Gas Chromatograph with a thermal conductivity detector. Fixed gases were separated on a 9.1 m by 2.2 mm Hayesep DB 100/120 SS column (Alltech) with helium as the mobile phase. HPLC measurement of daidzein and genistein has been described in Section 4.2.2.2.

7.2.4 Soybean Culture

Suspension cultures of *Glycine max* cv. Mandarin have been described in Section 4.2.5.

7.2.5 Grayscale and Concentration Correlation Experiments

Experiments were conducted to verify a linear relationship between light intensity (as grayscale values) and plant cell concentration (on a dry weight basis) in the DGC. A DGC was filled with plant cell culture and water to a total volume of 10 mL. The ratio of culture to water was varied to control cell concentration. Various plant morphologies were tested, including cultures that were unsieved, cultures passed through a 400 μm sieve, cultures passed through a 1 mm sieve, and cultures previously immobilized and grown in agar. The mean grayscale value for the DGC arena in each image was obtained using NIH Image (National Institutes of Health, http://rsb.info.nih.gov/NIH-IMAGE/).

7.2.6 Soybean Growth Experiments

The effects of several different types of chemoeffectors were tested: carbon source, nutrient salt, antibiotic, nitrogen source, hormone, vitamin, and isoflavonoid precursor. The chemoeffectors and their source flask concentrations are listed in

Image Acquisition and Processing

Images of the DGC arena were acquired over the course of each experiment with a CCD camera. Images were acquired at intervals from 1 to 3 days at 640 by 480 pixels resolution. In both image acquisition systems, variation in picture brightness (flickering) was observed as the image was continually refreshed. Triplicate images were taken and averaged to reduce the effect of this variation.

Table 7. In all cases, the sink flask contained none of the chemoeffector. For ampicillin and Timentin experiments, the sterile filtered antibiotics were added after autoclaving. For

the ammonium sulfate experiment, components of the B-5 basal salt mixture were added individually excluding ammonium sulfate to prepare the medium.

7.2.7 Image Acquisition and Processing

Images of the DGC arena were acquired over the course of each experiment with a CCD camera. Images were acquired at intervals from 1 to 3 days at 640 by 480 pixels resolution. In both image acquisition systems, variation in picture brightness (flickering) was observed as the image was continually refreshed. Triplicate images were taken and averaged to reduce the effect of this variation.

Table 7. List of chemical gradients used in DGC experiments.

Gradient Chemical(s)	Source Flask Concentration	Times Normal Value
Sucrose	20 and 30 g/L	1 and 1.5
Gamborg B5 Salts	9.3 g/L	3
Ampicillin	300 and 600 ppm	-
Timentin	500 ppm	-
Ammonium Sulfate	0.13, 0.40, and 0.67 g/L	1, 3, and 5
2,4-Dichlorophenoxyacetic acid (2,4-D)	2 and 5 ppm	2 and 5
Thiamine	10 ppm	1
Phenylalanine	0.1 and 1.0 g/L	-

Grayscale data were obtained over specified areas of the DGC with the plot profile function of NIH Image. Briefly, a profile window was chosen with dimensions

ranging from 4.2 to 4.6 cm along the gradient, and 3.3 to 3.8 cm perpendicular to the gradient. Profile window dimensions were chosen to exclude shadows from edges and concentration gradients due to the reservoir windows not spanning the entire width of the DGC. The plot profile function returned an average grayscale value between 0 and 255 for each pixel row perpendicular to the gradient. The initial image of each experiment was subtracted from the images at subsequent times to compensate for flaws in the DGC lid and non-uniform lighting.

7.2.8 Analytical

7.2.8.1 Post-experiment Sampling of Gel

Total sugar and/or cell concentration gradients were measured at the end of experiments. Four glass microscope slides were inserted into the gel perpendicular to the gradient dividing the slab into 5 equally sized sections. For total sugar and ampicillin, plugs of the entire depth of the agar were taken using a cut-off 1 mL autopipetor tip (approximately 5 mm diameter). Samples were taken along the gradient in two lines located 1 cm on either side of the centerline of the DGC, and centered between dividers. Gel plugs were stored frozen until assayed. The DGC gel was then partially frozen to facilitate removal of the individual sections.

7.2.8.2 Sugar Assays

Gel plugs in closed microfuge tubes were melted in a boiling water bath. Samples were centrifuged to settle any soybean tissue. Liquid samples from the supernatant were then assayed for total sugar concentration by the phenol-sulfuric method (Dubois *et al.*, 1956). Gel samples without sucrose were assayed to correct for agar interference in the

assay. Sucrose concentrations in the reservoir flasks were measured by HPLC. The isocratic mobile phase was 75% acetonitrile, 25% water, and 0.5% acetic acid flowing at 1.5 mL/min. Sucrose was detected at 6.8 minutes by a differential refractometer.

7.2.8.3 Ampicillin Assays

Gel plugs in microcentrifuge tubes were melted and centrifuged as for total sugar assays. Ampicillin stability during heating was verified experimentally. Microcentrifuge tubes containing gel with ampicillin were placed in a boiling water bath for 20 minutes. Concentrations as measured by HPLC at 5 minutes intervals did not decrease. A 0.200 mL volume of the melted gel was combined with 0.600 mL of 60% aqueous acetonitrile in a new microcentrifuge tube. The tube was vortex mixed, and injected into the HPLC. Ampicillin was quantified with the UV absorbance detector. The isocratic mobile phase was 25% acetonitrile, 75% water, and 0.5% acetic acid flowing at 1.0 mL/min. The ampicillin retention time was 9.5 minutes.

7.2.8.4 Dry Weight Assays of Gel Sections.

Gel sections were supplemented with approximately ten volumes of distilled water and heated on a hot plate to melt the agar. Water addition ensured the agar would not solidify upon cooling. Gel plugs used for total sugar assay were returned to their respective gel sections to account for soybean tissue in the plugs. Cell mass was collected on dried and tared Whatman 41 filter paper. Samples were dried overnight at 70°C and weighed.

7.2.8.5 Isoflavonoid Assays of Gel Sections

Gel sections were prepared as described above for dry weight assays except for the drying step. Cell mass which had been collected on filter paper was placed in tared microcentrifuge tubes. Extraction of cell tissue was as described in Section 4.2.8.3. Initial experiment samples, however, were extracted once with 80% aqueous ethanol and injected directly into the HPLC after centrifugation. Hydrolysis of samples was performed once it had been established that isoflavonoids were present in measurable quantities.

7.3 Theoretical

7.3.1 Unsteady-State Model of the DGC System

To study the effect of chemoeffector concentrations on plant cell growth, it is desirable to have a steady-state concentration gradient across the chamber. During the start-up phase while diffusion establishes the gradient, the largest variation from steady-state occurs. The system eventually reaches a pseudo-steady-state where reservoir flask concentrations change slowly due net diffusion across the chamber. It is desirable to minimize the time required for the pseudo-steady-state gradient to be established. Unsteady-state modeling of diffusion in the DGC provided a method for determining the time required for the 3-slab pouring method depicted in Figure 37 to approach steady state. Sucrose was chosen for the modeling studies as it was the focus of initial experiments.

Unsteady-state diffusion of sucrose through the gel is described by

$$\frac{\partial S}{\partial t} = D_S \nabla^2 S \qquad (29)$$

where S is the sucrose concentration and D_S is the diffusivity of sucrose. For the two-dimensional system depicted in Figure 37, Equation 1 becomes

$$\frac{\partial S}{\partial t} = D_S\left(\frac{\partial^2 S}{\partial y^2} + \frac{\partial^2 S}{\partial z^2}\right) \tag{30}$$

where y is the direction along the gradient and z is the vertical direction. The boundary conditions at the source and sink reservoir membranes are given by

$$\left.\frac{\partial S}{\partial y}\right|_{y=0} = \frac{k_S}{D_S}\left(S|_{y=0} - S_{Sink}\right) \tag{31}$$

for the sink reservoir and

$$\left.\frac{\partial S}{\partial y}\right|_{y=5} = \frac{-k_S}{D_S}\left(S|_{y=5} - S_{Source}\right) \tag{32}$$

for the source reservoir, where k_S is the membrane mass transfer coefficient. The source and sink flask concentrations are assumed to be constant throughout the experiment. This assumption was validated by the data. For all other boundaries, the no-flux boundary condition is applied

$$\underline{n} \cdot D_S \nabla S = 0 \tag{33}$$

where $\underline{n}$ is the unit normal vector. The source flask concentration (S_{Source}) was set at either 20 or 30 g/L. The sink flask concentration (S_{Sink}) was set at 0 g/L. The initial concentrations in the arena gel were chosen to be either those of the three-slab pouring method or a single slab initially containing no sucrose. The initial concentrations for the three-slab method were 20, 0, and 10 g/L for layers 1, 2, and 3, respectively. The initial concentrations for the single slab method were 0 g/L for all three layers.

Equations 2 through 5 were solved using the Partial Differential Equation (PDE) Toolbox in Matlab 4.2c (The Mathworks, Natick MA). The PDE Toolbox uses the finite element method with triangular elements. The PDE Toolbox was also used to determine the steady-state solution of the model using elliptic (no time dependence) equations. The steady-state solution was compared to the unsteady-state solution to determine the time necessary for the depth-averaged sucrose concentration to reach 95% of the steady-state concentration at each y-position in the chamber.

7.3.2 Parameter Determination

A diffusion coefficient (D_S) of 0.0183 cm^2/hr was calculated by a correlation (Cussler, 1984). The mass transfer coefficient (k_S) was measured experimentally. A DGC system was set up having one reservoir separated from the arena by a semi-permeable membrane, and the other three sealed-off. The membrane was coated with an approximately 1 mm thick layer of 0.3% agar to duplicate any agar effects on the membrane used in a DGC experiment. A sucrose solution was pumped through the reservoir from a flask containing 3 L of 30 g/L sucrose and recycled as in growth experiments. The DGC initially contained 45 mL of deionized water. A stir bar in the DGC arena kept the water well mixed. The mass balance on sucrose in the DGC arena (S) is

$$V_{arena}\frac{dS}{dt} = k_S A(S_{Source} - S) \qquad (34)$$

where V_{arena} is the volume of the arena, A is the area of the membrane (3.06 cm^2) available for mass transfer, and S_{Source} is the concentration of sucrose in the source flask. This equation can be solved with the initial condition $S=0$ to yield the following.

$$\ln\left(\frac{S_{bulk}}{S_{bulk}-S}\right)=\frac{k_S A}{V_{arena}}t \qquad (35)$$

Sucrose concentrations in the arena were measured over time by HPLC analysis. The value of k_S was found to be 0.26 cm/hr by fitting the model to data. The linearized model fit (not shown) had a coefficient of determination of 0.9988.

7.4 Results

7.4.1 Oxygen Limitations in the Immobilization Layer

Because the soybean cells are immobilized in agar, diffusion of oxygen from the head space could potentially limit the rate of growth. This hypothesis was tested in a preliminary DGC experiment where plant cells were uniformly distributed throughout a single slab of agar. After two weeks, the soybean had grown only near the surface of the gel in a layer approximately 3 mm thick. This system was closed, providing no replenishment of oxygen either by exchange of gas head space or reservoir media. Based on these results, plant cells were added only to the 4 mm thick top layer of agar (Layer 3 in Figure 37) in subsequent experiments.

During experiments conducted with a closed head space, the oxygen concentration in the head space, as measured by gas chromatography, was depleted by over 50% within 1 week (results not shown). To avoid such depletion in subsequent experiments, the head space was vented to the atmosphere through 0.22 μm sterile filters. Venting allowed the

DGC to maintain ambient oxygen concentrations throughout experiments (results not shown).

7.4.2 Simulation of Unsteady-State Diffusion Gradients.

For the three slab-pouring method, the model predicted 95% of steady-state would be reached within 2.1 days. The criteria for 95% of steady-state was that every finite-element node must be at greater than or equal to 95% of its steady-state value. For the single-slab method, with zero sucrose concentration throughout the gel, the corresponding time was 33.1 days. These numbers were the same source concentrations of both 20 and 30 g/L. Figure 38 shows three time profiles for the unsteady-state solution. The times shown are 1, 5, and 40 hour(s) (top to bottom) after initiation of diffusion. The side-view of chamber is depicted. The small graph on the top left is a legend for the sucrose concentration.

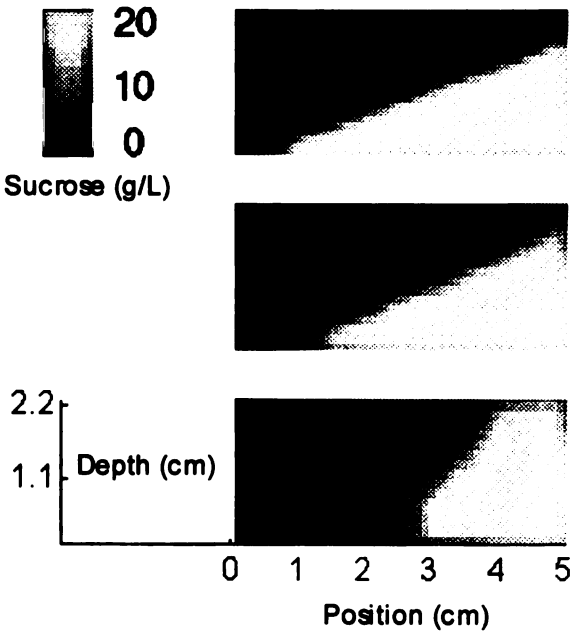

Figure 38. Simulation of approach to steady-state.

7.4.3 Grayscale and Concentration Correlation

Figure 39 shows grayscale values as a function of soybean concentration for 4 brightness settings. Each line and data set corresponds to a different brightness setting. Concentrations are given in relative units as a percent of soybean suspension (1 mm sieve) per total volume of suspension and water. In all cases, ranges existed where the grayscale values of acquired images were found to increase linearly with cell concentration. Outside of the

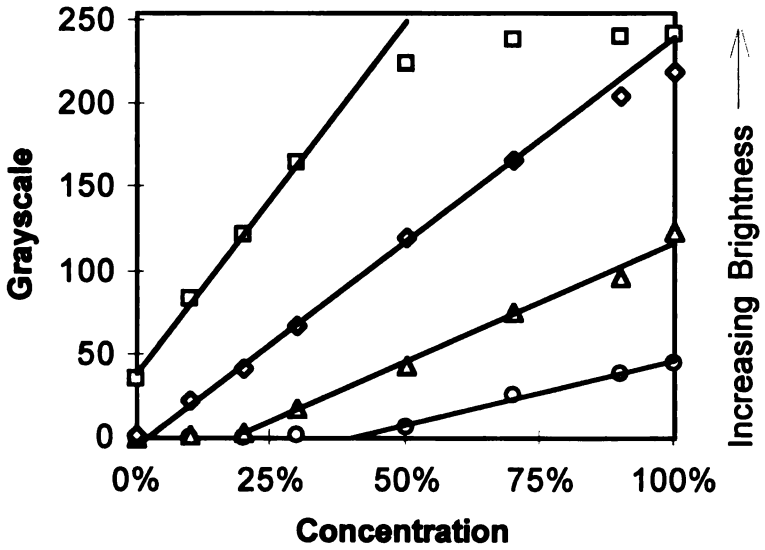

Figure 39. Correlation of image grayscale with plant-cell density.

linear range, the grayscale response becomes black and white saturated at low and high concentrations, respectively. At the highest brightness setting shown in Figure 39, grayscale is a linear function of concentration from 0 to 40%. Past 40% the response is saturated. The next three lower settings have linear ranges from 0 to 80%, 20 to 100%, and 40 to 100% respectively. The four culture types of varied morphologies produced results similar to those shown in Figure 39 although the slopes varied.

7.4.4 Growth Studies

7.4.4.1 Linearity of Diffusion Gradients

Example total sugar assays from soybean growth experiments are shown in Figure 40 for a 0 to 20 g/L gradient and in Figure 41 for a 0 to 30 g/L gradient. Results are shown for plugs taken on both sides of the centerline. The gradients predicted by the model are also shown in Figure 40 and Figure 41. At the source end of the gradient, the model agreed well with experimental data. However, total sugar assays were higher than model predictions toward the sink end of the gradient. The cause of this trend was not determined although interference by medium components was experimentally disproved. The total sugar assay of the soybean media without sucrose produced no absorbance.

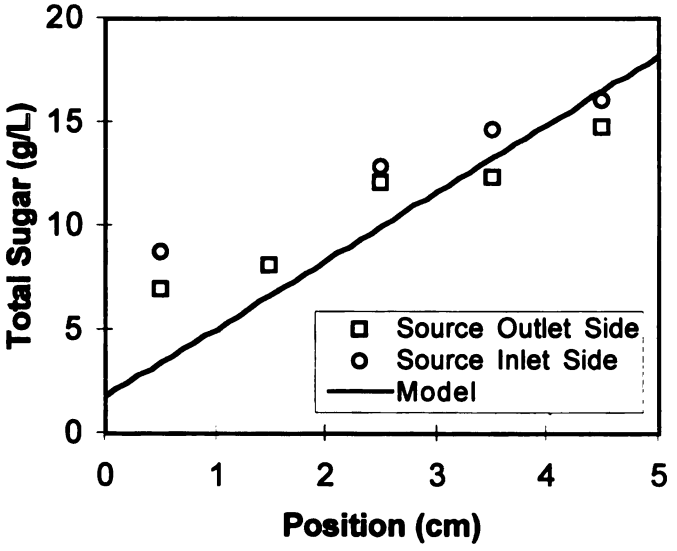

Figure 40. Total sugar gradient data and model for a 0 to 20 g/L experiment.

Sucrose concentrations in the source and sink flasks were measured for several experiments in order to verify pseudo-steady-state conditions. Losses from source flasks ranged from 0.08 to 0.41 g/L-week. For six different DGC experiments, source flask

losses were 0.26±0.13 g/L-week at a 95% confidence level. A 20 g/L source flask would therefore have an average decrease in concentration of only 1.3% per week.

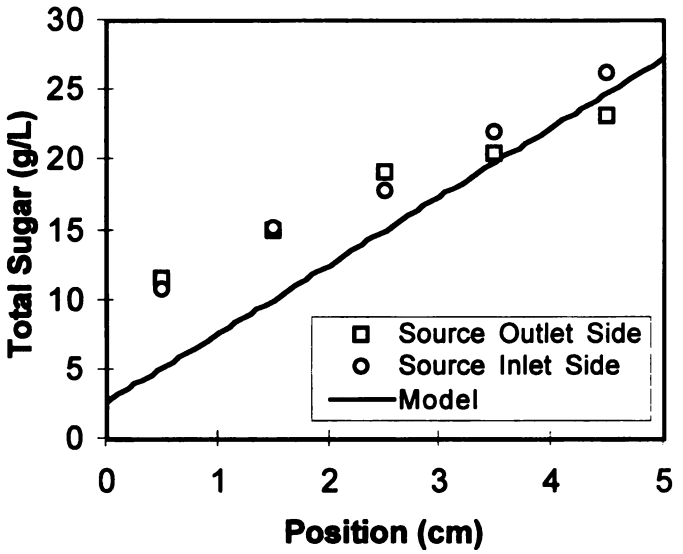

Figure 41. Total sugar gradient data and model for a 0 to 30 g/L experiment.

7.4.4.2 Effect of Sucrose

The effect of sugar concentration on soybean growth was studied in DGC experiments with reservoir flask concentrations of 0 to 20 g/L and 0 to 30 g/L. Figure 42 shows the final day image of the DGC for a 0 to 20 g/L experiment. Figure 43 shows the plot of grayscale values versus position on various days for the same experiment. As in all results shown, the source reservoir is on the right (y=5 cm), and the sink reservoir is on the left (y= 0 cm). The dark to light trend from left to right depicts increasing soybean concentration and grayscale. The series of grayscale plots shows both the spatial and temporal dependence of plant cell concentration. A maximum in concentration and thus growth rate is seen near the source reservoir.

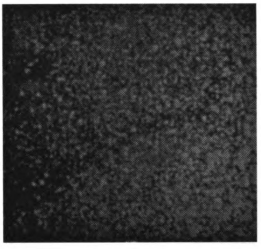

Figure 42. Image from day 13 of a 0 to 20 g/L sucrose experiment.

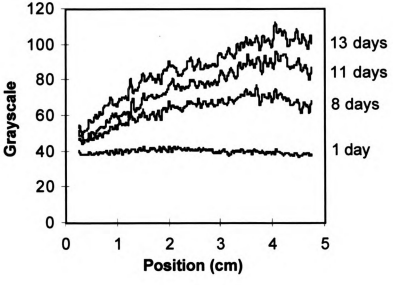

Figure 43. Grayscale profiles for a 0 to 20 g/L experiment.

Decreased soybean growth at higher sucrose concentrations was observed in one of the 0 to 20 g/L experiments and all of the 0 to 30 g/L experiments. Figure 44 shows an example grayscale obtained for a 0 to 30 g/L experiment. The maximum cell concentration occurred slightly past 1 cm from the sink reservoir. Based on total sugar assays of the gel, a concentration of approximately 14 g/L was determined to be optimal for growth

(maximum cell concentration). Essentially no growth occurred at concentrations above 20 g/L.

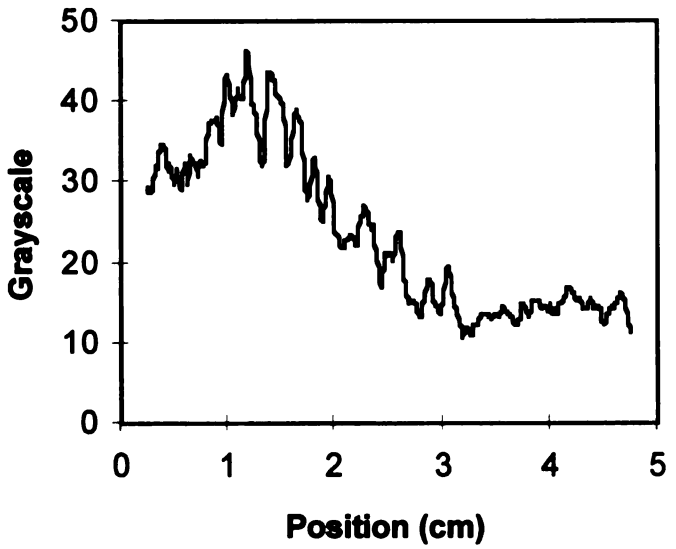

Figure 44. Grayscale profile from day 14 of a 0 to 30 g/L experiment.

Figure 45 and Figure 46 show the chamber image and final grayscale plots for a second 0 to 30 g/L experiment. In contrast to other experiments, the plant cell concentration also varied perpendicular to the gradient. Plant cell concentrations were higher in the outlet half of the chamber at high sucrose concentrations, as seen in both the chamber image and grayscale plots of each side. This result is explained by total sugar assay data. Figure 47 shows total sugar concentrations for the experiment. While the gradient was linear on the source outlet side, the gradient did not appear to be linear on the source inlet side. Furthermore, past roughly the 3 cm position the total sugar concentrations were significantly higher on the source inlet side. The outlet side of the chamber in which total sugar concentrations reached less than 20 g/L had growth all the way to the source-reservoir edge of the DGC. The inlet side, however, reached over 25

g/L, and growth stopped at approximately 20 g/L. Maximum growth appeared to have occurred at approximately 10 g/L total sugar.

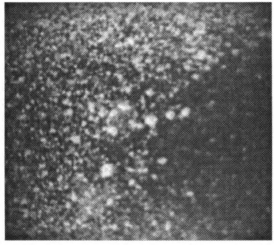

Figure 45. Image from day 14 of a 0 to 30 g/L sucrose experiment.

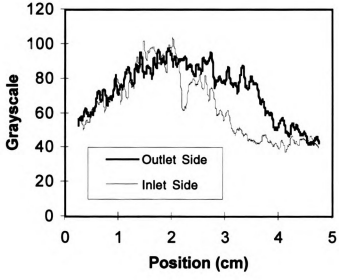

Figure 46. Grayscale profiles for inlet and outlet halves of the DGC.

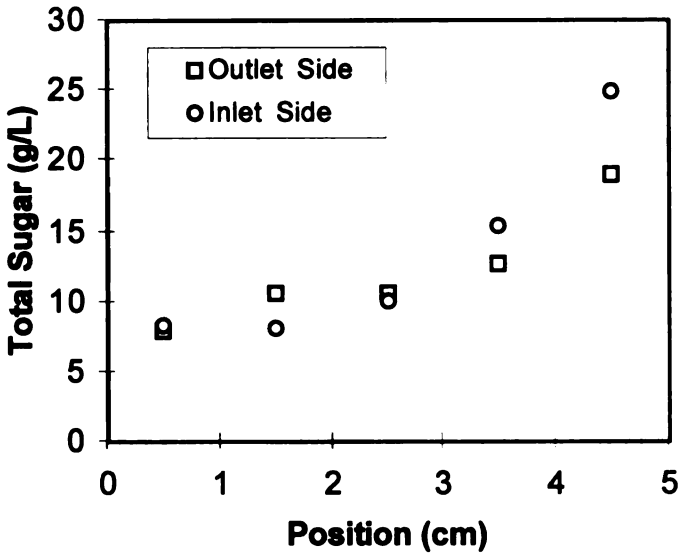

Figure 47. Total sugar assays for inlet and outlet halves of the DGC.

7.4.4.3 Effect of 1-B5 Medium Components

Three components of Gamborg 1-B5 medium were tested for their effect on soybean growth: basal salt mixture, 2,4-D, and ammonium sulfate. Figure 48 shows the final day image and Figure 49 shows the grayscale plot for a basal salt experiment with sink and source flask concentrations of 0 g/L and 9.3 g/L respectively. Soybean growth was significantly affected by salt concentration. Maximum growth occurred around the recommended concentration (3.1 g/L) used in 1-B5 medium. Less marked results were seen with the 2,4-D experiment ranging from 0 to 2 ppm (results not shown). Maximum growth occurred near the center of the chamber which corresponds to the normal concentration of 2,4-D (1 ppm) in the Gamborg 1-B5 medium. The experiment utilizing an ammonium sulfate gradient of 0 to 0.67 g/L showed little effect of nitrogen concentration on growth (results not shown). The gradient ranged from 0 to 5 times the normal medium concentration in the sink and source flasks respectively. The grayscale

plot on the final day was essentially flat except for somewhat lower values near the sink reservoir. These results indicate that nitrogen levels above that in the normal 1-B5 medium did not enhance or retard growth.

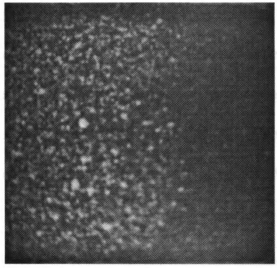

Figure 48. Image from day 13 of Gamborg basal salts experiment.

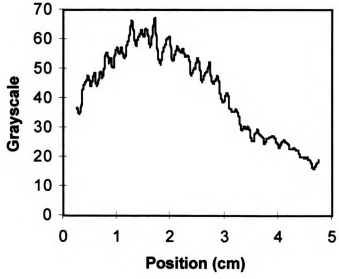

Figure 49. Grayscale profile from day 13 of Gamborg basal salts experiment.

7.4.4.4 Effect of Antibiotics

Figure 50 shows the results for a Timentin gradient ranging from 0 to 500 ppm in the sink and source flasks respectively. Soybean concentration appears to diminish beyond the 2 cm position. Figure 51 shows grayscale results for replicate experiments using a 0 to 300 ppm ampicillin gradient. While the magnitude of the grayscale varies between replicates due to camera effects and/or differences in cell density, the grayscale trends with respect to position are in good agreement. Ampicillin appears to inhibit growth around the 4 cm position. Figure 52 shows a comparable experiment for a 0 to 600 ppm ampicillin gradient. In this experiment, inhibition appears to start at the center of the chamber.

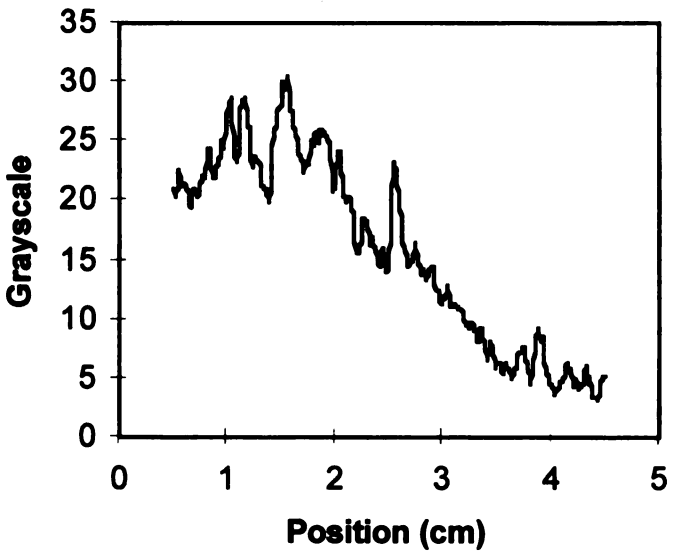

Figure 50. Grayscale profile for day 11 of a Timentin experiment.

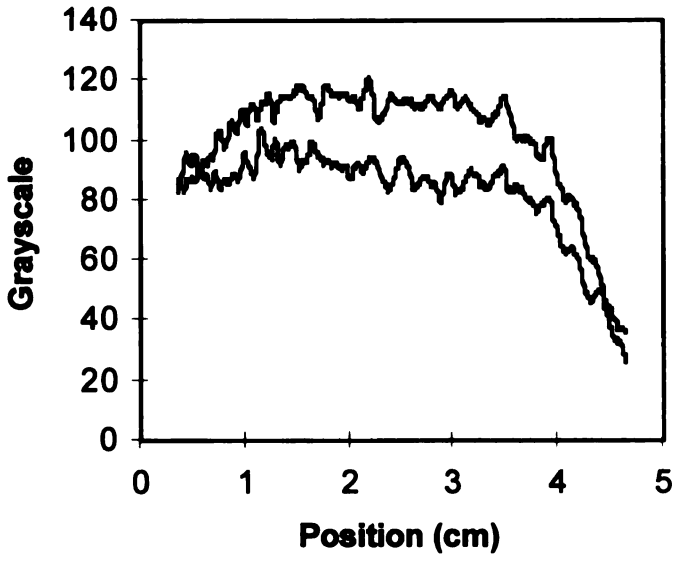

Figure 51. Grayscale profiles for day 15 of replicate 300 ppm ampicillin experiments.

Ampicillin gradients were measured for the 300 and 600 ppm experiments. All three experiments had essentially linear gradients of ampicillin (results not shown). However, these concentrations were well below expected values. The average concentration for the 300 ppm experiments at the 4.5 cm position was 84 ppm. The average concentration for the 600 ppm experiment at the 4.5 cm position was only 34 ppm. Values much closer to source flask concentrations were expected. A significant difference between these experiments was their duration. The 300 ppm experiments lasted 15 days while the 600 ppm experiment lasted 23 days. Assays of the reservoir source flasks indicated an average decrease of 43% for the 300 ppm experiments and a decrease of 54% for the 600 ppm experiment.

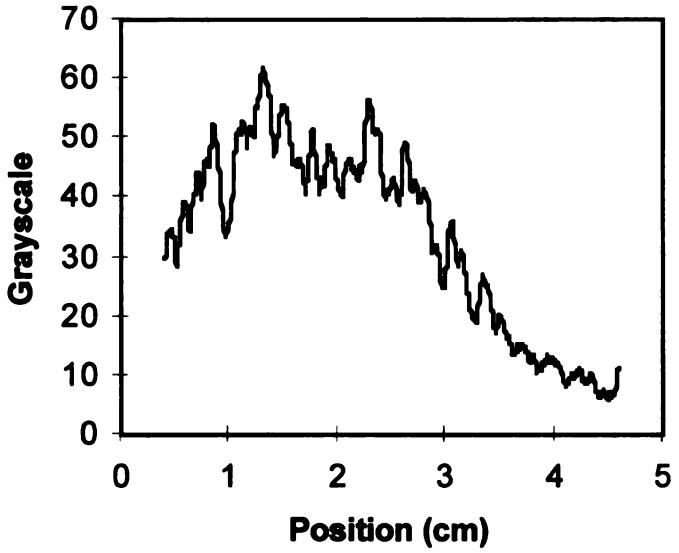

Figure 52. Grayscale profile for day 23 of 600 ppm ampicillin experiment.

7.4.5 Isoflavonoid Production Studies

Three DGC experiments were run with gradients of ammonium sulfate, which is the sole source of reduced nitrogen supplied in the Gamborg 1-B5 medium. Daidzein and genistein concentrations for experiments with source flask concentrations of 1, 3, and 5 times the normal value are shown in Figure 53, Figure 54, and Figure 55, respectively. Concentrations are reported as μg isoflavonoid per g of dry cell mass. Figure 53 shows a clear trend of increasing isoflavonoid production with increasing supply of nitrogen. A similar trend is not seen in Figure 54 or Figure 55. Similarities are limited to a maximum genistein level at intermediate values. Soybean stock cultures were also different among the runs however. Soybean suspension culture used in Figure 53 was grown in ammonium sulfate free medium for the 2 week cycle prior to use.

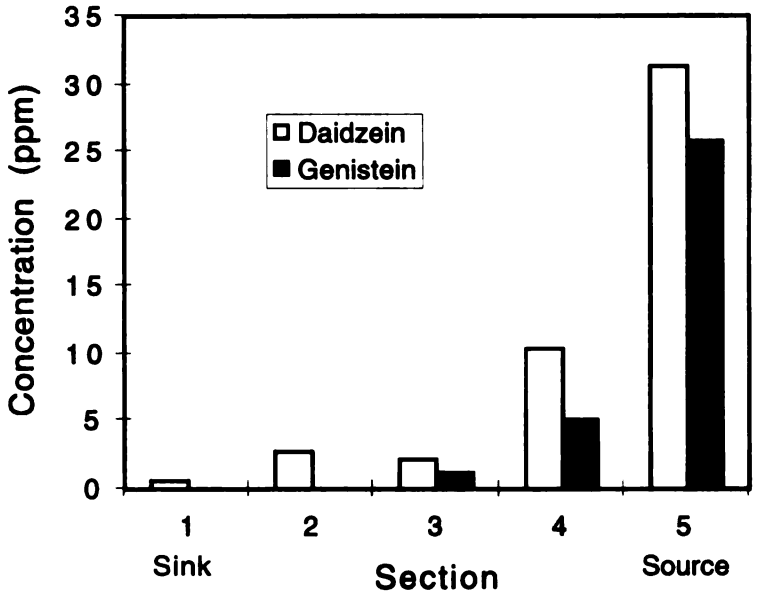

Figure 53. Free isoflavonoid concentrations for 0 to 1x nitrogen gradient.

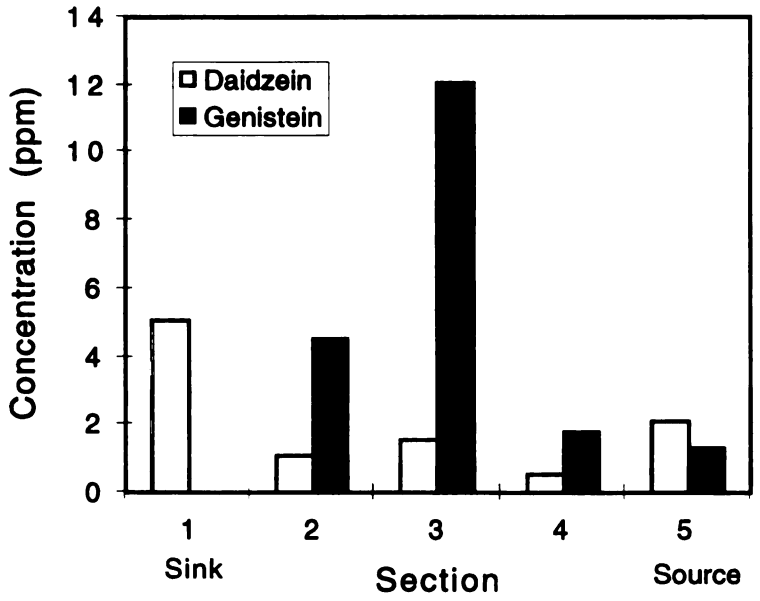

Figure 54. Free isoflavonoid concentrations for 0 to 3x nitrogen gradient.

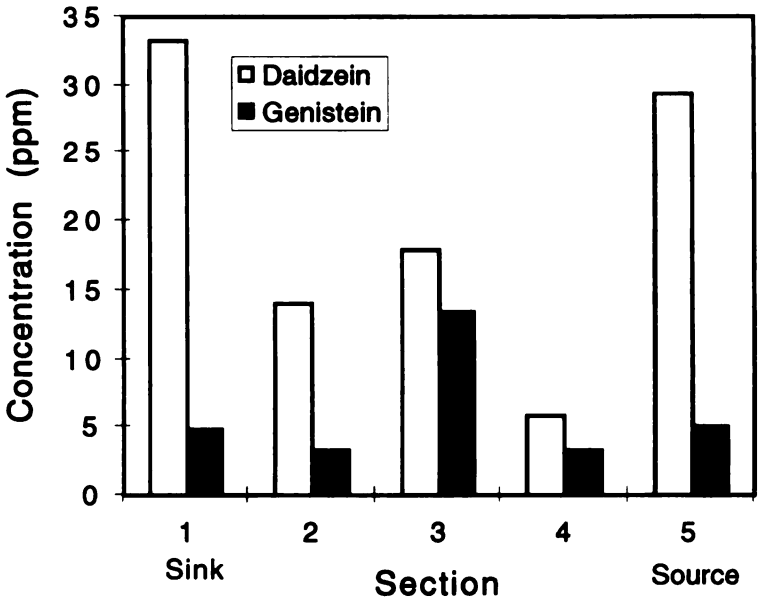

Figure 55. Total isoflavonoid concentrations for 0 to 5x nitrogen gradient.

Two other medium components were tested, thiamine and 2,4-D. The results for the thiamine experiment are shown in Figure 56. A trend of increasing isoflavonoid concentrations with thiamine is illustrated. Isoflavonoids were not detected in sections 1 and 2, explained in part by the low quantity of tissue which was available for extraction. Figure 57 shows the results of the 2,4-D experiment with a source reservoir concentration of 5 ppm. Maximum isoflavonoid concentrations occur in the second section, where 2,4-D is expected to be at 1 to 2 ppm.

Phenylalanine, a precursor to daidzein and genistein, was tested in 2 experiments. Figure 58 and Figure 59 show the results for 0 to 1.0 g/L and 0 to 0.1 g/L phenylalanine experiments, respectively. The 0 to 1 g/L gradient produced a flat profile for both isoflavonoids. The 0 to 0.1 g/L gradient produced a maximum however. Production is

maximum in the second section, with the greatest contrast between sections 2 and 3. The maximum is expected to be at approximately 50 ppm phenylalanine.

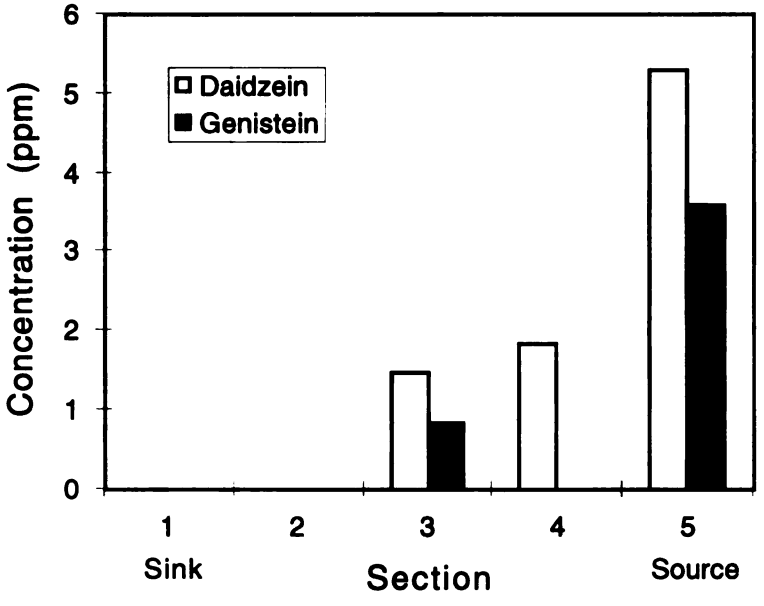

Figure 56. Free isoflavonoid concentrations for 0 to 1x thiamine gradient.

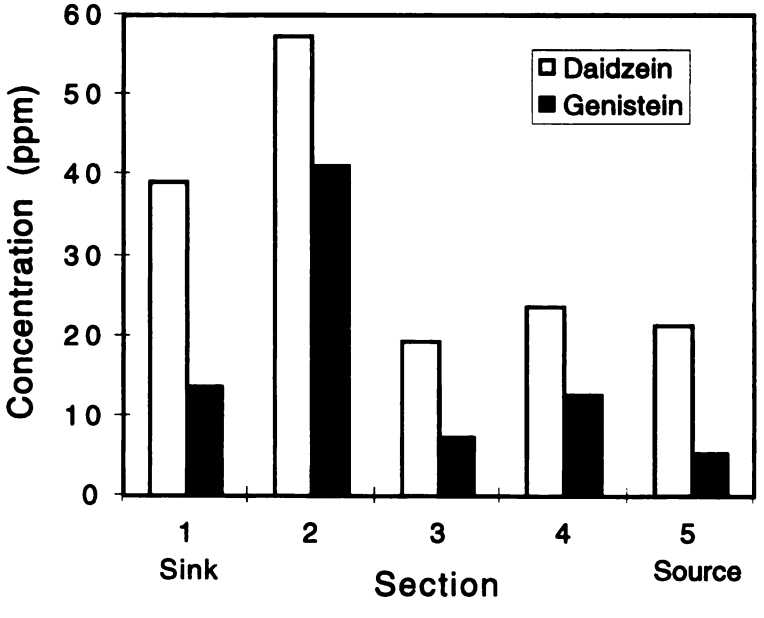

Figure 57. Total isoflavonoid concentrations for 0 to 5x 2,4-D gradient.

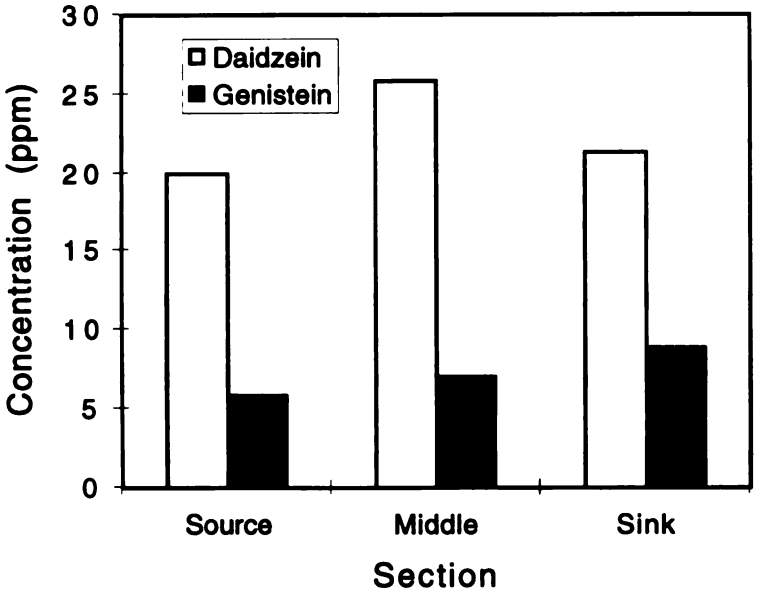

Figure 58. Free isoflavonoid concentrations for 0 to 1 g/L phenylalanine gradient.

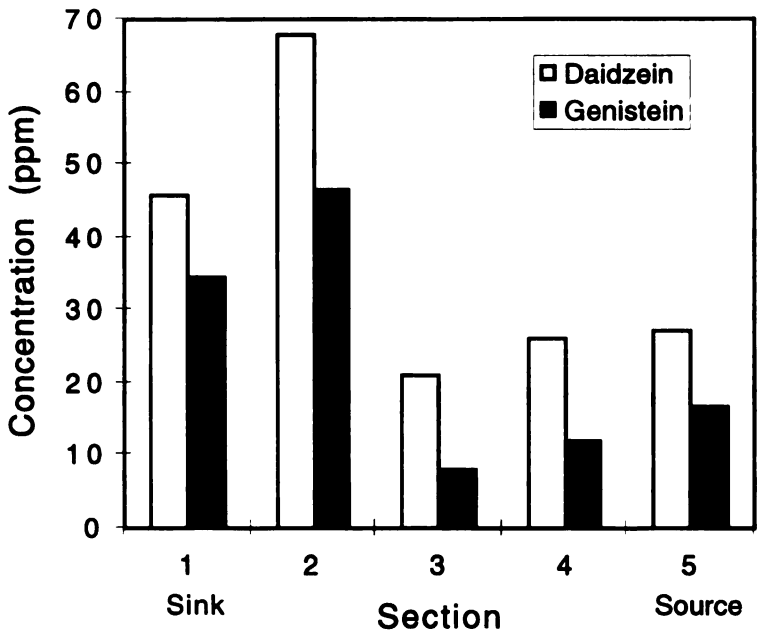

Figure 59. Total isoflavonoid concentrations for 0 to 0.1 g/L phenylalanine gradient.

7.5 Discussion

7.5.1 Correlation of Grayscale and Concentration

Image acquisition and analysis was found to provide a suitable, non-invasive, on-line method for monitoring plant cell growth in the DGC. An important feature of the image acquisition software used in this work was the adjustable brightness setting. As seen in Figure 39, no single setting allowed for a linear relationship across the entire range of concentrations. S-curves with black and white saturation at either extreme are seen. By adjusting the brightness, however, a linear region can be obtained for the concentration of interest. A large range of concentrations could potentially be spanned by using multiple brightness settings. The trade-off for decreased brightness, and therefore the ability to work in a linear response range at higher concentrations, is a loss of sensitivity. This trend is seen in Figure 39 as decreasing slopes for decreasing brightness settings. An optimum setting could be chosen for a particular application by finding the brightest setting which gave a linear response over the entire concentration range of interest.

Cell density data from the final day of several experiments were collected in order to supplement grayscale data. Correlation of final day cell density and grayscale from sections was poor as indicated by low coefficient of determination (r^2 = 0.31±0.33) values. While sections of a grayscale image are exactly the same size, DGC gel sectioning introduced error. Calculations assume that all sections are equal. Residual, unmelted gel can remain with the plant tissue when dried and weighed, increasing the measured cell mass. For some experiments, the concentration gradient was shallow across the sections, yielding a flat plot of grayscale versus concentration, and thus a low coefficient of

determination. It should be noted that these problems were not present in the greyscale and dry weight correlation work described above. Image analysis provided greater sensitivity and precision within any single experiment than dry weight measurement.

7.5.2 Suitability of DGC for Growth Studies

Sugar gradient data and modeling indicated that the DGC method can approximate steady-state conditions in order to study plant cell culture growth. Diffusion of sucrose across the arena and consumption by plant cells, were found to have a minimal impact on reservoir flask sucrose concentrations. Although non-linear gradients could arise due to cellular consumption of metabolites, no evidence of such gradients was seen except for Figure 47 which is likely explained by reservoir non-idealities discussed below.

For the linear gradients shown in Figure 40 and Figure 41, the total sugar concentrations were higher than model predictions. This result may be explained in part by extracellular hydrolysis of sucrose to glucose and fructose by cell wall invertases (Fowler, 1982). The hydrolysis is a rapid process compared to consumption (Hooker and Lee, 1992) and may, therefore, increase the concentration driving force for sucrose diffusion across the DGC arena. The total sugar assay used in this study would collectively quantify the sucrose and its hydrolysis products glucose and fructose.

Measured ampicillin concentrations were significantly lower than expected at the end of the experiments. Degradation and uptake by plant cells are two possible explanations. In either case, the actual concentrations to which the cells were exposed were different than those predicted assuming a linear gradient based on initial ampicillin concentration. The results indicate that whenever possible, assays of the chemoeffector

should be conducted when working with a new compound and/or culture to determine the significance of uptake or degradation. In cases where degradation is not significant, then such results would provide information about the rate of cellular uptake.

7.5.3 Non-Ideality of DGC Reservoirs

Several sucrose experiments yielded inlet- and outlet-side concentration gradients for total sugar that were not equal. Examples of this trend are shown in Figure 40 and Figure 47. This result is attributed to flow patterns in the reservoir. To prevent swelling of the gel or flooding of the arena, low reservoir flow rates were used initially. These low flow rates may have led to concentration gradients in the x-direction within the reservoirs. In subsequent experiments having a flow rate greater than approximately 6 mL/h, the problem did not reappear.

7.5.4 Determination of Optimum Growth Conditions

The optimal concentrations of Gamborg salts and 2,4-D were essentially that of Gamborg 1-B5 medium. This was not the case for sucrose gradient experiments however, which suggested that sugar concentrations became inhibitory above 15 g/L to the immobilized soybean cultures. In the original report on formulation of the B5 medium (Gamborg *et al.*, 1968), the authors found that soybean cell yields increased with sucrose concentration up to 20 g/L sucrose. Furthermore, plant cell growth kinetics are commonly described by a Monod model when sucrose or glucose is the carbon and energy substrate (Hooker and Lee, 1992; van Gulik *et al.*, 1992; Guardiola *et al.*, 1995; Westgate *et al.*, 1991; Schnapp *et al.*, 1991). The Monod model is incapable of describing substrate inhibition. Other reports of sucrose inhibition at this level are unknown to the authors.

Cell growth can be studied under steady-state conditions using other experimental systems such as a CSTR. However, several different steady-states would need to be achieved to determine the effect of the dependent variable for a range of values. Such information can be obtained in a single DGC experiment. Genetic instability of some plant cultures adds complexity to the comparison of multiple experiments. DGC studies yield a continuum of data from a single inoculum. While multiple replicates could be run in CSTRs or shake flasks, this approach is expensive due to the demand for equipment or manpower. Finally, image capture provides a quick and non-invasive method of data acquisition not available in the other systems.

7.5.5 Determination of Optimum Isoflavonoid Conditions

DGC experiments which focused on isoflavonoid quantification were performed after the methods for growth studies had been established. The chemoeffectors chosen for these studies were largely those used in growth studies, with the addition of a vitamin and an isoflavonoid precursor. Nitrogen was chosen for study as its levels affect secondary metabolism in numerous biological systems. Nitrogen is also present in the amino acid phenylalanine. The conversion of phenylalanine to cinnamic acid by phenylalanine ammonium lyase (PAL) is the branch point from primary to secondary metabolism (Barz and Welle, 1992). As ammonium sulfate is the only reduced nitrogen source, its availability was expected to be important (Gamborg *et al.*, 1968). By the same logic, phenylalanine was also tested. It was hypothesized that a small pool of phenylalanine, and thus a slow conversion by PAL, could be rate limiting in the isoflavonoid pathway. The hormone 2,4-D was chosen as its negative effect on secondary metabolite production

has been reported. Thiamine was chosen as the vitamin which is provided in the highest quantity in the soybean medium.

The nitrogen studies shown in Figure 53, Figure 54, and Figure 55 do not show a consistent trend such as an optimum level of ammonium sulfate. Three gradient slopes were tested in search of an optimum level. However, the results indicate that the history of the cell culture used in the study is important. The experiment illustrated in Figure 53 used cells which had been deprived of ammonium sulfate, while the others did not. The 0 to 1x experiment was conducted with the assumption that nitrogen was not rate limiting under normal conditions, but that a rate limitation could be induced. While the effect was significant for this first experiment, additional runs focused on conditions useful for bioreactor operation. Increased ammonium sulfate levels would only be of value if isoflavonoid production was enhanced for normal (non-deprived) cells. The results in Figure 54 and Figure 55 indicate that there is not a significant benefit from elevated nitrogen levels.

Supplementation of phenylalanine appeared to have a marginal effect on isoflavonoid production. For the steep 1 g/L gradient shown in Figure 58, the flat profile is inconclusive. Supplementation may have had no effect. Alternatively, the effect may have been saturated very close to the sink reservoir. The latter was hypothesized and tested with the 0.1 g/L experiment. Figure 59 indicates that isoflavonoid production is effected by supplementation. The results also indicate that bioreactor operation may benefit from supplementation, but not with a large improvement in productivity. While a comparison of concentrations from these experiments would be useful, this must be done

with caution as Figure 58 reports only free isoflavonoids while Figure 59 reports total isoflavonoids. In general, comparison between DGC experiments which use different inoculums must be done cautiously. While replicate growth studies have demonstrated consistency with DGC methods, variation in plant cell culture can lead to dramatic differences in isoflavonoid levels over time.

7.6 Conclusions

The Diffusion Gradient Chamber (DGC) has been demonstrated as a tool for studying the effects of chemical concentrations on plant cell culture growth and product formation. Image acquisition provided a sensitive, non-invasive method for tracking growth over the course of an experiment, based on the linear relationship between image grayscale and cell concentration. Medium components and antibiotics were found to affect soybean cell culture growth. Optimal concentrations for Gamborg B5 salts and 2,4-D were found to be in the range of normal medium component values. Inhibition of growth was seen for the antibiotics ampicillin and Timentin, and for total sugar concentrations above 15-20 g/L. Nitrogen source, phenylalanine, 2,4-D, and thiamine were found to affect production of daidzein and genistein. Optimal conditions for productivity appeared to be within recommended medium values excepting a potential benefit from phenylalanine supplementation.

8. SUMMARY AND CONCLUSIONS

Continuous isoflavonoid production from soybean with biocatalyst throughput was demonstrated in a MFB bioreactor for over 2 months. Plug-flow biocatalyst movement was observed, utilizing a magnetic valve for solids. Both biocatalyst microscopy and Thiele modulus calculations indicated that intra-biocatalyst oxygen diffusion was not significant.

Continuous operation has been demonstrated past start-up to the point of steady growth rates and sugar concentrations. However, modeling indicated that achievement of steady-state is dependent on the inherently long, liquid residence time. Contamination of the long-term continuous bioprocess, and plant cell growth on the exterior of the immobilization matrix remain concerns for process feasibility. A simple control strategy was able to maintain DO and CO_2 near target levels. Model results predicted an optimum integer interval between biocatalyst exchange of 4 days. While isoflavonoid productivity was improved from earlier runs, concentrations were well below current shake flask levels, due in part to the use of antibiotics. Daidzein, but not genistein, productivity exceeded the target level indicating commercial potential. Research is needed to better understand the relationship between isoflavonoid production kinetics and bioreactor process variables.

Based on solenoid power per volume calculations, the MFB bioreactor is feasible at large scale, but may require the use of a third (gas) phase. If needed, the gas phase could be provided by microbubbles which do not increase solenoid power consumption like

traditional sparged bubbles. The MFB scales up favorably with regard to power per volume requirements. Calculations indicate that an order of magnitude reduction in power consumption can be achieved over a traditional CSTR fermenter. Added capital costs for the solenoid were estimated to be reasonable.

The Diffusion Gradient Chamber (DGC) was demonstrated as a tool for studying the effects of chemical concentrations on plant cell culture growth and product formation. Image acquisition provided a sensitive, non-invasive method for tracking growth over the course of an experiment, based on the linear relationship between image grayscale and cell concentration. The DGC was used for determining optimal medium constituent concentrations, and inhibitory levels of toxic compounds. Secondary metabolite (isoflavonoid) accumulation was also studied. Optimal conditions for productivity appeared to be within recommended medium values excepting a potential benefit from phenylalanine supplementation. However, DGC studies could be expected to yield significant insight to productivity improvements for a plant bioprocess where medium optimization studies have yet to be done.

LIST OF REFERENCES

9. LIST OF REFERENCES

Adesanya, S.A., O'Neill, M.J., Roberts, M.F. (1986) Structure-related fungitoxicity of isoflavonoids, *Physiol. and Mol. Plant Path.*, **29**, 95-103.

Aiba, S., Humphrey, A.E., Millis, N.F. (1973) *Biochemical Engineering*, Academic Press, New York.

Akiyama, T., Ishida, J., Nakagawa, S., Ogawara, H., Watanabe, S., Itoh, N., Shibaya, M., Fukami, Y. (1987) Genistein, a specific inhibitor of tyrosine-specific protein kinases, *J. Biol. Chem.*, **262**, 5592-5595.

Ames, T.T., Thompson, V.S., Worden, R.M. (1995) A Three Phase Magnetofluidized Bed Bioreactor for Production of Plant Secondary Metabolites, *Annual Meeting of American Institute of Chemical Engineers*, Miami Beach, FL, November 14, 1995.

Ames, T.T., Worden, R.M. (1997) Continuous Production of Daidzein and Genistein from Soybean in a Magnetofluidized Bed Bioreactor. *Biotech. Prog.*, in press.

Ananta, M., Subroto, A., Doran, P. (1995) Oxygen transfer and culture characteristics of self-immobilized *Solanum aviculare* aggregates, *Biotech. Bioeng.*, **47**, 541-549.

Andrews, G. (1988) Fluidized-bed bioreactors. *Biotechnology and genetic engineering reviews*, **6**, 151-169.

Archambault, J. (1991) Large-scale (20 L) culture of surface-immobilized *Catharanthus roseus* cells, *Enzyme Microb. Technol.*, **13**, 882-892.

Atkinson, B., Mavituna, F. (1983). *Biochemical Engineering and Biotechnology Handbook*, Stockton Press, New York, 263.

Bailey, J.E., Ollis, D.F. (1986) *Biochemical Engineering Fundamentals*, McGraw Hill, New York.

Balaban, R.S., Mandel, L.J. (1990) Optical methods for the study of metabolism in intact cells, *Noninvasive Techniques in Cell Biology*, Eds. J.K. Foskett and S. Grinstein, Wiley-Liss, New York, 213-236.

Barz, W., Welle, R. (1992) Biosynthesis and metabolism of isoflavones and pterocarpan phytoalexins in chickpea, soybean and phytopathogenic fungi, *Phenolic Metabolism in Plants*, Ed. H.A. Stafford and R.K. Ibrahim, Plenum Press, New York, 139-165.

Bate, N.J. (1994) Quantitative relationship between phenyalanine ammonia-lyase levels and phenylpropanoid accumulation in transgenic tobacco identifies a rate-

determining step in natural product synthesis, *Proc. Natl. Acad. Sci.*, **91**, 7608-7612.

Bramble, J.; Graves, D.; Brodelius, P. Plant cell culture using a novel bioreactor: the magnetically stabilized fluidized bed. *Biotechnology Progress* **1990**, *6*, 452-457.

Bramble, J.L., Graves, D.J., Brodelius, P. (1990) Plant cell culture using a novel bioreactor: The magnetically stabilized fluidized bed, *Biotechnol. Prog.*, **6**, 452-457.

Bredwell, M.D., Telgenhoff, M.D., Worden, R.M. (1994) Enhancement of gas mass transfer using microbubble dispersions, *Annual Meeting of American Institute of Chemical Engineers*, San Fransico, CA, November 13-18, 1994.

Bredwell, M.D., Telgenhoff, M.D., Worden, R.M. (1995a) Formation and coalescence properties of microbubbles, *Appl. Biochem. Biotechnol.*,**51/52**, 501-509.

Bredwell, M.D., Telgenhoff, M.D., Worden, R.M. (1995b) Effects of Using Microbubble Dispersions on Synthesis Gas Fermentations, *Annual Meeting of American Institute of Chemical Engineers*, Miami Beach, FL, November 14, 1995.

Brodelius, P.E. (1990) Transport and accumulation of secondary metabolites, *Progress in Plant Cellular and Molecular Biology*, Proceedings of the VIIth International Congress on Plant Tissue and Cell Culture, Eds. H.J.J. Nijkamp, L.H.W. van der Plas and J. van Aartrijk, Kluwer Academic Publishers, Boston.

Brown, D., Groom, C., Vitanik, M., Brown, M., Cooper, J., Arditti, J. (1982) Effects of fungicides and bactericides on orchid seed germination and shoot tip cultures *in vitro*, *Plant Cell Tissue Organ Culture*, **1**, 165-180.

Caboche, M., Lark, K.E. (1981) Preferential replication of repeated DNA sequences in nuclei isolated from soybean cells grown in suspension culture, *P.N.A.S.*, **78**, 1731-1735.

Chappell, J., Halbrock, K. (1984) Transcription of plant defense genes in response to UV light or fungal elicitor, *Nature*, **311**, 76-78.

Cho, G.H., Kim, D., Pedersen, H., Chin, C. (1988) Ethephon enhancement of secondary metabolite synthesis in plant cell cultures, *Biotechnol. Prog.*, **4**, 184-188.

Cho, M.J., Harper, J.E. (1991) Effect of inoculation and nitrogen on isoflavonoid concentration in wild-type and modulation-mutant soybean roots, *Plant Physiol.*, **95**, 435-442.

Christou, P. (1994) The biotechnology of crop legumes. *Euphytica*, **74**, 165-185.

Cussler, E.L. (1984) *Diffusion: Mass transfer in fluid systems*. Cambridge University Press, Cambridge.

Darvill, A.G., Albersheim, P. (1984) Phytoalexins and their elicitors: A defense against microbial infection in plants, *Ann. Rev. Plant Physiol.*, **35**, 243-275.

Dorgelo, E., van der Meer, A., Wesselingh, J. (1985) Measurement of the axial dispersion of particles in a liquid fluidized bed applying a random walk method, *Chem. Eng. Sci.*, **40**, 2105-2111.

Dörnenburg, H., Knorr, D. (1995) Strategies for the improvement of secondary metabolite production in plant cell cultures, *Enzyme and Microbial Technology*, **17**, 674-684.

Dougall, D.K. (1986) Accumulation of natural products in plant tissue cultures revisited, *New Zealand J. Technol.*, **2**, 71-76.

Dubois, M., Gilles, K., Hamilton, J.K., Rebers, P.A., Smith, F. (1956) *Anal. Biochem.*, **28**, 350.

Einsele, A. (1976) Scaling of bioreactors, theory and reality, *5th Int. Ferm. Symp.*, Berlin, Paper 4.13.

Elridge, A.C., Kwolek, W. (1983) Soybean isoflavones: Effect of environment and variety on composition, *J. Agric. Food Chem.*, **31**, 394-396.

Emerson, D., Worden, R.M., Breznak, J.A. (1994) A diffusion gradient chamber for studying microbial behavior and separating microorganisms, *Appl. Environ. Microbiol.*, **60**, 1269-1278.

Facchini, P., DiCosmo, F. (1991) Plant cell bioreactor for the production of photoberberine alkaloids from immobilizaed *Thalictrum rugosum* cultures, *Biotech. Bioeng.*, **37**, 397-403.

Fett, W.F., Zacharius, R.M. (1982) Bacterially induced glyceollin production in soybean cell suspension cultures, *Plant Sci. Lett.*, **24**, 303-309.

Fogler, H.S. (1986) *Elements of Chemical Reaction Engineering*, Prentice-Hall, New Jersey.

Fogler, H.S. (1992) *Elements of chemical reaction engineering, 2nd edition,* Prentice Hall, Englewood Cliffs, New Jersey.

Fotsis, T., M. Pepper, H. Adlercreutz, G. Fleischmann, J. Hase, R. Montesana, and L. Schweigerer (1993) Genistein, a dietary-derived inhibitor of *in vitro* angiogenesis, *Proc. Natl. Acad. Sci.*, **90**, 2690-2694.

Fotsis, T., Pepper, M., Adlercreutz, H., Fleischmann, G., Hase, J., Montesana, R., Schweigerer, L. (1993) Genistein, a dietary-derived inhibitor of in vitro angiogenesis. *Proc. Natl. Acad. Sci.*, **90**, 2690-2694.

Fowler, M.W. (1982) *J. Chem. Tech. Biotechnol.*, **32**, 338-346.

Freund, V.S., Worden, R.M. (1990) Gas hold-up in a magnetically stabilized three-phase fluidized bed bioreactor, *Annual Meeting of American Institute of Chemical Engineers*, Chicago, IL, Nov 11-16.

Froment, G., Bischoff, K. (1979) *Chemical Reactor Analysis and Design,* John Wiley & Sons: New York.

Gamborg, O., Miller, R., Ojima, K. (1968) Nutrient requirements of suspension cultures of soybean root cells, *Experimental Cell Research*, **50**, 151-158.

Gazaway, W.S., Hagan, A.K. (1989) Sclerotium blight, In: *Compendium of Soybean Diseases*, 3rd ed., Eds. J.B. Sinclair, and P.A. Backman, APS Press, St. Paul, Minn., 48-49.

Graham, M.Y., Graham, T.L. (1991) Rapid accumulation of anionic peroxidases and phenolic polymers in soybean cotyledon tissues following treatment with *Phytophthora megasperma* f. sp. *Glycinea* wall glucan, *Plant Physiol.*, **97**, 1445-1455.

Graham, T., Kim, J., Graham, M. (1990) Role of constitutive isoflavone conjugates in the accumulation of glyceollin in soybean infected with *Phytophthora megasperma*, *Mol. Plant-Microbe Interact.*, **3**, 157-166.

Graham, T.L. (1991) A rapid, high resolution high performance liquid chromatography profiling procedure for plant and microbial aromatic secondary metabolites, *Plant Physiol.*, **95**, 584-593.

Graham, T.L. (1991b) Flavonoid and isoflavonoid distribution in developing soybean seedling tissues and in seed and root exudates, *Plant Physiol.*, **95**, 594-603.

Guardiola, J., Iborra, J.L., Canovas, M. (1995) A model that links growth and secondary metabolite production in plant cell suspension cultures, *Biotechnol. Bioeng.*, **46** 291-297.

Hahlbrock, K., Lamb, C.J., Purwin, C., Ebel, J., Fautz, E., Schafer, E. (1981) Rapid response of suspension-cultured parsley cells to the elicitors from *Phytophthora megasperma* var. *sojae*, *Plant Physiol.*, **67**, 768-773.

Holden, M.A., Yeoman, M.M. (1987) Optimization of product yield in immobilised plant cell cultures, *Bioreactors and Biotransformations*, Eds. G.W. Moody and P.B. Baker, Elsevier Applied Science Publishers, New York.

Homberg, H., Geiger, H. (1980) Fluorescence and structure of flavones, *Phytochemistry*, **19**, 2443-2449.

Hooker, B.S., Lee, J.M. (1992) Application of a new structured model to tobacco cell cultures, *Biotech. Bioeng.*, **39**, 765-774.

Hu, T., Wu, J. (1987) Study on the characteristics of a biological fluidized bed in a magnetic field, *Chem. Eng. Res. Des.*, **65**, 238-242.

Hubbard, D.W. (1987) Scale-up strategies for bioreactors, *Biotechnology Processes: Scale-up and Mixing*, Ho, C.S., Oldshue, J.Y. eds., American Institute of Chemical Engineers, New York.

Jacobsen, B.J., Meronuck, R.A. (1989) Postharvest Pathology, In: *Compendium of Soybean Diseases*, 3rd ed., Eds. J.B. Sinclair, Backman, P.A., APS Press, St. Paul, Minn., 80-82.

Jaraiz-M., E., Wang, Y., Zhang, G., Levenspiel, O. (1984) Theory and operational characteristics of the magnetic valve for solids, *AIChE J.*, **30**, 951-966.

Jaraiz-M., E., Zhang, G., Wang, Y., Levenspiel, O. (1984b) The magnetic distributor-downcomer (MDD) for fluidized beds, *Power Technol.*, **38**, 53-61.

Jende-Strid, B. (1993) Genetic control of flavonoid biosynthesis in barley, *Hereditas*, **119**, 187-204.

Jing, Y., Nakaya, K., Han, R. (1993) Differentiation of promyelocytic leukemia cells HL-60 induced by daidzein *in vitro* and *in vivo*, *Anticancer Res.*, **13**, 1049-1054.

Jing, Y., Waxman, S. (1995) Structural requirements for differentiation-induction and growth-inhibition of mouse erythroleukemia cells by isoflavones, *Anticancer Res.*, **15**, 1147-1152.

Kalk, J.P., Langlykke, A.F. (1986) Cost estimation for biotechnology projects, Manual of Industrial Microbiology & Biotechnology, Demain, A.L., Solomon, N.A. eds., American Society for Microbiology, Washington D.C.

Kaster, J.A., Michelsen, D.L., Velander, W.H. (1990) Increased oxygen transfer in a yeast fermentation using a microbubble dispersion, *Appl. Biochem. Biotechnol.*, **24**, 469-784.

Kim, D., Pedersen, H., Chin, C. (1991) Cultivation of *Thalictrum rugosum* cell suspension in an improved airlift bioreactor: Stimulatory effect of carbon dioxide and ethylene on alkaloid production, *Biotechnol. Bioeng.*, **38**, 331-339.

Kochs, G., Grisebach, H. (1987) Induction and characterization of a NADPH-dependent flavone synthase from cell cultures of soybean, *Z. Naturforsch*, **42**, 343-348.

Kosslak, R.M., Bookland, R., Barkei, J., Paaren, H.E., Appelbaum, E.R. (1987) Induction of *Bradyrhizobium japonicum* common *nod* genes by isoflavones isolated from *Glycine max*, *Proc. Natl. Acad. Sci.*, **84**, 7428-7432.

Kudou, S., Fleury, Y., Welti, D., Magnolato, D., Uchida, T., Kitamura, K., Okubo, K. (1991) Malonyl isoflavone glycosides in soybean seeds (*Glycine max* Merrill), *Agric. Biol. Chem*, **55**, 2227-2233.

Leckie, F., Scragg, A., Cliffe, K. (1991) Effect of bioreactor design and agitator speed on the growth and alkaloid accumulation by cultures of *Catharanthus roseus*, *Enzyme Microb. Technol.*, **13**, 296-305.

Lee, C.W., Shuler, M.L. (1991) Different shake flask closures alter gas phase composition and ajmalicine production in *Catharanthus roseus* cell suspensions, *Biotechnol. Tech.*, **5**, 173-178.

Lee, H.P., Gourley, L., Duffy, S.W., Esteve, J., Lee, J., Day, N.E. (1991) Dietary effects on breast-cancer risk in Singapore, *The Lancet*, **337**, 1197-1200.

Liao, J.C., Delgado, J. (1993) Advances in Metabolic Control Analysis, *Biotechnol. Prog*, **9**, 221-223.

Lindsey, K., Yeoman, M.M. (1984) The synthetic potential of immobilised cells of *Capsicum frutescens* Mill cv. Annuum, *Planta*, **162**, 495-501.

Liu, Y., Hamby, R., Colberg, R. (1991) Fundamental and practical developments of magnetofluidized beds: a review, *Power Technology*, **64**, 3-41.

Longe, T.A. (1989) Colloidal gas aphrons: Generation, flow characterization and application in soil and groundwater decontamination, Ph.D. Dissertation, Virginia Polytechnic Institute and State University.

Maurel, B., Pareilleux, A. (1985) Effect of carbon dioxide on the growth of cell suspensions of *Catharanthus roseus*, *Biotechnol. Lett.*, **7**, 313-318.

McCabe, W.L., Smith, J.C., Harriott, P. (1993) *Unit Operations of Chemical Engineering, Fifth Ed.* McGraw-Hill, New York, 350-357.

McKelvey, S.A., Gehrig, J.A., Hollar, K.A., Curtis, W.R. (1993) Growth of plant root cultures in liquid- and gas-dispersed reactor environments, *Biotechnol. Prog.*, **9**, 317-322.

Menczel, L., Nagy, F., Kiss, Z.R., Maliga, P. (1981) Streptomycin resitant and sensitive somatic hybrids of *Nicotiana tabacum* and *Nicotiana knightiana*: correlation of resistance to *N. tabacum* plastids, *Theor. Appl. Genet.*, **59**, 191-195.

Messina, M., Barnes, S. (1991) The role of soy products in reducing risk of cancer, *J. Natl. Cancer Inst.*, **83**, 541-545.

Miller, K.J., Hadley, J.A., Gustine, D.L. (1994) Cyclic -1,6-1,3-glucans of *Bradyrhizobium japonicum* USDA 110 elicit isoflavonoid production in the soybean (*Glycine max*) host, *Plant Physiol.*, **104**, 917-923.

Mol, J., de Lange, P., Oostdam, A., van der Plas, L. (1990) Use of genetic engineering to improve yields in cell cultures, e.g. (anti)sense DNA technology, In *Progress in plant cellular and molecular biology*; Nijkamp, H., Van der Plas, L., Van Aartrijk, J. Eds., Kluwer Academic Publishers: Boston, 712-716.

Montgomery, D.B. (1969) *Solenoid Magnet Design*, Wiley-Interscience, New York.

Mousavi, Y., Aldercreutz, H. (1993) Genistein is an effective stimulator of sex hormone-binding globulin production in heptocarcinoma human liver cancer cells and suppresses proliferation of these cells in culture, *Steroids*, **58**, 301-304.

Mueller, S., Yeh, Y., Chen, W.-T. (1992) Tryosine phosphorylation of membrane protein mediates cellular invation by transformed cells, *J. Cell Biol.*, **119**, 1309-1325.

Mustelin, T., Burn, P. (1993) Regulation of *src* family tyrosine kinases in lymphocytes, *TIBS*, June, 215-220.

Naim, M., Gestetner, B., Zilkah, S., Birk, Y., Bondi, A. (1974) Soybean isoflavones: Characterization, determination, and antifungal activity, *J. Agr. Food Chem.*, **22**, 806-809.

Okada, W., Fukuda, H., Morikawa, H. (1981) Kinetic expressions of ethanol production rate and ethanol consumption rate in baker's yeast cultivation, *J. Ferment. Technol.*, **59**, 103-109.

Okura, A., Arakawa, H., Oka, H., Yoshinari, T., Monden, Y. (1988) Effect of genistein on topoisomerase activity and on the growth of [Val 12]Ha-*ras*-transformed NIH 3T3 cells, *Biochem. Biophysical Research*, **157**, 183-189.

Orr, J.D., Edwards, R., Dixon, R.A. (1993) Stress responses in alfalfa (*Medicago sativa* L.), *Plant Physiol.*, **101**, 847-856.

Panda, A., Mishra, S., Bisaria, V., Bhojwani, S. (1989) Plant cell reactors--a perspective, *Enzyme Microb. Technol.*, **11**, 386-397.

Partridge, J.E., Keen, N.T. (1977) Soybean phytoalexins: Rates of synthesis are not regulated by activation of initial enzymes in flavonoid biosynthesis, *Phytopathology*, **67**, 50-55.

Perry, R.H., Green, D.W., Maloney, J.O. (1984) *Perry's chemical engineers' handbook, 6th edition,* McGraw-Hill, New York.

Pollock, K, Barfield, D., Shields, R. (1983) The toxicity of antibiotics to plant cell cultures, *Plant Cell Reports*, **2**, 36-39.

Porter, P.M., Banwart, W.L., Hassett, J.J. (1986) Phenol acids and flavonoids in soybean root and leaf extracts, *Environ. and Exptl. Bot.*, **26**, 65-73.

Rao, S. (1990) Root flavonoids, *The Botanical Review*, **56**, 2-85.

Reinhard, E., Kreis, W., Barthlen, U., Helmbold, U. (1989) Semicontinuous cultivation of *Digitalis lanata* cells: production of β-methyldigoxin in a 300-L airlift bioreactor, *Biotechnology and Bioengineering,* **34**, 502-508.

Rosenshine, I., Duronio, V., Finlay, B. (1992) Tyrosine protein kinase inhibitors block invasin-promoted bacterial uptake by epithelial cells, *Infection and Immunity*, **60**, 2211-2217.

Rosensweig, R.E. (1978) Process for operating a magnetically stabilized bed, U.S. Patent 4 115 927.

Rosensweig, R.E. (1979) Fluidization: hydrodynamic stabilization with a magnetic field, *Science*, **204**, 57-60.

Rosensweig, R.E., Siegell, J.H., Lee, W.K., Mikus, T. (1981) Magnetically stabilized fluidized solids, *AIChE Symposium Series*, **77**, 8.

Sahai, O., Knuth, M. (1985) Commercializing plant tissue culture processes: Economics, problems and prospects, *Biotechnol. Prog.*, **1**, 1-9.

Schlatmann, J.E., Moreno, P.R., Vinke, J.L., ten Hoopen, H.J., Verpoorte, R., Heijnen, J.J. (1997) Gaseous metabolites and the ajmalicine production rate in high density cell cultures of *Catharanthus roseus*, *Enzyme Microb. Technol.*, **20**, 107-115.

Schlatmann, J.E., Nuutila, A.M., van Gulik, W.M., ten Hoopen, H.J.G., Verpoorte, R., Heijnen, J.J. (1993) Scaleup of ajmalicine production by plant cell cultures of *Catharanthus roseus*, *Biotech. Bioeng.*, **41**, 253-262.

Schmidt, S. (1995) Development of Novel Methods to Measure Random and Chemotactic Microbial Motility at the Community Level, Studienarbeit, Istitut fur Verfahrenstechnik, Supervising Professor at Michigan State University: R. Mark Worden, East Lansing MI.

Schnapp, S. R., Curtis, W. R., Bressan, R. A., Hasegawa, P. M. (1991) Estimation of growth yield and maintenance coefficient of plant cell suspensions, *Biotech. Bioeng.*, **38**, 1131-1136.

Schneckenburger, H., Reuter, B.W., Schoberth, S.M. (1985) Fluorescence techniques in biotechnology, *Trends in Biotechnology*, **3**, 257-261.

Scholar, E.M., Toews, M.L. (1994) Inhibition of invasion of murine mammary carcinoma cells by the tyrosine kinase inhibitor genistein, *Cancer Lett.*, **87**, 159-162.

Sebba, F. (1987) *Foams and Biliquid Foams - Aphrons*, John Wiley and Sons, Ltd., New York.

Shuler, M. (1981) Production of secondary metabolites from plant tissue culture--problems and prospects, *Ann. N. Y. Acad. Sci.*, 65-79.

Shuler, M., Hirasuna, T., Prince, C., Bringi, V. (1990) Bioreactor considerations for producing flavors and pigments from plant tissue culture, In *Biotechnology and food process engineering*, Scwartzberg, H., Rao, M., Eds., Marcel Dekker, New York, 45-65.

Siegell, J.H. (1988) Magnetically frozen beds, *Powder Technology*, **55**, 127-132.

Smith, J.M., Davison, S.W., Payne, G.F. (1990) Development of a strategy to control the dissolved concentrations of oxygen and carbon dioxide at constant shear in a plant cell bioreactor, *Biotechnol. Bioeng.*, **35**, 1088-1101.

Takano, H., Furu-une, H., Burgess, J.G., Manabe, E., Hirano, M., Okazaki, M., Matsunaga, T. (1993) Production of ultrafine calcite particles by coccolithophorid algae grown in a biosolar reactor supplied with sunlight, *App. Biochem. Biotechnol.*, **39**, 159-167.

Taya, M., Yoyama, A., Kondo, D., Kobayashi, T., Matsui, C. (1989) Growth characteristics of plant hairy roots and their cultutres in bioreactors, *J. Chem. Eng. Japan*, **22**, 84-89.

Ten Hoopen, H., Van Gulik, W., Meijer, J. (1990) Possibilities, problems, and pifalls of large-scale plant cell cultures, In *Progress in plant cellular and molecular biology*, Nijkamp, H., Van der Plas, L., Van Aartrijk, J. Eds., Kluwer Academic Publishers, Boston, 673-681.

Thompson, V., Worden, R. (1997) Phase holdup, liquid dispersion, and gas-to-liquid mass transfer measurements in a three-phase magnetofluidized bed, *Chem. Eng. Sci.*, **52**, 279-295.

Thompson, V.S. (1993) Characterization of a three-phase magnetically stabilized fluidized bed bioreactor, Ph.D. Dissertation, Michigan State University, East Lansing, MI.

Thompson, V.S., Worden, R.M. (1991) Axial dispersion in a three-phase, magnetically stabilized bioreactor, *Annual Meeting of American Institute of Chemical Engineers*, Los Angeles, CA, November 17, 1991.

Thompson, V.S., Worden, R.M. (1992) The effect of tracer diffusion on liquid axial dispersion in a three phase fluidized bed bioreactor, *Chem. Eng. Sci.*, **47**, 3435-3441.

Uchimiya, H., Handa, T., Brar, D. (1989) Transgenic plants, *Journal of biotechnology*, **12**, 1-20.

Urushibara, S., Kitayama, Y., Watanabe, T., Okuno, T., Watarai, A., Matsumoto, T. (1992) New flavonol glycosides, major determinants inducing the green fluorescence in the guard cells of *Allium cepa*, *Tetrahedron Letters*, **33**, 1213-1216.

van Gulik, W. M., ten Hoopen, H. J., Heijnen, J. J. (1992) Kinetics and stoichiometry of growth of plant cell cultures of *Catharanthus roseus* and *Nicotiana tabacum* in batch and continuous fermentors, *Biotech. Bioeng.*, **40**, 863-874.

van Gulik, W.M., Nuutila, A.M., Vinke, K.L., ten Hoopen, H.J., Heijnen, J.J. (1994) Effects of carbon dioxide, air flow rate, and innoculation density on the batch growth of *Catharanthus roseus* cell suspensions in stirred fermentors, *Biotechnol. Prog.*, **10**, 335-339.

van Gulik, W.M., ten Hoopen, H.J., Heijnen, J.J. (1993) A structured model describing carbon and phosphate limited growth of *Catharanthus roseus* plant cell suspensions in batch and chemostat culture, *Biotechnol. Bioeng.*, **41**, 771-780.

van't Riet, K. (1983) Mass transfer in fermentation, *Trends in Biotechnology*, **1**, 113-119.

Vieth, W. (1994) Gene expression with plant cells, In *Bioprocess engineering: kinetics, mass transport, reactors and gene expression*, John Wiley & Sons, New York, 265-324.

Voirin, B. (1983) UV spectral differentiation of 5-hydroxy- and 5-hydroxy-3-methoxyflavones with mono-(4';), di-(3',4') or tri-(3',4',5')-substituted b rings, *Phytochemistry*, **10**, 2107-2145.

Wang, H., Murphy, P.A. (1994) Isoflavone composition of American and Japanese soybeans in Iowa: Effects of variety, crop year, and location, *J. Agric. Food Chem.*, **42**, 1674-1677.

Wang, H., Murphy, P.A. (1994b) Isoflavone Content in Commercial Soybean Foods, *J. Agric. Food Chem.*, **42**, 1666-1673.

Watanabe, T., Kondo, K., Oishi, M. (1991) Induction on *in vitro* differentiation of mouse erythroleukemia cells by genistein, an inhibitor of tyrosine protein kinases, *Cancer Research*, **51**, 764-768.

Waugh, R., Brown, J. (1991) Plant gene structure and expression, *Plant genetic engineering*, Grierson, D. Ed; Chapman and Hall, New York, 1-37.

Wei, H., Bowen, R., Cai, Q., Barnes, S., Wang, Y. (1995) Antioxidant and antipromotional effects of the soybean isoflavone genistein, *Proc. Soc. Exp. Biol. Med.*, **208**, 124-130.

Wei, H., Wei, L., Frenkel, K., Bowen, R., Barnes, S. (1993) Inhibition of tumore promoter-induced hydrogen peroxide formation *in vitro* and *in vivo* by genistein, *Nutrition and Cancer*, **20**, 1-12.

Weng, D., Chen, L., Han, Y., Zhu, W., Xu, S., Ouyang, F. (1992) Continuous ethanol fermentation in a three-phase magnetic fluidized bed bioreactor, *AIChE Symposium Series on Fluidized Processes*, **289**, 107-115.

Westgate, P. J., Curtis, W. R., Emery, A. H., Hasegawa, P. M. and Heinstein, P. F. (1991) Approximation of continuous growth of *Cephalotaxus harringtonia* plant cell cultures using fed-batch operation, *Biotech. Bioeng.*, **38**, 241-246.

Westgate, P.J., Emery, A.H., Hasegawa, P.M., Heinstein, P.F. (1991) Growth of *Cephalotaxus harringtonia* plant-cell cultures, *Appl. Microbiol. Biotechnol.*, **34**, 798-803.

Westrin, B., Axelsson, A. (1991) Diffusion in gels containing immobilized cells: a critical review, *Biotech. and Bioeng.*, **38**, 439-446.

Whitney, P.J. (1992) Novel bioreactors for the growth of roots transformed by *Agrobacterium rhizogenes*, *Enzyme Microb. Tech.*, **14**, 13-17.

Widman, M., Emerson, D., Chiu, C., Worden, R., Breznak, J., Hoppensteadt, F. (1995) Modeling of microbial chemotaxis in a diffusion gradient chamber, *Annual Meeting of American Institute of Chemical Engineers*, Miami Beach, FL, November 14, 1995.

Widman, M.T., Emerson, D., Chiou, C., Worden, R.M. (1997) Modeling microbial chemotaxis in a diffusion gradient chamber, *Biotech. Bioeng.*, in press.

Worden, R.M., Donaldson, T.L. (1987) Dynamics of a biological fixed film for phenol degradation in a fluidized bed bioreactor, *Biotech. and Bioeng.*, **30**, 398-412.

Worden, R.M., Emerson, D., Breznak, J.A. (1993) Quantitative analysis of chemotaxis in a Diffusion Gradient Chamber, *Annual Meeting of American Institute of Chemical Engineers*, St. Louis, MO, November 7-12.

Yamada, Y. (1984) Selection of cell lines for high yields of secondary metabolites, *Cell Culture and Somatic Cell Genetics of Plants*, **1**, 629-636.

Yanagihara, K., Ito, A., Toge, T., Numoto, M. (1993) Antiproliferative effects of isoflavones on human cancer cell lines established from the gastrointestinal tract, *Cancer Res.*, **53**, 5815-5821.

Yang, W., Jaraiz-M., E., Levenspiel, O., Fitzgerald, T.J. (1982) A magnetic control valve for flowing solids: Exploratory studies, *Ind. Eng. Chem. Process Des. Dev.*, **21**, 717-721.

Yun, D., Hashimoto, T., Yamada, Y. (1992) Metabolic engineering of medicinal plants: transgenic *Atropa belladonna* with an improved alkaloid composition, *Proc. Natl. Acad. Sci. USA*, **89**, 11799-11803.

Zacharius, R.M., Kalan, E.B. (1990) Isoflavonoid changes in soybean cell suspensions when challenged with intact bacteria or fungal elicitors, *J. Plant Physiol.*, **135**, 732-736.

Zhong, J., Seki, T., Kinoshita, S., Yoshida, T. (1991) Effect of light irradiation on anthocyanin production by suspended culture of *Perilla frutescens*, *Biotech. Bioeng.*, **38**, 653-658.